CHAPTER 4 RESULT AND DISCUSSION

4.1 Introduction

In this chapter, unconfined compression test results of polymer modified asphalt concrete (PMA) prepared by different directions of compaction at different densities are presented. The stress-strain and strength characteristics of different directions of compaction were discussed. The equivalent modulus and Poisson's ratio of PMA by different directions of compaction were also compared and discussed. Moreover, the results of hot-mixed asphaltic concrete (HMA) that were studied in the past were also compared with the results of PMA.

4.2 Continuous monotonic loading

4.2.1 Stress-strain relations

Figs. 4.1a-4.1c compare the unconfined compression test results which were obtained by continuous monotonic loading (ML) at constant strain rate ($\dot{\varepsilon}$) of 0.03%/min by using apparatus A. The PMA specimens were compacted in vertical and horizontal directions at different densities of: 1.90 g/cm^3 (PMA-1V and PMA-1H), 2.15 g/cm^3 (PMA-2V and PMA-2H) and 2.37 g/cm^3 (PMA-3V and PMA-3H) and had the voids in mineral aggregates (VMA) of 31.369 %, 22.339 %, and 14.392 %, respectively. Note that the strain values (ε) presented in Figs. 4.1a-4.1c were the ones measured by using LVDT.

The results shown in Figs. 4.2a and 4.3a compares the representatives of stress-strain relation for specific directions of compaction and densities. That is, Fig. 4.2a compares the stress-strain relations of the vertically compacted PMA specimens; and, Fig. 4.3athe horizontally compacted PMA specimens at different densities.

Figs. 4.2b and 4.3b show the stress-strain relations normalized by the maximum stress and maximum strain for vertical and horizontal compactions, respectively.

It may be seen from Figs. 4.2b and 4.3b that different stress-strain behaviors for the same direction of compaction were collapsed into a similar manner.

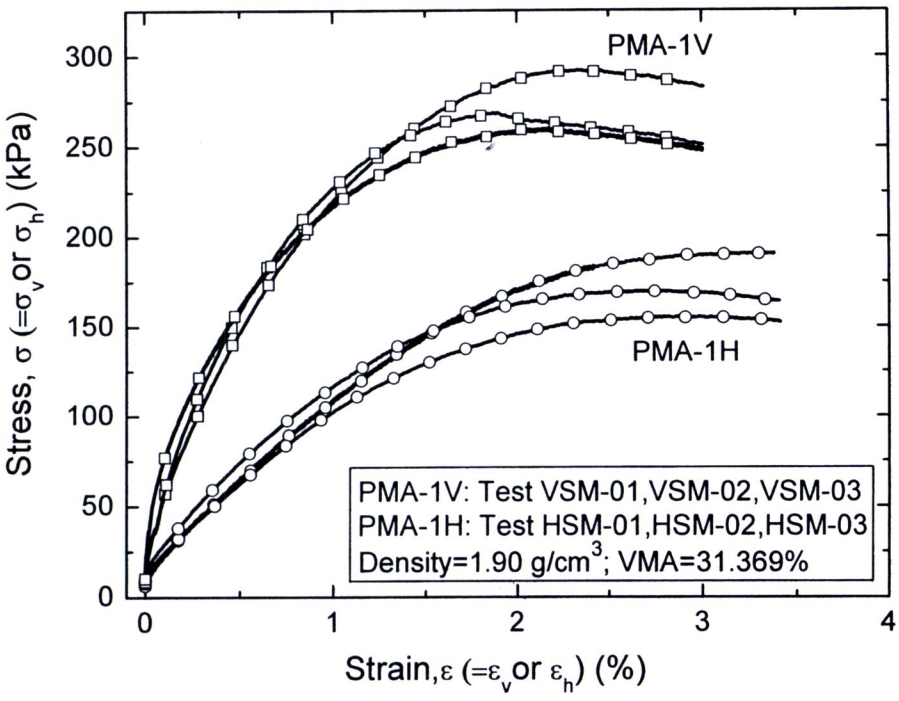

Figure 4.1(a) Continuous monotonic loading test results on PMA specimens compacted in vertical and horizontal directions at the density of 1.90 g/cm^3

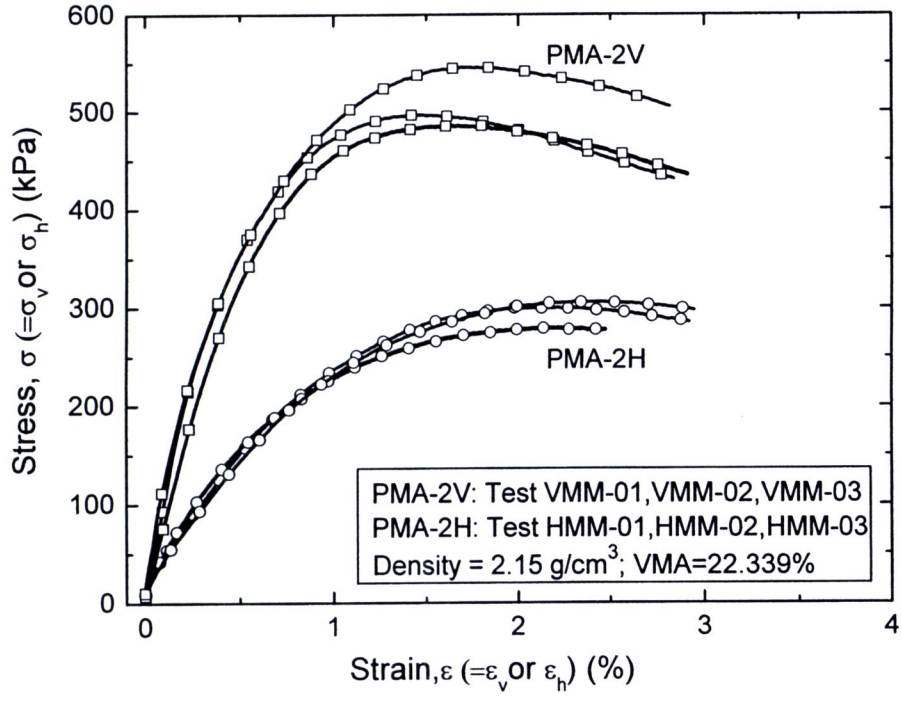

Figure 4.1(b) Continuous monotonic loading test results on PMA specimens compacted in vertical and horizontal directions at the density of 2.15 g/cm^3

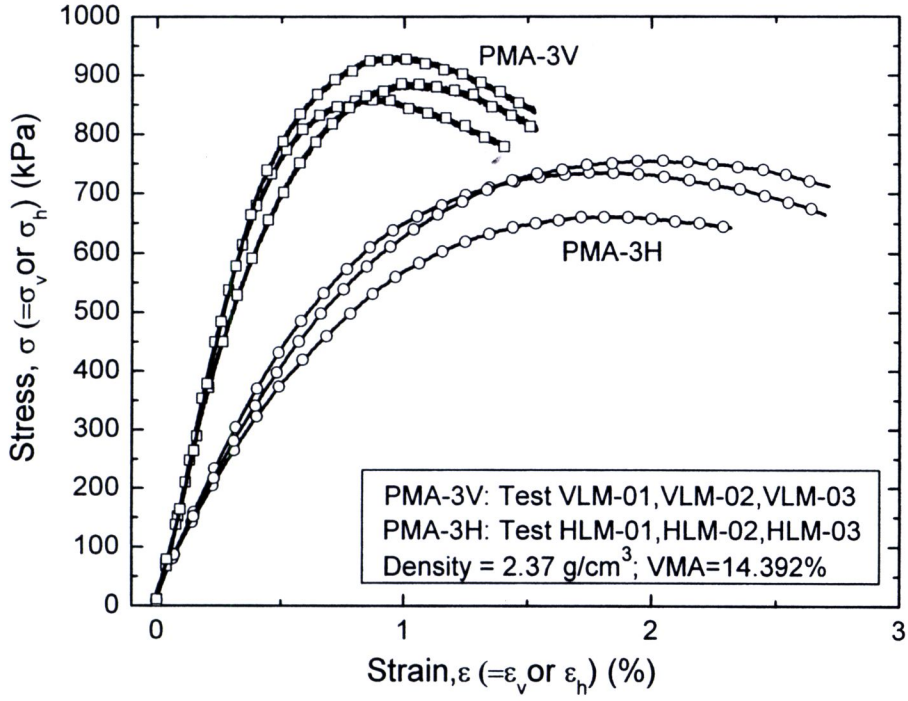

Figure 4.1(c) Continuous monotonic loading test results on PMA specimens compacted in vertical and horizontal directions at the density of 2.37 g/cm^3

THE NATIONAL RESEARCH COUNCIL OF THAILAND
RESEARCH LIBRARY

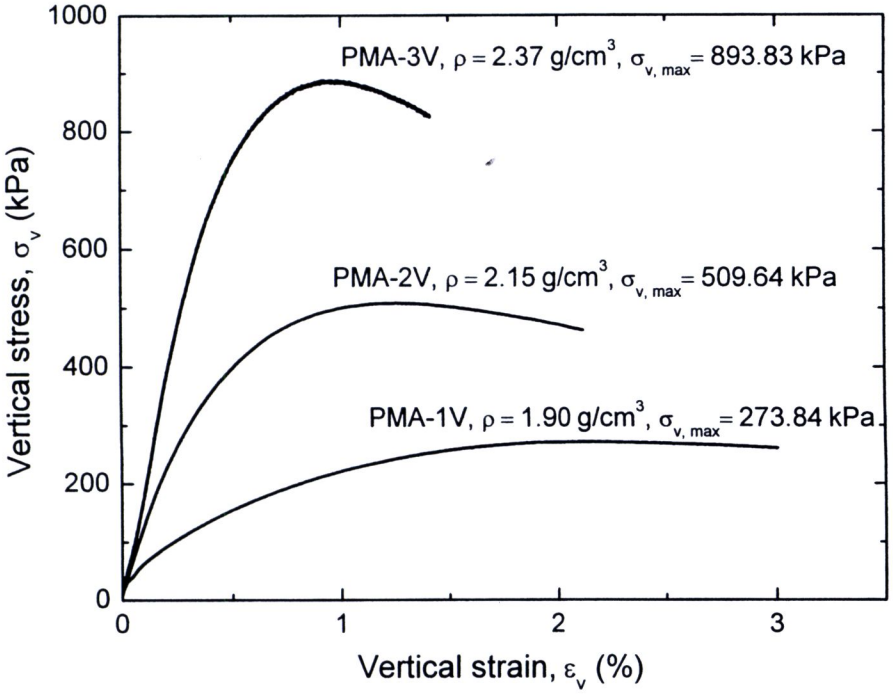

Figure 4.2(a) Comparison of the relationships between vertical stress and vertical strain of the vertically compacted PMA specimens at different densities

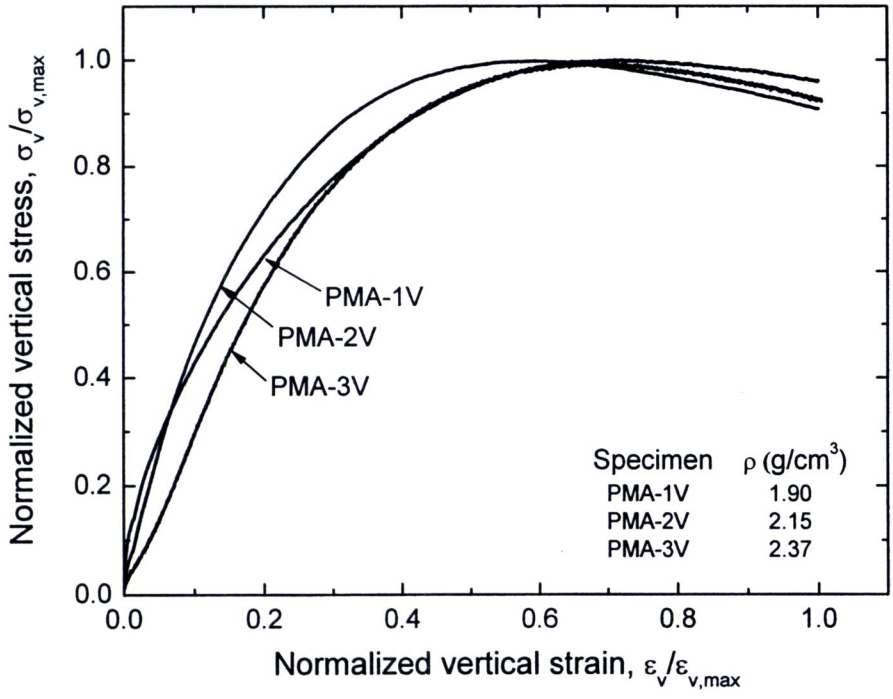

Figure 4.2(b) Relationships between vertical stress and vertical strain of the vertically compacted PMA specimens at different densities normalized by maximum vertical stress and maximum vertical strain

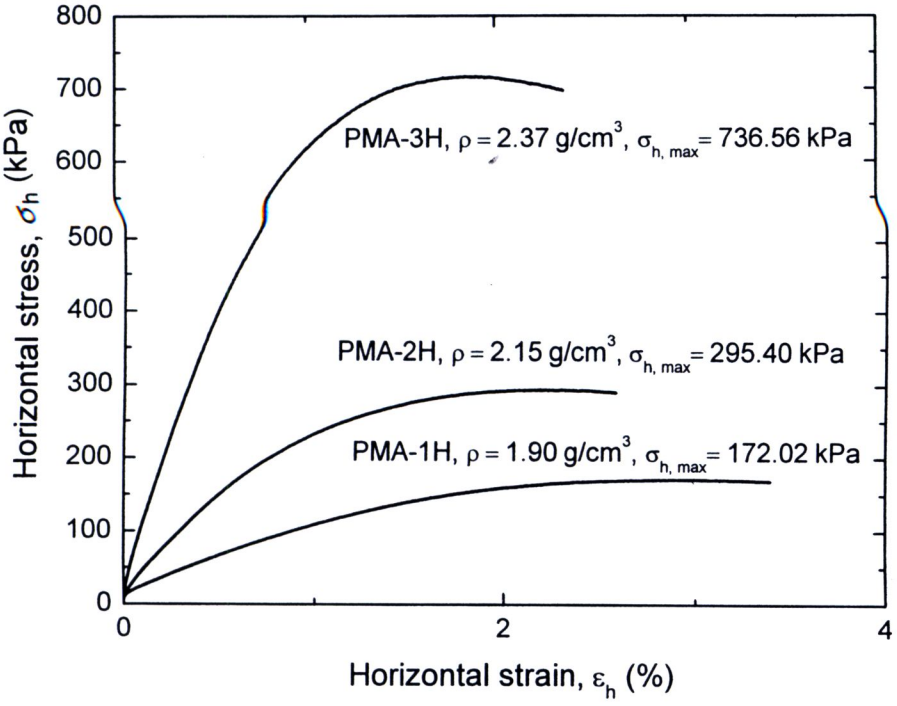

Figure 4.3(a) Comparison of the relationships between horizontal stress and horizontal strain of the horizontally compacted PMA specimens at different densities

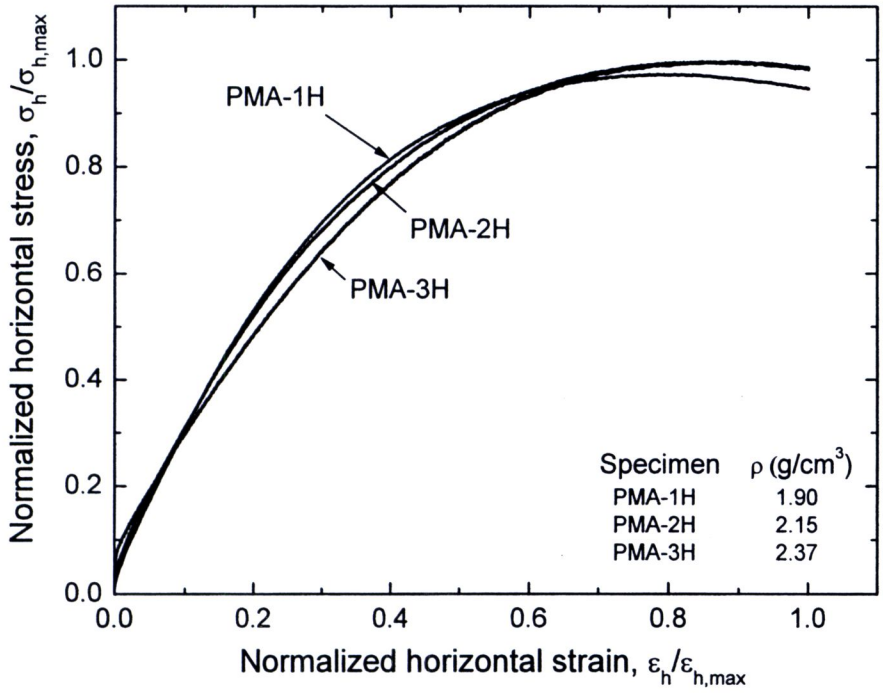

Figure 4.3(b) Relationships between horizontal stress and horizontal strain of the horizontally compacted PMA specimens at different densities normalized by maximum vertical stress and maximum vertical strain

4.2.2 The maximum stress and secant modulus (E_{50})

The peak values of vertical and horizontal stresses ($\sigma_{v,max}$ and $\sigma_{h,max}$) of PMA specimens having different directions of compaction at different densities are summarized in Table 4.1. It should be noted here that the respective $\sigma_{v,max}$ and $\sigma_{h,max}$ values were used to configure the input loading histories in which combinations of sustained loading (SL) and cycles of unload and reload were performed.

Table 4.1 Summary of maximum stress and secant modulus (E_{50}) of PMA specimens having different directions of compaction and different densities

Density (g/cm^3)	Direction of compaction	Test name	$\sigma_{v,max}$ or $\sigma_{h,max}$ (kPa)	E_{50} (MPa)	Avg. σ_{max} (kPa)	Avg. E_{50} (MPa)
1.90	vertical	VSM-01	292.31	29.52	273.84	35.02
		VSM-02	260.31	40.29		
		VSM-03	268.90	35.26		
	horizontal	HSM-01	190.83	11.42	172.02	12.27
		HSM-02	155.52	11.51		
		HSM-03	169.73	13.89		
2.15	vertical	VMM-01	545.97	85.95	509.64	82.61
		VMM-02	496.80	89.75		
		VMM-03	486.16	72.13		
	horizontal	HMM-01	305.83	28.35	295.40	30.46
		HMM-02	300.14	30.58		
		HMM-03	280.23	32.45		
2.37	vertical	VLM-01	860.51	193.57	893.83	184.13
		VLM-02	933.32	187.63		
		VLM-03	887.67	171.20		
	horizontal	HLM-01	662.18	79.79	736.56	85.52
		HLM-02	735.57	92.74		
		HLM-03	755.51	84.04		

Fig. 4.4 shows the relationships between the maximum vertical or horizontal stress and the density of PMA specimen. Fig. 4.5 shows the relationships between the E_{50} and the density of PMA specimen. The following trends of behavior may be seen from Figs. 4.4 and 4.5:

1) Considering the test results in terms of maximum stresses ($\sigma_{v,max}$ and $\sigma_{h,max}$) and at the same of direction of compactions (vertical or horizontal compactions). Values of the maximum stresses and secant modulus (E_{50}) increased with an increase in the densities of PMA. The increases of the maximum stresses and the E_{50} with the densities of PMA were at the increasing rate. This shows the significance of compaction on PMA to obtain higher density for increasing the strength and stiffness properties.

2) Considering the difference of directions of compaction while at the same density, the strength of the vertically compacted PMA specimen was higher than the horizontally compacted PMA specimen. The deformation of vertically compacted PMA specimen at which the maximum stress exhibited was noticeably smaller than the horizontally compacted PMA specimen. As a result, the E_{50} value for the vertically compacted specimens was larger than the horizontally compacted ones.
3) As PMA specimens were prepared by compaction, when the direction of compaction compared to the direction of loading was changed between vertically and horizontally compacted specimens the behaviors of the strength and deformation of PMA also change.

From test results on PMA, it was found that the strength and deformation behaviors of PMA are anisotropic. This implies that the material properties are direction dependent. Therefore, it is reasonable to assert that PMA may exhibit significant anisotropic behavior due to the compaction.

The strength and the E_{50} behaviors of the vertically compacted PMA specimen were quantitatively greater than the ones of horizontally compacted PMA specimen. It may be due to the following reasons:

1) In the process of compaction, aggregate particles were arranged in forms of a layer that has a small thickness in the direction vertical to the direction of compaction. So, when the aggregate receive the force in the same direction (direction of compaction), they would be stronger than the other directions.
2) There is preloading force in the same direction of loading to the specimen. That is, while the aggregate particles were compacted, the aggregate particle arranged in each layers would receive the force in the same direction as the force at testing specimen.
3) The joint between the layers of vertically compacted PMA specimen is normal to the direction of loading. When the vertically compacted PMA specimen receive the force from loading, a joint was pressed down such that the friction and the connection between the layers became stronger than the joints in the direction parallel to the direction of loading.

The E_{50} value that obtained from this study (PMA at 2.15 g/cm^3) when compared with the E value which obtained from falling weight deflectometer (FWD) (Moryadee, 2009), the E_{50} value of PMA is greater than the E value of FWD about 20%. It may be due to the following reasons:

1) The specimens were use in FWD testing have a thickness 50 mm only but in this study used the specimens with a thickness of 150 mm. So the results from these two cases are different.
2) FWD tests were tested by put the specimens on the sand which is the strength less than asphaltic concrete. Therefore the E values from FWD is less than the E_{50} values from PMA which tests by does not put specimens on the low strength materials.

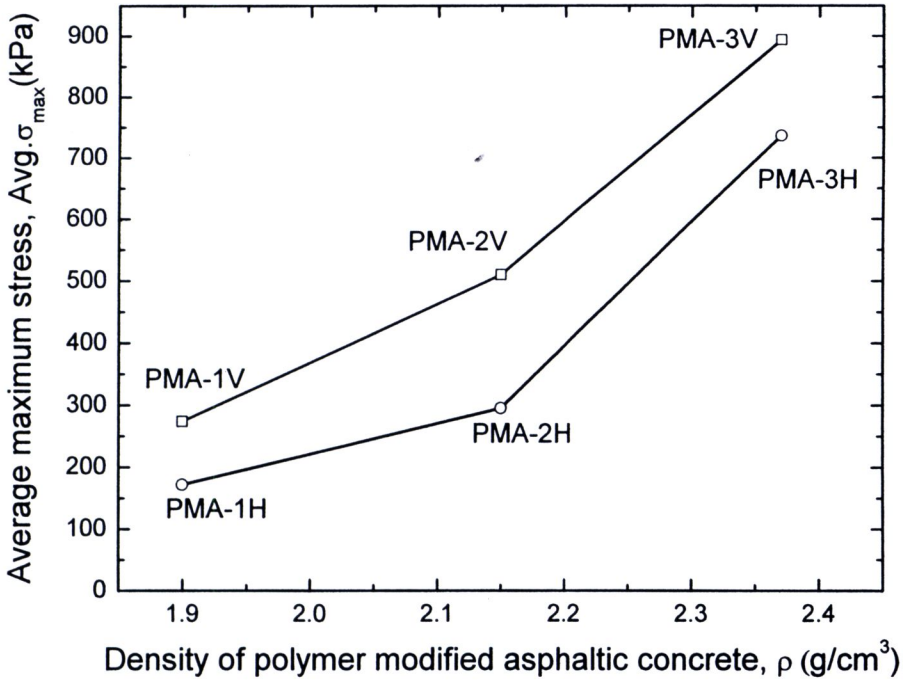

Figure 4.4 Relationships between the maximum stress ($\sigma_{v,max}$ and $\sigma_{h,max}$) and the density of PMA specimen

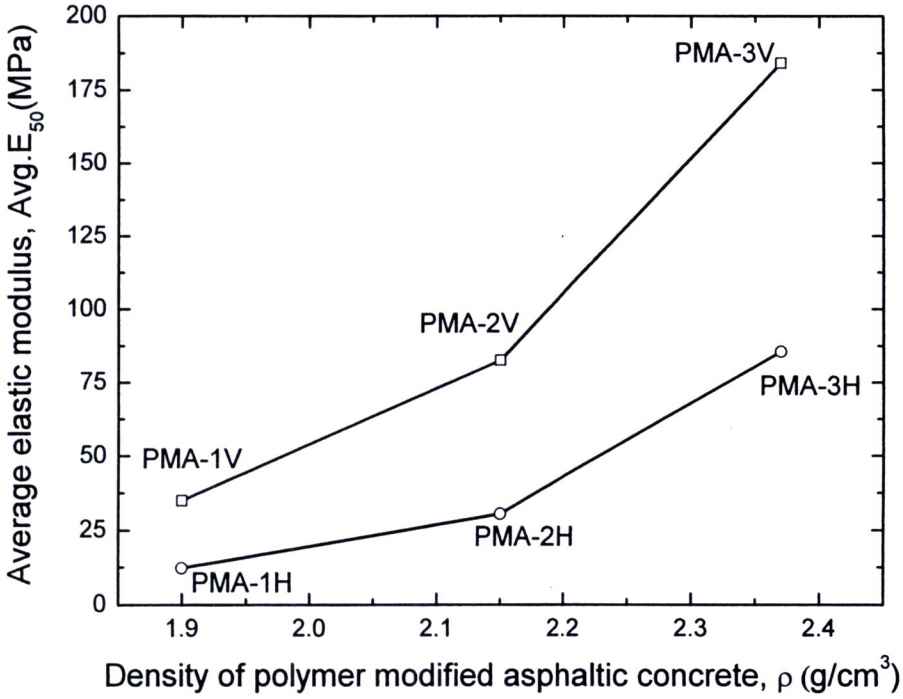

Figure 4.5 Relationships between the elastic modulus (E_{50}) and the density of PMA specimen

The peak values of vertical and horizontal stresses ($\sigma_{v,max}$ and $\sigma_{h,max}$) of PMA and HMA specimen having different directions of compaction at different densities are summarized in Table 4.2. In addition, Fig. 4.6 shows the comparison of the maximum stresses among PMA and HMA specimens prepared by vertical and horizontal compactions for different densities. Fig. 4.7 shows the comparison of the secant modulus (E_{50}) among PMA and HMA specimens prepared by vertical and horizontal compactions for different densities. The following trends of behavior may be seen from these figures:

1) PM-AC increased the compressive strength of PMA specimen for all densities and directions of compaction tested. PM-AC increased the compressive strength in the specimens with low density more than the ones with high density. That is, for the PMA specimens with low density (1.90 g/cm^3), the value of $\sigma_{v,max}$ is 2.93 times the value for HMA. However, at the higher density (2.37 g/cm^3), this ratio became only 1.26.
2) The value of the strength and the E_{50} of PMA were always higher than the ones of HMA when consider at the same direction of compaction. Interestedly, the ratio of the E_{50} value of PMA to HMA specimens was seemed to be constant for each direction of compaction, irrespective of different density. That is, the ratio was about 2.0 and 1.5 for vertical and horizontal directions, respectively. It showed that the development of the E_{50} by using PMA instead of HMA values in the vertical compaction was more than the horizontal compaction.

Table 4.2 Summary of the average of maximum stress and secant modulus (E_{50}) of PMA and HMA specimens having different directions of compaction and different densities

PMA				HMA		Ratio	
Density (g/cm3)	**Direction**	**Avg.$\sigma_{v,max}$ (kPa)**	**Avg. E_{50} (MPa)**	**Avg.$\sigma_{v,max}$ (kPa)**	**Avg. E_{50} (MPa)**	**Avg.$\sigma_{v,max}$ (kPa)**	**Avg. E_{50} (MPa)**
1.9	Horizontal	172.02	12.27	70.37	8.1	2.44	1.51
	Vertical	273.84	35.02	93.43	16.35	2.93	2.14
2.15	Horizontal	295.4	30.46	168.34	17.64	1.75	1.72
	Vertical	509.64	82.61	264.55	37.12	1.92	2.22
2.37	Horizontal	736.56	85.52	425.64	65.62	1.73	1.3
	Vertical	893.83	184.13	706.66	84.47	1.26	2.18

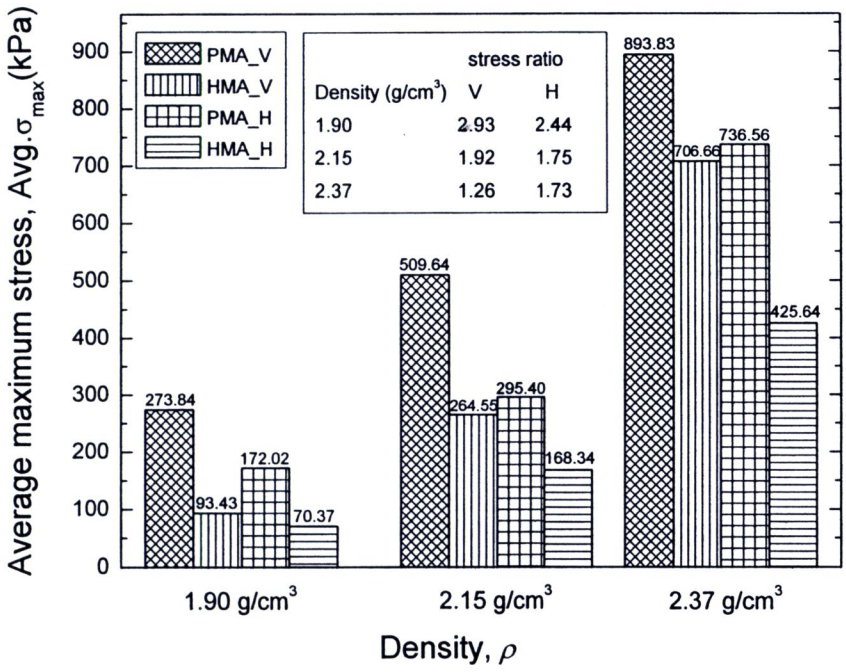

Figure 4.6 Comparison of the maximum stresses among PMA and HMA specimens prepared by vertical and horizontal compactions for different densities

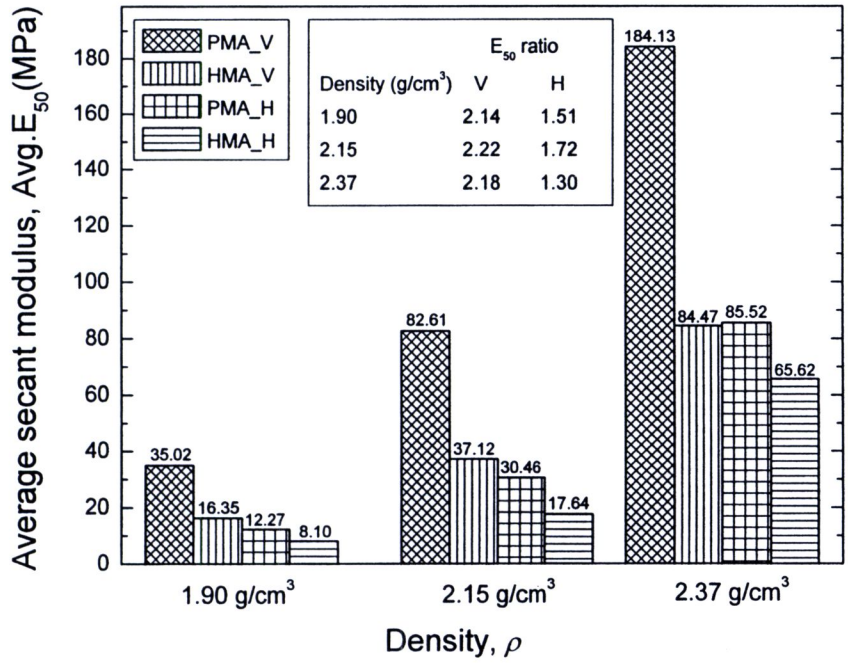

Figure 4.7 Comparison of the secant modulus (E_{50}) among PMA and HMA specimens prepared by vertical and horizontal compactions for different densities

4.3 Minute cyclic loading

4.3.1 Stress-strain relations

Test results employing minute-amplitude cyclic loading histories (as explained in Section 3.8) were presented and discussed in this section. Figs. 4.8(a) through 4.10(a) show the σ_v - ε_v relations from continuous ML tests intervened by 180 minutes sustained loading (SL) after which ten minute-amplitude unload/reload cycles were performed at constant stress rate $|\dot{\sigma}|$ of 3.556 kPa/min by using apparatus B on PMA specimens having different densities equal to 1.90 g/cm^3 (PMA-1V), 2.15 g/cm^3 (PMA-2V) and 2.37 g/cm^3 (PMA-3V) and had the voids in mineral aggregates (VMA) of 31.369 %, 22.339 %, and 14.392 % from tests VSC-01, VMC-01 and VLC-01, respectively. Figs. 4.11(a) through 4.13(a) show σ_h - ε_h relations for PMA-1H, PMA-2H and PMA-3H from tests HSC-01, HMC-01 and HLC-01, respectively. Figs. 4.14(a) through 4.16(a) show $\varepsilon_h - \varepsilon_v$ relations for PMA-1V, PMA-2V and PMA-3V from tests VSC-01, VMC-01 and VLC-01, respectively. Figs. 4.17(a) through 4.19(a) show $\varepsilon_v - \varepsilon_h$ relations for PMA-1H, PMA-2H and PMA-3H from tests VSC-01, VMC-01 and VLC-01, respectively. Moreover, in the series (b) of Figs 4.8 through 4.19 show the zoomed-up portions of respective figures in (a) series. The following trends of behavior may be seen from these figures:

1) Creep strains during SL before minute-amplitude cyclic loading are noticeably significant. That is, residual strains caused by subsequent minute-amplitude cyclic loading become much smaller. Therefore, the behaviors during this minute-amplitude cyclic loading were essentially elastic. The results from this study were obtained from the elastic behavior only.
2) Lateral expansion always occurred during the axial compression. In particular for Figs. Series (b), the additional compressions by sustained loading (from 'a' to 'b') and by minute cycles (from 'b' to 'c') are associated with lateral expansion of specimen. However, the flow characteristic was not significantly affected by intermissions of sustained and cyclic loadings.

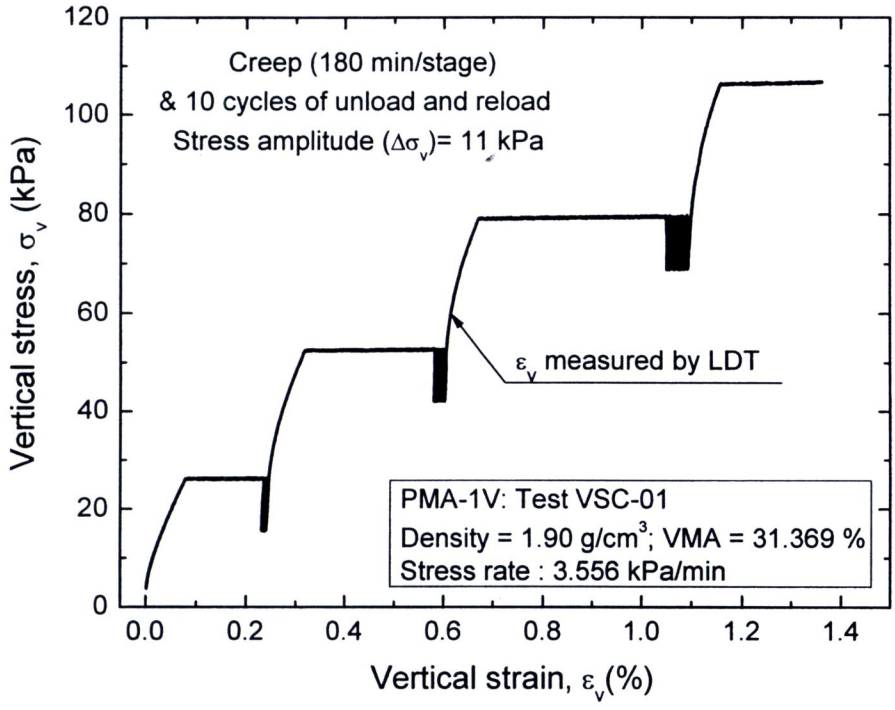

Figure 4.8(a) Relationship between vertical stress and vertical strain obtained from minute-amplitude cyclic loading test on PMA-1V from test VSC-01, density = 1.90 g/cm^3 and VMA = 31.369 %

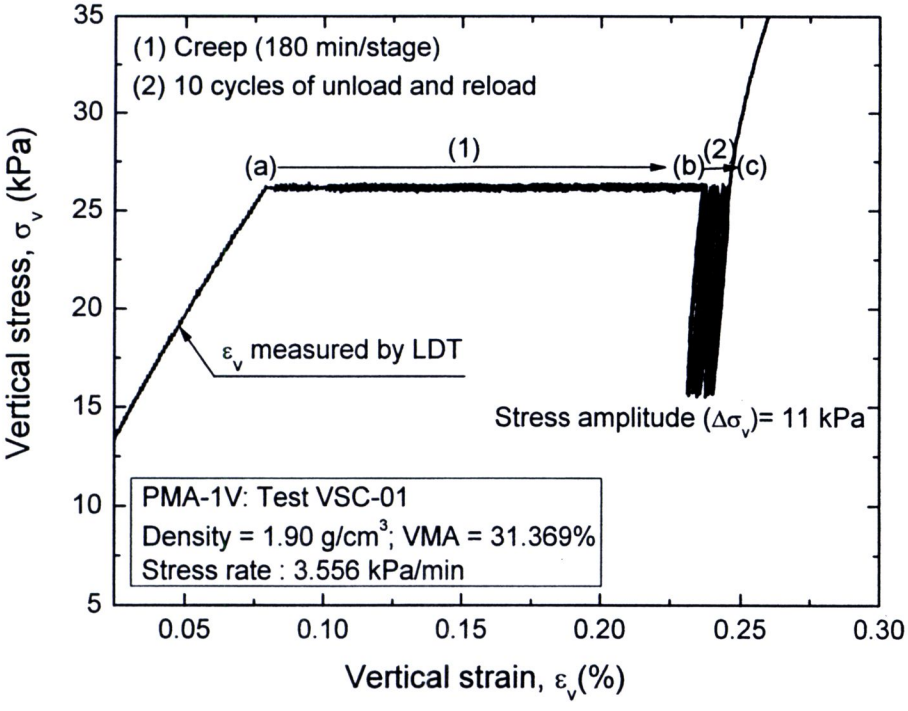

Figure 4.8(b) Close-up of σ_v - ε_v relations obtained from minute-amplitude cyclic loading test on PMA-1V from test VSC-01, density = 1.90 g/cm^3 and VMA = 31.369 %

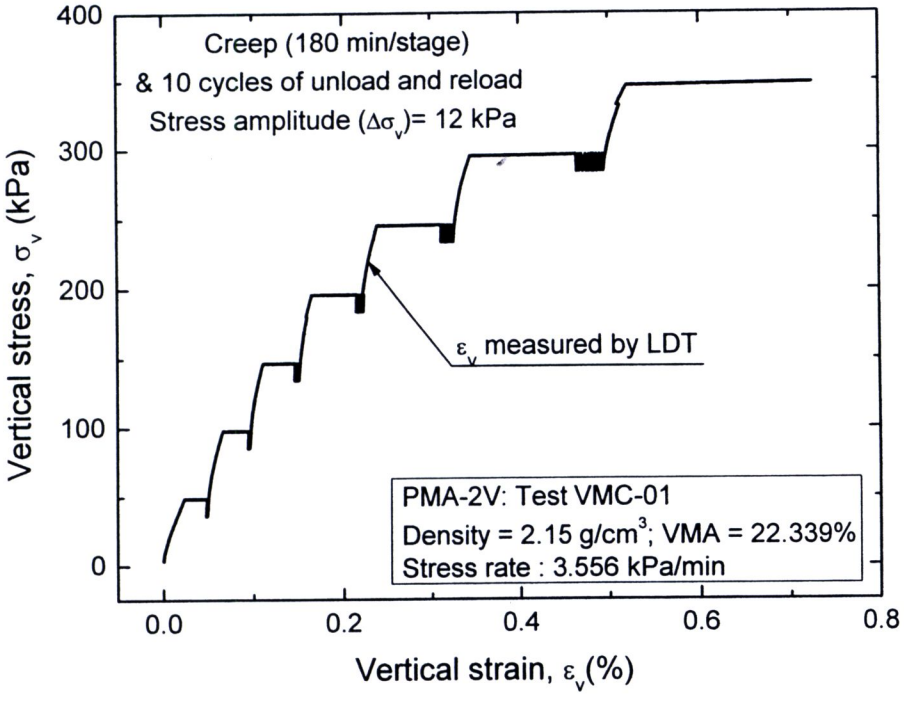

Figure 4.9(a) Relationship between vertical stress and vertical strain obtained from minute-amplitude cyclic loading test on PMA-2V from test VMC-01, density = 2.15 g/cm^3 and VMA = 22.339 %

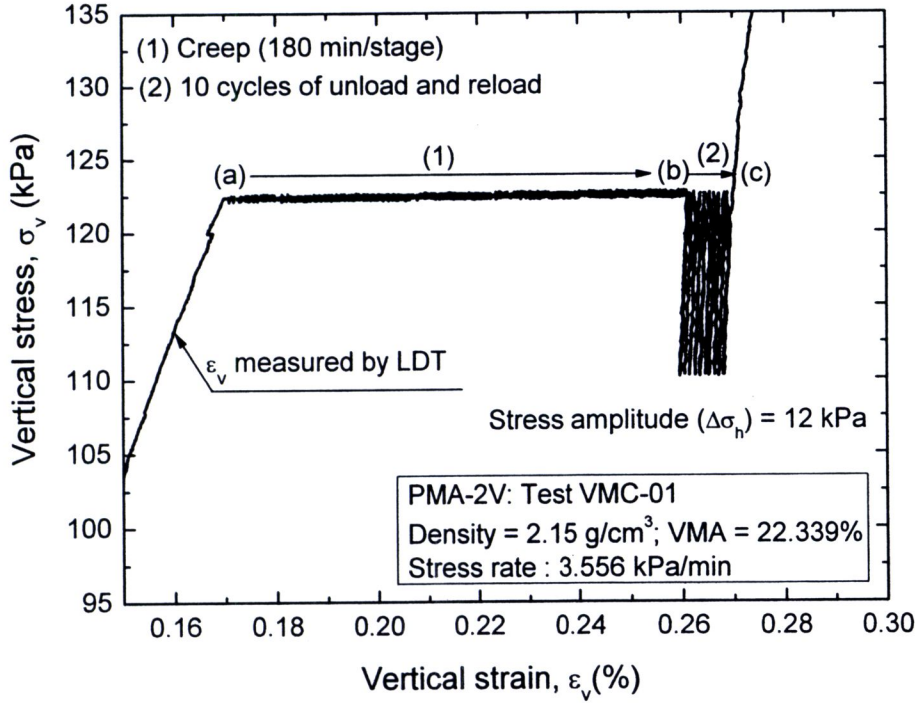

Figure 4.9(b) Close-up of σ_v - ε_v relations obtained from minute-amplitude cyclic loading test on PMA-2V from test VMC-01, density = 2.15 g/cm^3 and VMA = 22.339 %

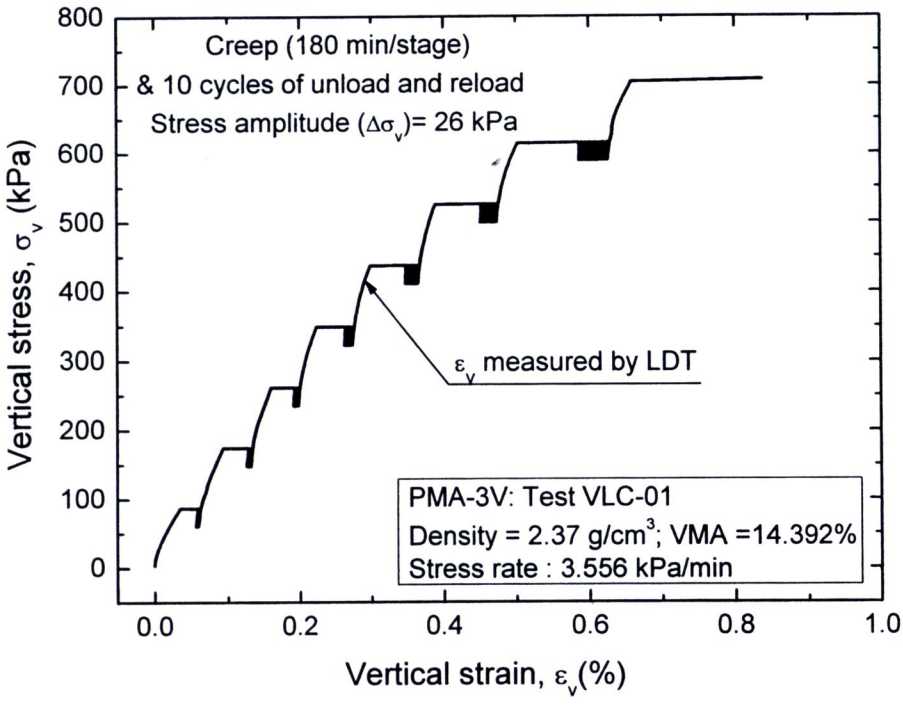

Figure 4.10(a) Relationship between vertical stress and vertical strain obtained from minute-amplitude cyclic loading test on PMA-3V from test VLC-01, density = 2.37 g/cm^3 and VMA = 14.392 %

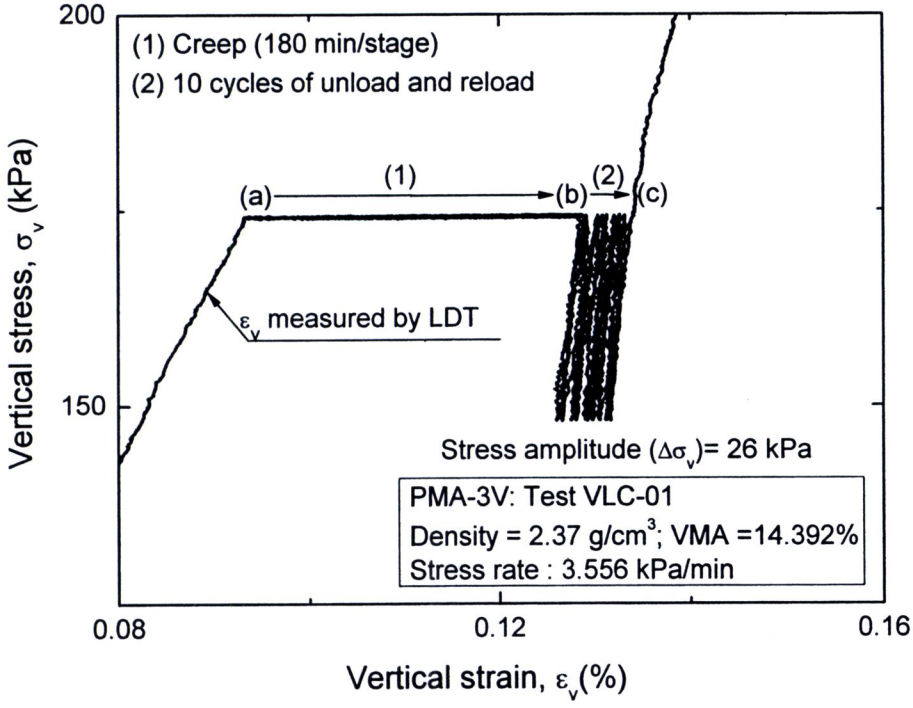

Figure 4.10(b) Close-up of σ_v - ε_v relations obtained from minute-amplitude cyclic loading test on PMA-3V from test VLC-01, density = 2.37 g/cm^3 and VMA = 14.392 %

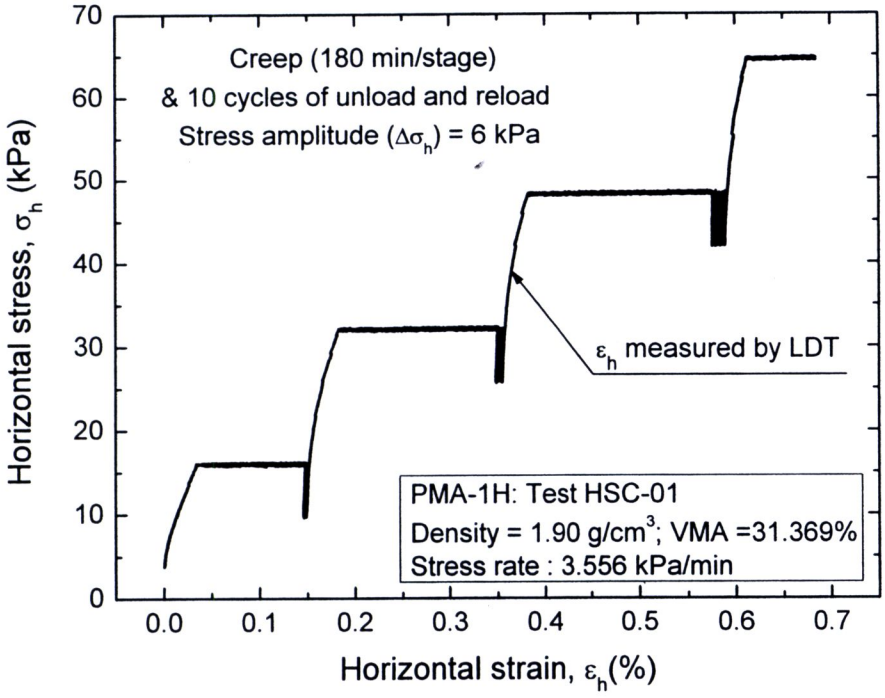

Figure 4.11(a) Relationship between horizontal stress and horizontal strain obtained from minute-amplitude cyclic loading test on PMA-1H from test HSC-01, density = 1.90 g/cm^3 and VMA = 31.369 %

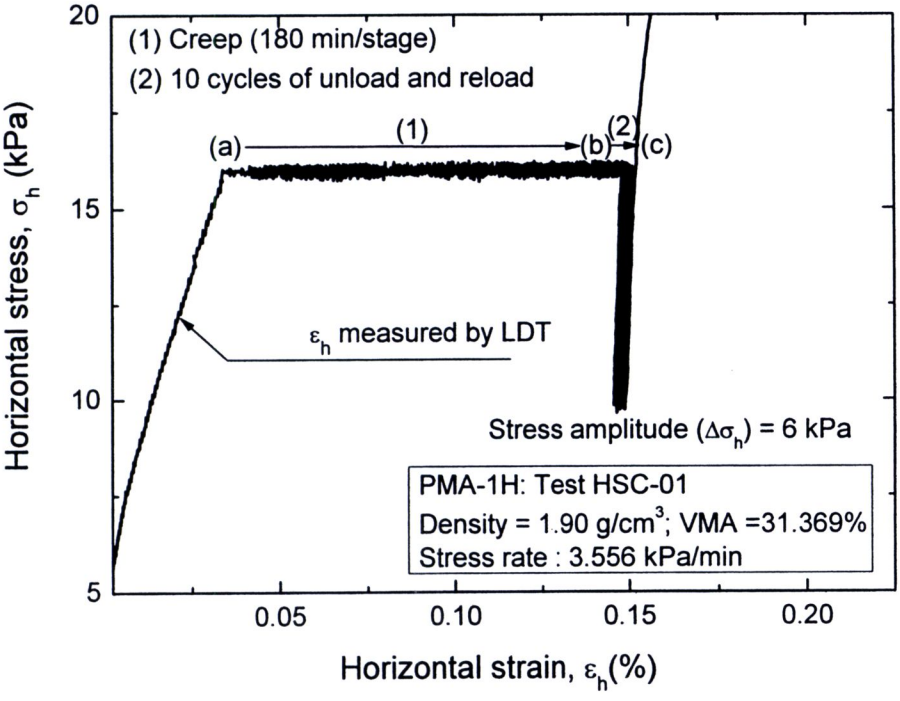

Figure 4.11(b) Close-up of σ_h - ε_h relations obtained from minute-amplitude cyclic loading test on PMA-1H from test HSC-01, density = 1.90 g/cm^3 and VMA = 31.369 %

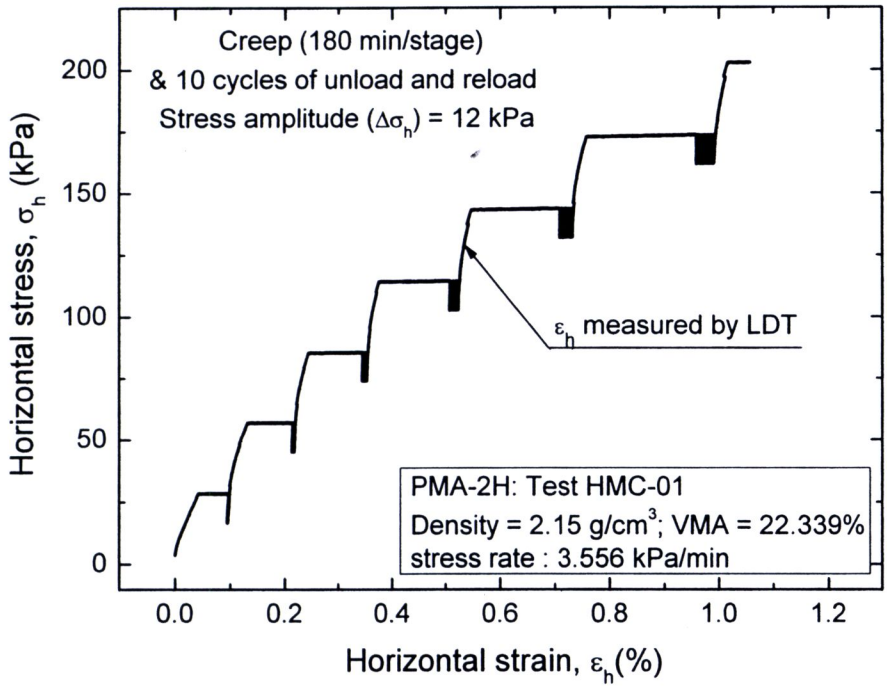

Figure 4.12(a) Relationship between horizontal stress and horizontal strain obtained from minute-amplitude cyclic loading test on PMA-2H from test HMC-01, density = 2.15 g/cm^3 and VMA = 22.339 %

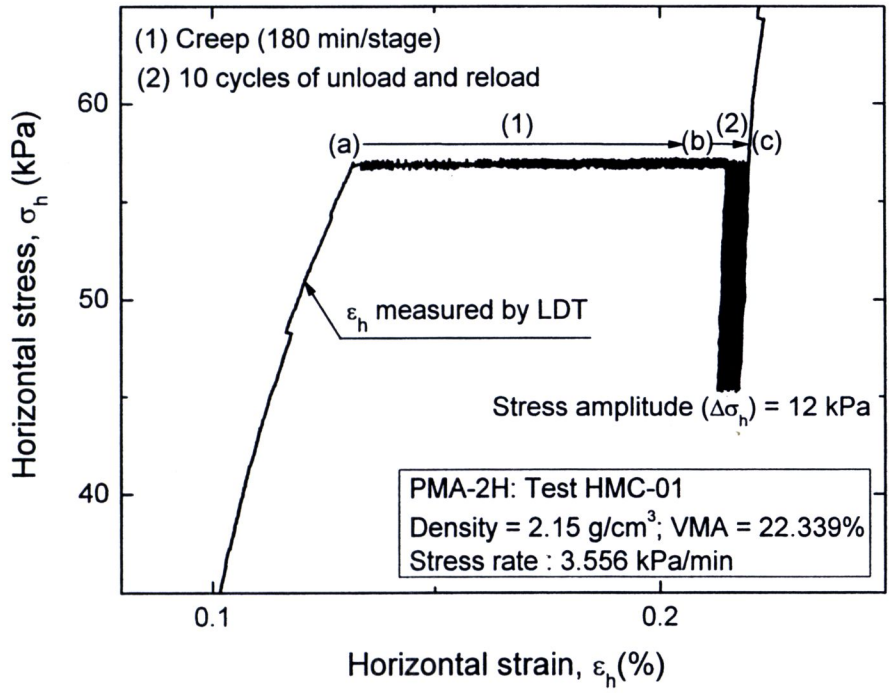

Figure 4.12(b) Close-up of σ_h - ε_h relations obtained from minute-amplitude cyclic loading test on PMA-2H from test HMC-01, density = 2.15 g/cm^3 and VMA = 22.339 %

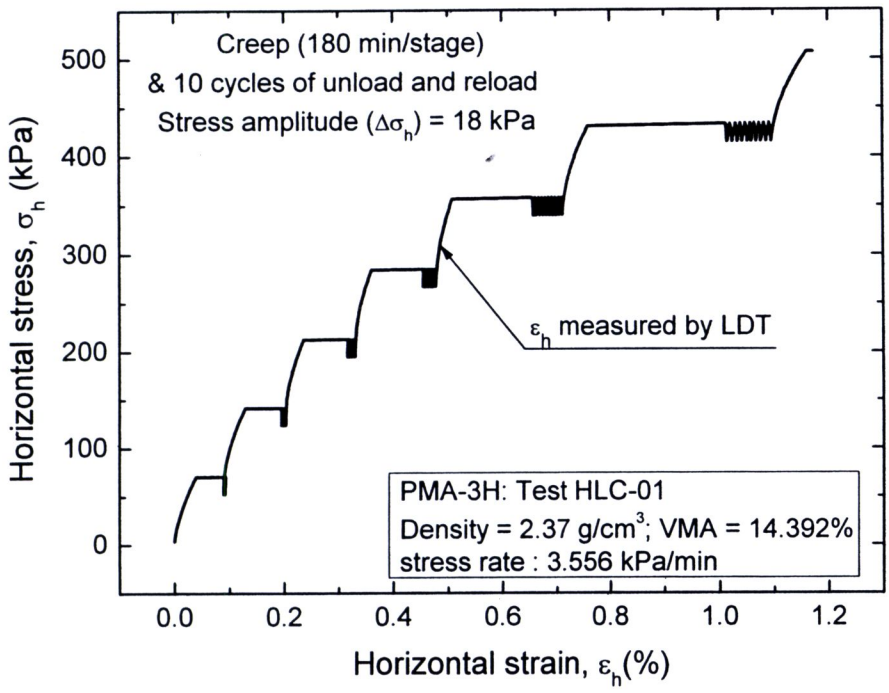

Figure 4.13(a) Relationship between horizontal stress and horizontal strain obtained from minute-amplitude cyclic loading test on PMA-3H from test HLC-01, density = 2.37 g/cm^3 and VMA = 14.392 %

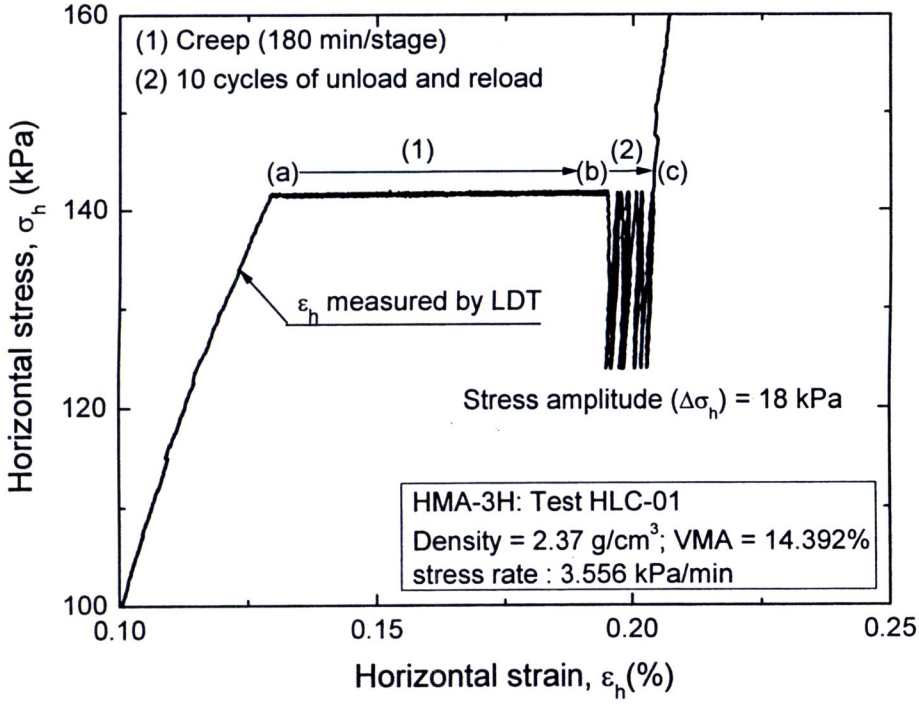

Figure 4.13(b) Close-up of σ_h - ε_h relations obtained from minute-amplitude cyclic loading test on PMA-3H from test HMC-01, density = 2.37 g/cm^3 and VMA = 14.392 %

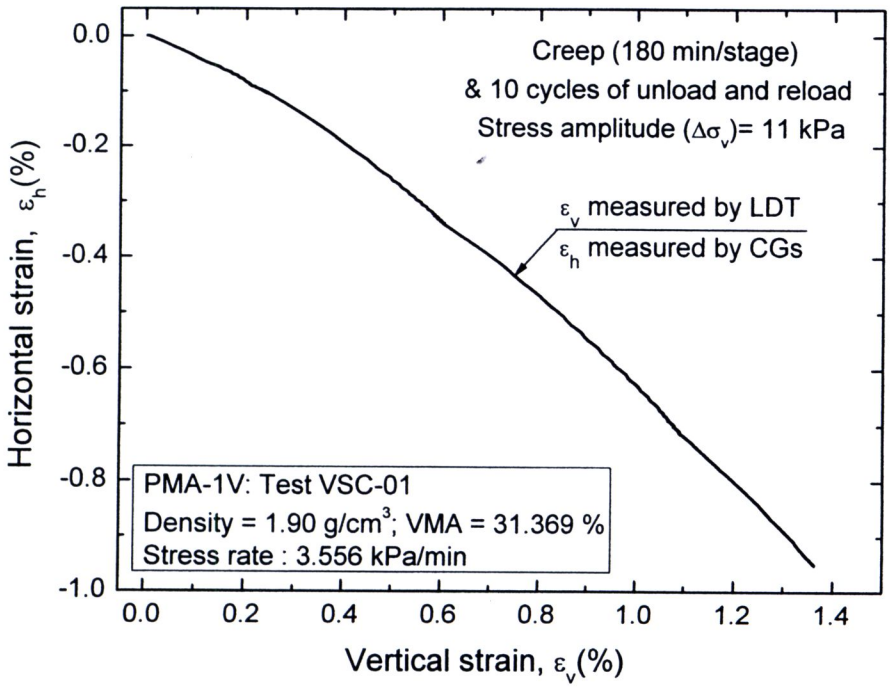

Figure 4.14(a) Relationship between horizontal strain and vertical strain obtained from minute-amplitude cyclic loading test on PMA-1V from test VSC-01, density = 1.90 g/cm^3 and VMA = 31.369 %

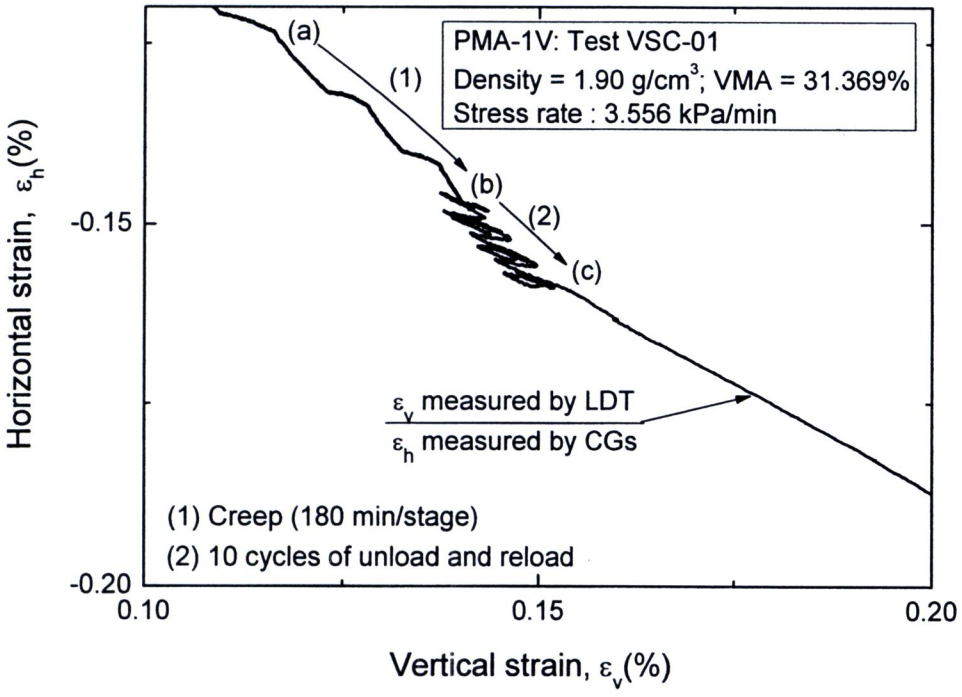

Figure 4.14(b) Close-up of ε_h - ε_v relations obtained from minute-amplitude cyclic loading test on PMA-1V from test VSC-01, density = 1.90 g/cm^3 and VMA = 31.369 %

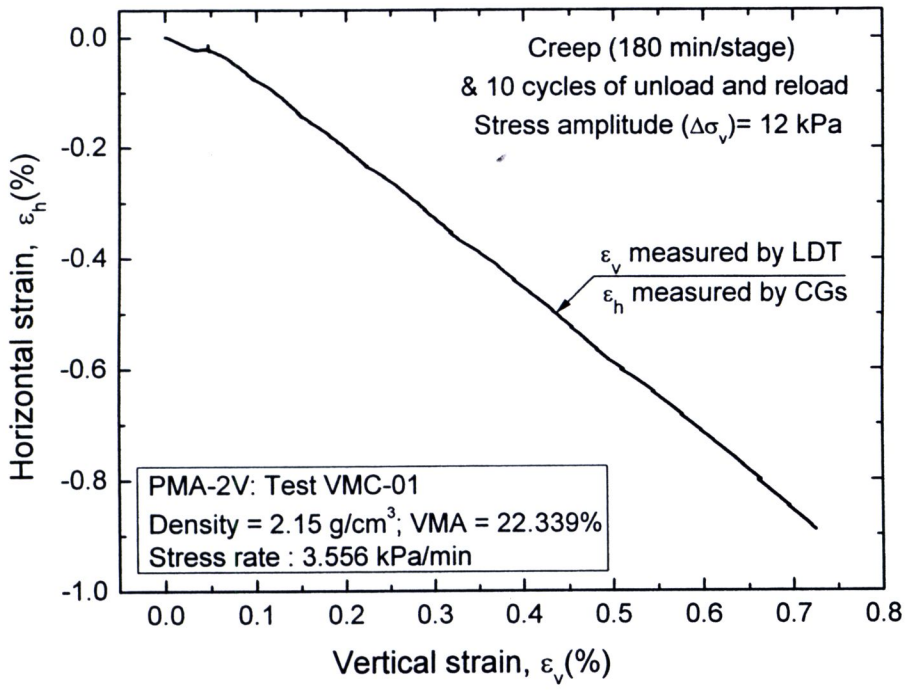

Figure 4.15(a) Relationship between horizontal strain and vertical strain obtained from minute-amplitude cyclic loading test on PMA-2V from test VMC-01, density = 2.15 g/cm^3 and VMA = 22.339 %

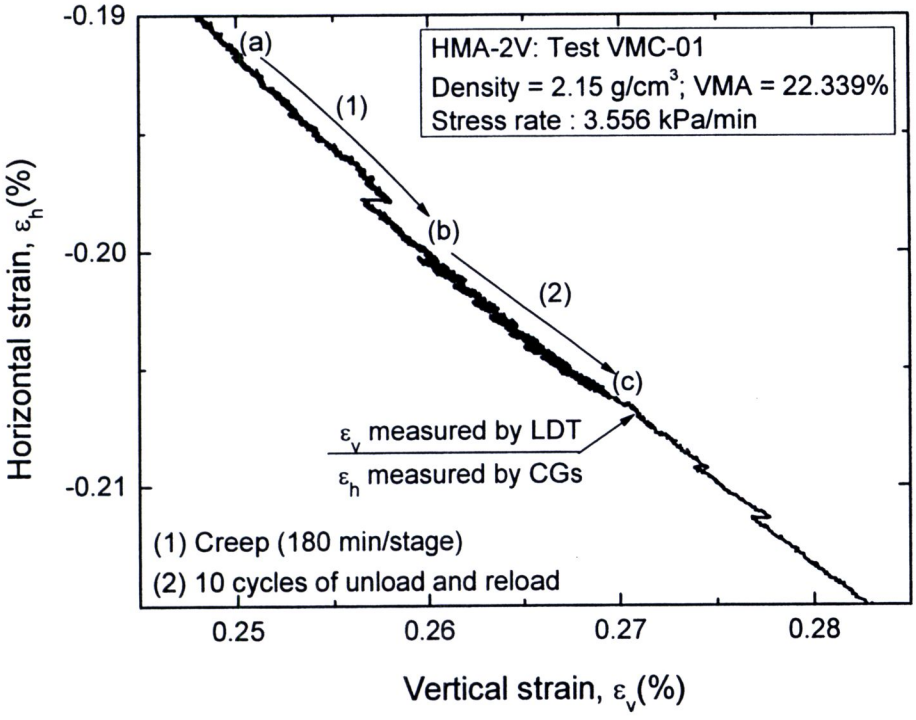

Figure 4.15(b) Close-up of ε_h - ε_v relations obtained from minute-amplitude cyclic loading test on PMA-2V from test VMC-01, density = 2.15 g/cm^3 and VMA = 22.339 %

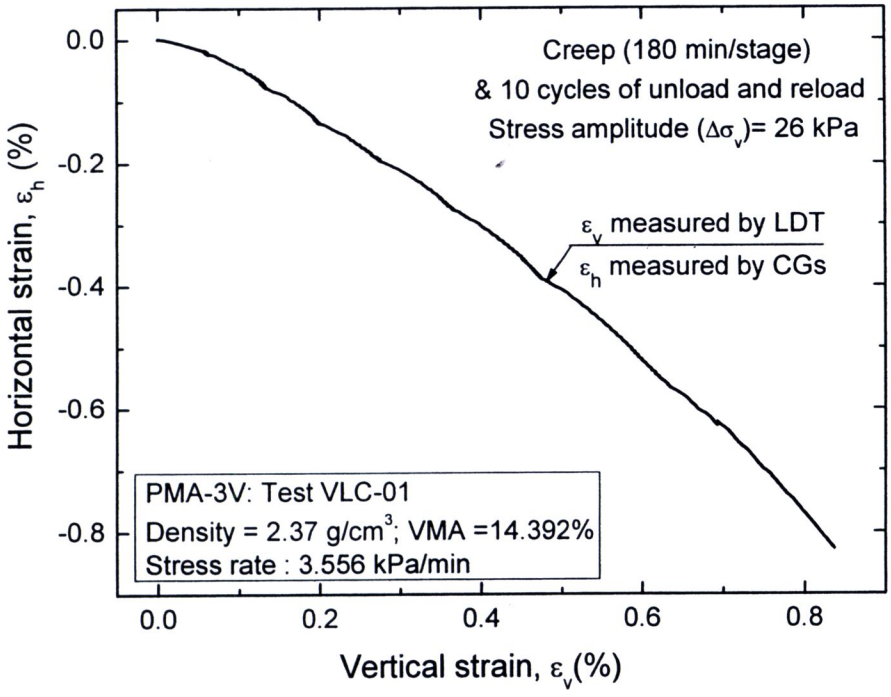

Figure 4.16(a) Relationship between horizontal strain and vertical strain obtained from minute-amplitude cyclic loading test on PMA-3V from test VLC-03, density = 2.37 g/cm^3 and VMA = 14.392 %

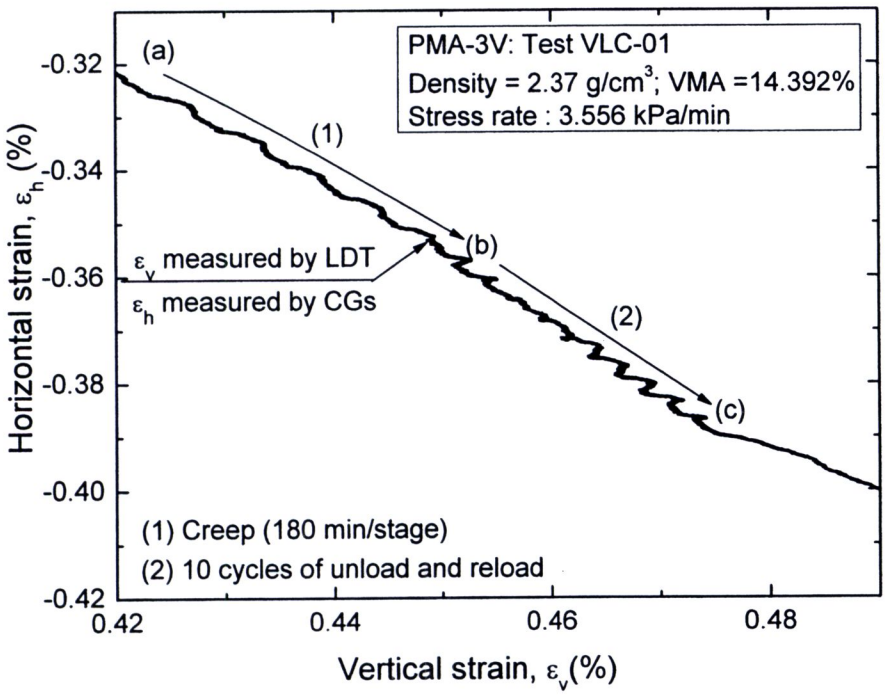

Figure 4.16(b) Close-up of ε_h - ε_v relations obtained from minute-amplitude cyclic loading test on HMA-3V from test VLC-03, density = 2.37 g/cm^3 and VMA = 14.392 %

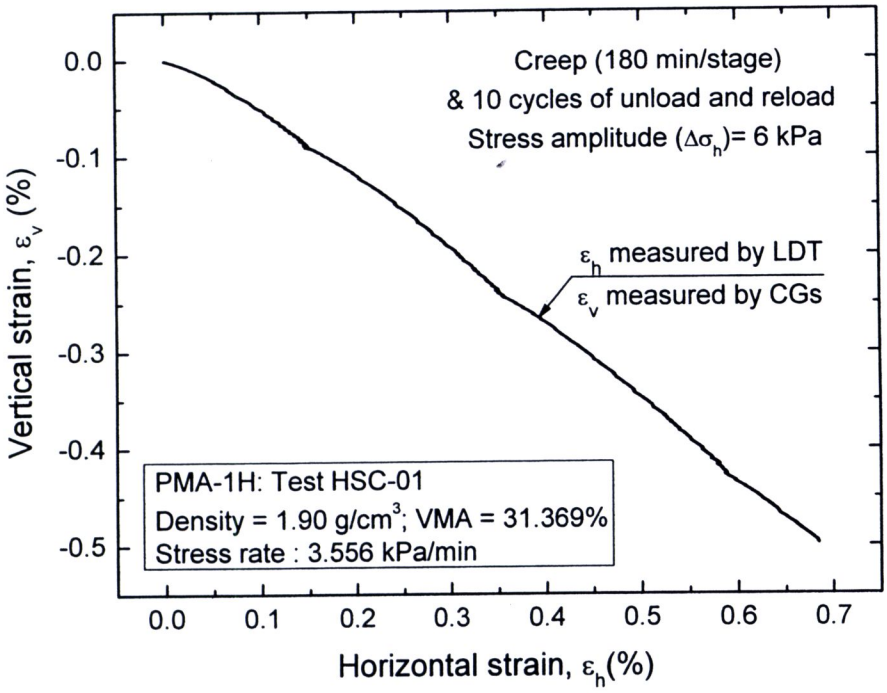

Figure 4.17(a) Relationship between vertical strain and horizontal strain obtained from minute-amplitude cyclic loading test on PMA-1H from test HSC-01, density = 1.90 g/cm^3 and VMA = 31.369 %

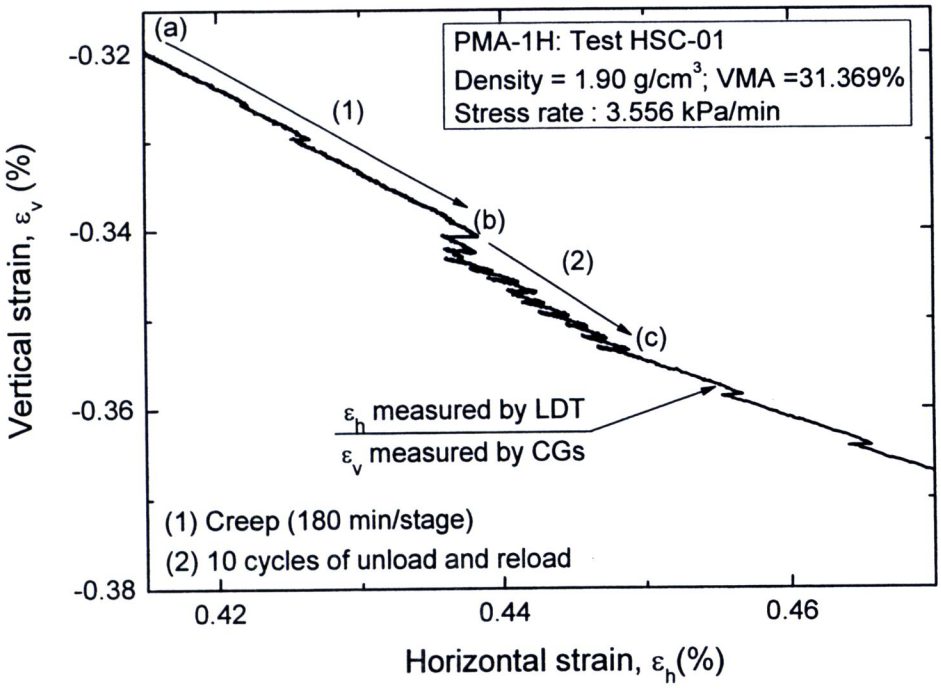

Figure 4.17(b) Close-up of ε_v - ε_h relations obtained from minute-amplitude cyclic loading test on PMA-1H from test HSC-01, density = 1.90 g/cm^3 and VMA = 31.369 %

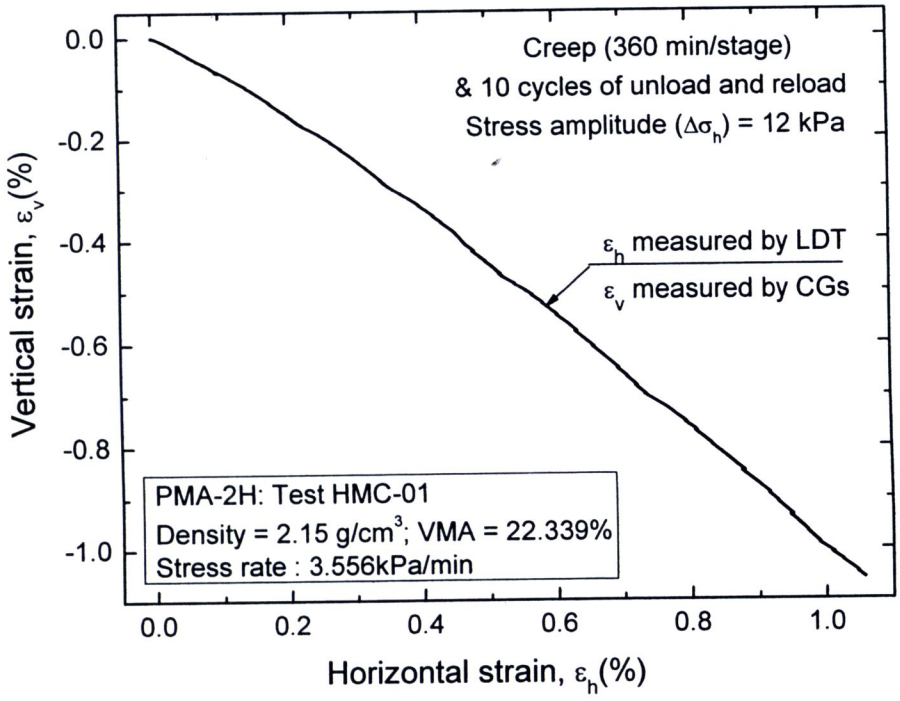

Figure 4.18(a) Relationship between vertical strain and horizontal strain obtained from minute-amplitude cyclic loading test on PMA-2H from test HMC-01, density = 2.15 g/cm^3 and VMA = 22.339 %

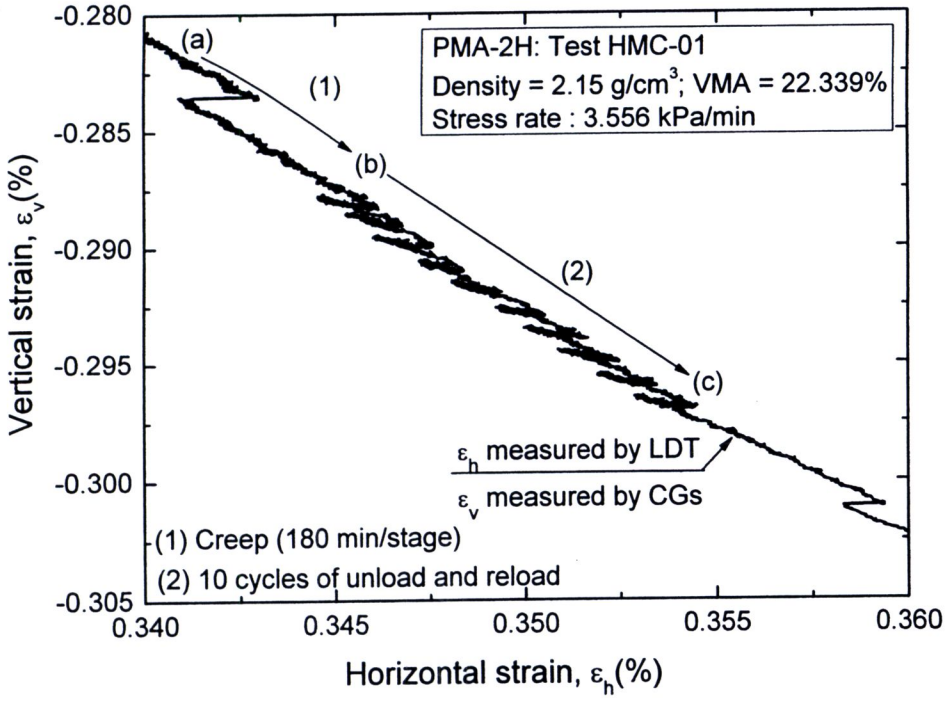

Figure 4.18(b) Close-up of ε_v - ε_h relations obtained from minute-amplitude cyclic loading test on PMA-2H from test HMC-01, density = 2.15 g/cm^3 and VMA = 22.339 %

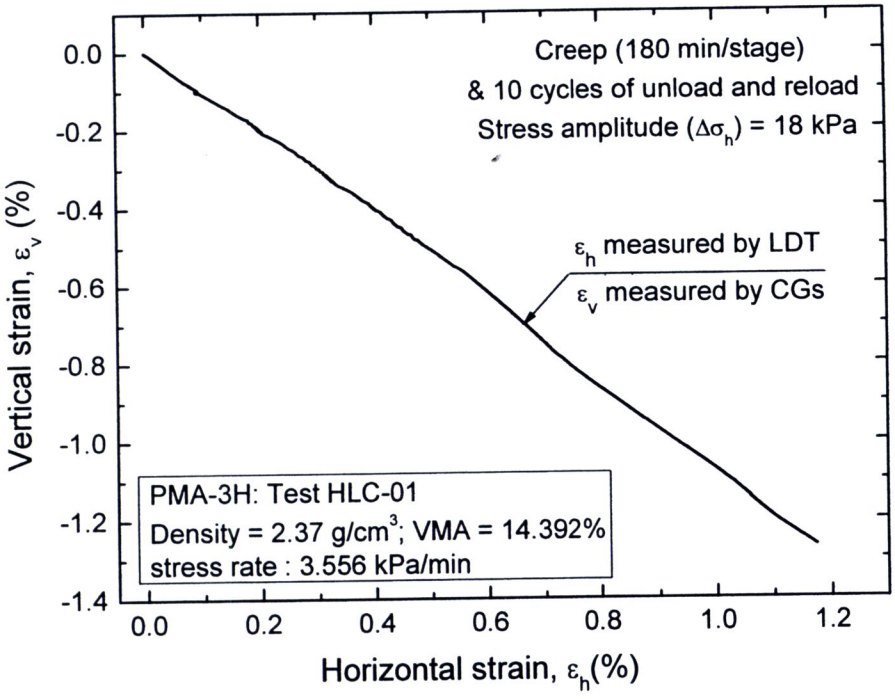

Figure 4.19(a) Relationship between vertical strain and horizontal strain obtained from minute-amplitude cyclic loading test on PMA-3H from test HLC-01, density = 2.37g/cm^3 and VMA = 14.392 %

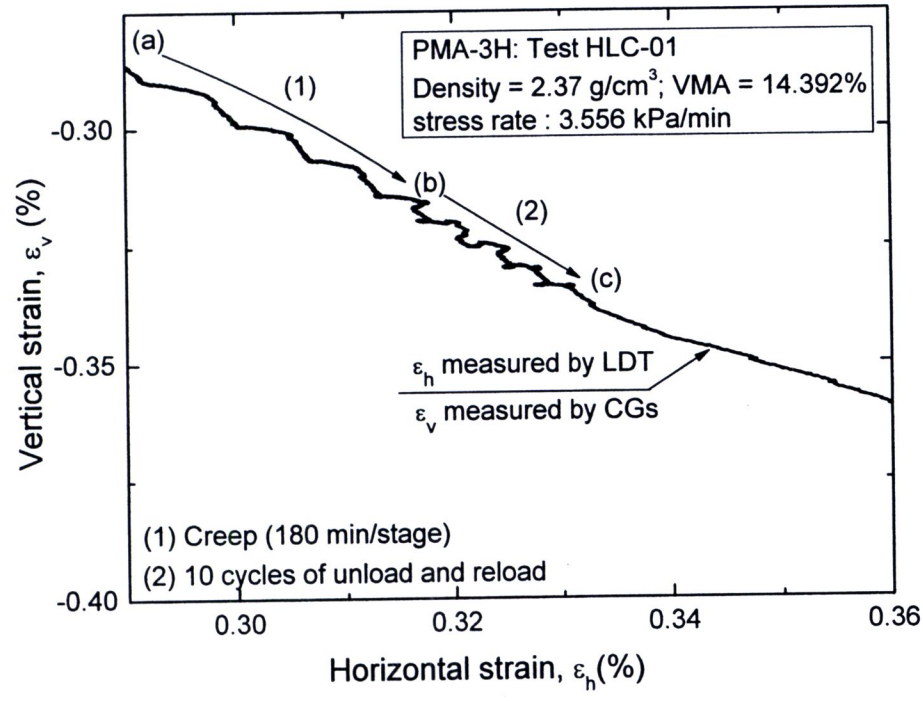

Figure 4.19(b) Close-up of ε_v- ε_h relations obtained from minute-amplitude cyclic loading test on PMA-3H from test HLC-01, density = 2.37 g/cm^3 and VMA = 14.392 %

4.3.2 Equivalent modulus and Poisson's ratio

The equivalent modulus is the Young's modulus that is the result with equivalent elastic behavior. For the equivalent elastic modulus, $E_{v,eq}$ and $E_{h,eq}$ are defined as the slope of the apparently linear portion from unload cycle on respective σ_v - ε_v and σ_h - ε_h curves as shown in Figs 4.20(a) and 4.20(b). For Poisson's ratio, ν_{vh} and ν_{hv} are defined as the slope of the apparently linear portion from unload cycle on respective ε_h - ε_v and ε_v - ε_h curves as shown in Figs. 4.21(a) and 4.21(b). For the test results that showed a limited linear range of ε_h - ε_v and ε_v - ε_h relation during unloading of minute-amplitude cyclic loading, the following were performed:

1) Time histories of ε_v and ε_h were plotted. (Fig. 4.23)
2) Respective ε_v – time and ε_h – time relations during unloading of minute-amplitude cyclic loading that exhibited linear behavior were fitted to determine $d\varepsilon_v / dt$ and $d\varepsilon_h / dt$ values (Fig. 4.23).
3) Equivalent Poisson's ratios were then determined from the respective ratio of the $d\varepsilon_h / dt$ to the $d\varepsilon_v / dt$ (Fig. 4.23).

For vertical compaction specimen, the $E_{v,eq}$ - value and the $\nu_{vh,eq}$ - value were determined from σ_v - ε_v and ε_h - ε_v relations of which ε_h and ε_v values were obtained by CGs and LDTs, and the horizontal specimen, the $E_{h,eq}$ - value and the $\nu_{hv,eq}$ - value were evaluated from σ_h - ε_h and ε_v - ε_h relations of which ε_v and ε_h values were obtained by CGs and LDTs. These values were obtained by ten minute-amplitude unload/reload cycles performed after SL. The equivalent modulus values were obtained from the average of the ones obtained from the unloading branches of the sixth to the tenth loops (5 loops in total).

Figs. 4.25(a) through 4.25(c) and Figs. 4.27(a) through 4.27(c) respectively show the $E_{v,eq}$ - value and the $\nu_{hv,eq}$ - value plotted against σ_v value in full-log scale for vertically compacted PMA specimens at different densities equal to 1.90 g/cm^3 (PMA-1V), 2.15 g/cm^3 (PMA-2V) and 2.37 g/cm^3 (PMA-3V). Figs 4.26(a) through 4.26(c) and Figs. 4.28(a) through 4.28(c) respectively show the $E_{h,eq}$ - value and the $\nu_{hv,eq}$ - value plotted against σ_h value in full-log scale for horizontally compacted PMA specimens at different densities equal to 1.90 g/cm^3 (PMA-1H), 2.15 g/cm^3 (PMA-2H) and 2.37 g/cm^3 (PMA-3H). Three densities of vertical and horizontal PMA specimen, 1.90 g/cm^3, 2.15 g/cm^3 and 2.37 g/cm^3 have the voids in mineral aggregates (VMA) of 31.369 %, 22.339 %, and 14.392 %, respectively. Figs. 4.29(a) and 4.30(a) show the comparisons of $E_{v,eq}$ - values and $\nu_{hv,eq}$ - values for different densities of vertically compacted PMA specimens and Figs. 4.29(b) and 4.30(b) show the comparisons of $E_{h,eq}$ - values and $\nu_{vh,eq}$ - values for different densities of horizontally compacted PMA specimens.

To eliminate the effect of the different densities and void ratio of PMA specimens, the equivalent elastic modulus $E_{v,eq}$ and $E_{h,eq}$ have been normalized by a void ratio function $f(e) = (2.17 - e)^2 / (1 + e)$ (Hardin and Richart, 1963). Fig 4.31(a) and 4.31(b) show the relation between the equivalent elastic modulus normalized by a void ratio function and the reference stress. However, the value of void ratio (e) used in the void ratio function is obtained from the specimens before the start of shearing (e_0), which may not be truly realistic. Because during the test the volume of specimens changed, the void ratio (e) in the specimens was also changed. Figs. 4.32(a) and 4.32(b) show the relation between the equivalent elastic modulus normalized by a void ratio function in which the void ratios were the ones at the current stress state ($e_{current}$). It is to be noted that the values of

void ratio were determined as the ratio of void volume to aggregate volume, ignoring the presence of binder. Details are available in Appendix B.

Fig 4.33(a) and 4.33(b) show the relation between the equivalent Poisson's ratio and the stress level. The following trends of behavior may be seen from these figures:

1) The equivalent elastic modulus $E_{v,eq}$ and $E_{h,eq}$ increase significantly with an increase in the respective vertical and horizontal stresses. When the stress value approaches zero, $E_{v,eq}$ bounds for E_{v0} and $E_{h,eq}$ bounds for E_{h0} . On the other hand, the equivalent Poisson's ratio $\nu_{vh,eq}$ and $\nu_{hv,eq}$ decreases with an increase in the respective vertical and horizontal stresses. When the stress value approaches zero, $\nu_{vh,eq}$ bounds for ν_{vh0} and $\nu_{hv,eq}$ bounds for ν_{hv0} .
2) Observation 1) implies that, at small strain level near the origin, the σ-ε behaviors are significantly elastic for all specimens prepared at different densities.
3) The equivalent elastic modulus of the vertically compacted PMA specimen ($E_{v,eq}$) was higher than the equivalent elastic modulus of horizontally compacted PMA specimen ($E_{h,eq}$). Also, the equivalent Poisson's ratio of the vertically compacted specimens ($\nu_{vh,eq}$) was higher than the equivalent Poisson's ratio of the horizontally compacted specimens ($\nu_{hv,eq}$) when compared at the same density.
4) Considering the equivalent elastic modulus normalized by the void ratio function $E_{v,eq} / f(e)$ and $E_{h,eq} / f(e)$: Where $f(e) = (2.17 - e)^2 / (1 + e)$ (Hardin and Richart, 1963) with different void ratio values e_0 and $e_{current}$, they were plotted against level stress in full-log scale as shown in Fig. 4.30. Then, lines were best fitted to the data with the same slope for each respective direction of compaction. It was found that: $m_{v(e_0)} = 0.445$, $m_{v(e_{current})} = 0.445$, $m_{h,e_0} = 0.431$ and $m_{h(e_{current})} = 0.432$. It could seen that, *m*-values with e_0 and $e_{current}$ were equal for the same direction of compaction. However, the product of equation of void ratio function with the e_0 and $e_{current}$ are different. However, it is only 3.67 % for the vertically compacted PMA specimen and 2.28 % of the horizontally compacted PMA specimen.
5) Observation 4) implies that, the difference by using different void ratio, e_0 and $e_{current}$ results in insignificant difference in the equivalent elastic modulus. Therefore, in this study, the value of e_0 was used in the void ratio function because the value of e_0 was determined easier than $e_{current}$. In addition, the use of e_0-value can be compared with results from other research in which the e_0-value was also in the void ratio function.
6) The void ratio function $f(e) = (2.17 - e)^2 / (1 + e)$ (Hardin and Richart, 1963) was successfully used to normalize the elastic modulus. It could be seen that, test results after normalization appeared to be systematic.
7) It could be seen that, the behavior of equivalent modulus in that it depends on the stress level for different $E_{v,eq}$ and $E_{h,eq}$ is significantly similar. Therefore, the elastic behavior of PMA may consider to be significantly depending on the friction between the aggregate particles. On the other hand, the $\nu_{vh,eq}$ -values and $\nu_{hv,eq}$ -values for the different densities can be written in the relationship with σ / σ_{max} for each direction.

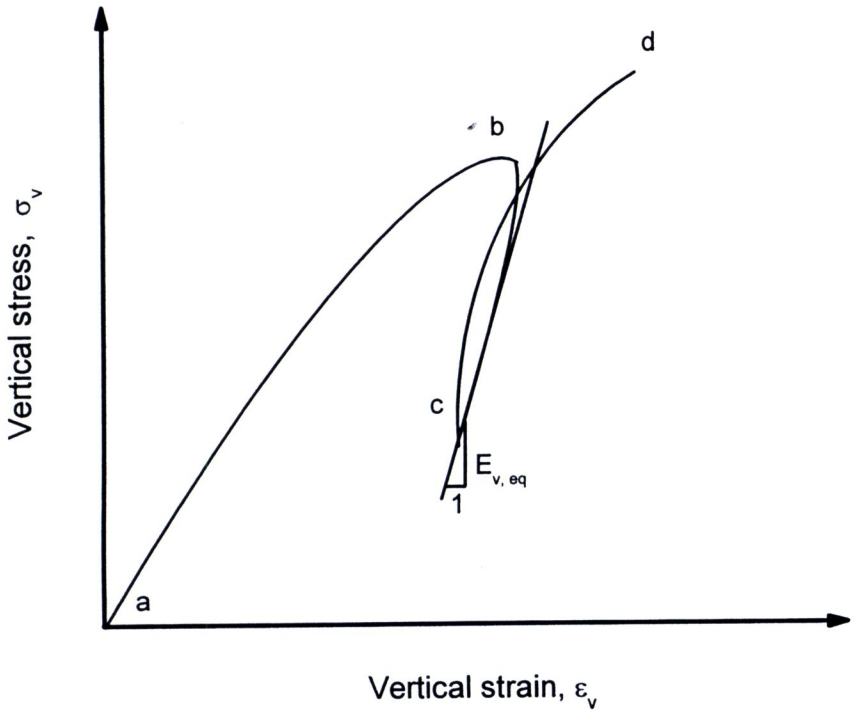

Figure 4.20(a) Definition of equivalent elastic modulus for vertically compacted specimen

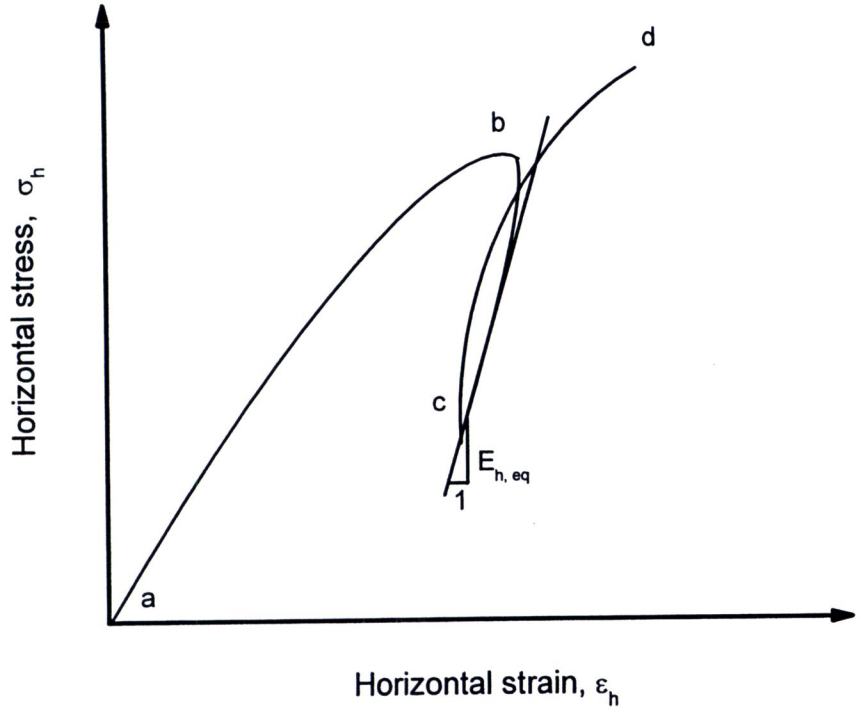

Figure 4.20(b) Definition of equivalent elastic modulus for horizontally compacted specimen

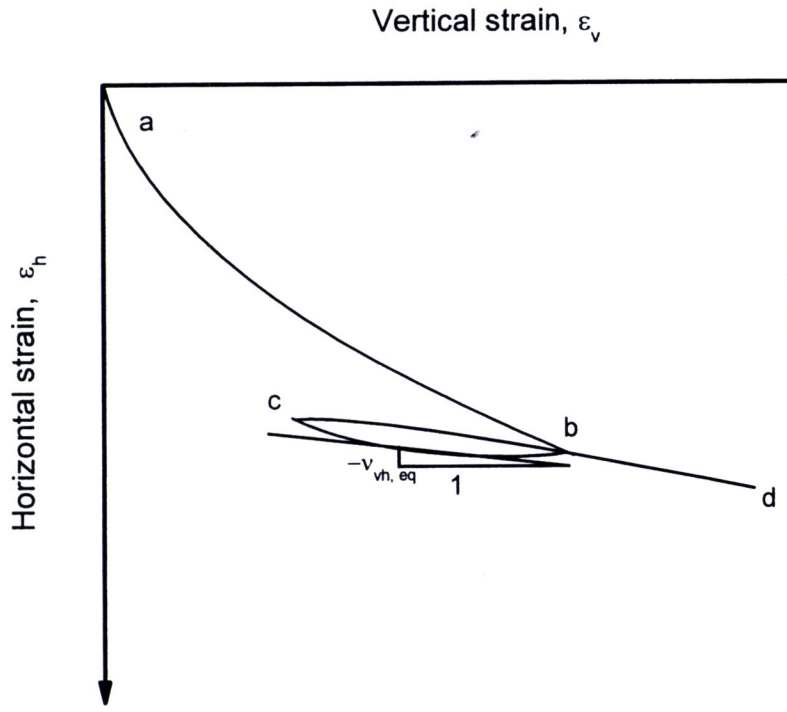

THE NATIONAL RESEARCH COUNCIL OF THAILAND
RESEARCH LIBRARY

Figure 4.21(a) Definition of equivalent Poisson's ratio for vertically compacted specimen

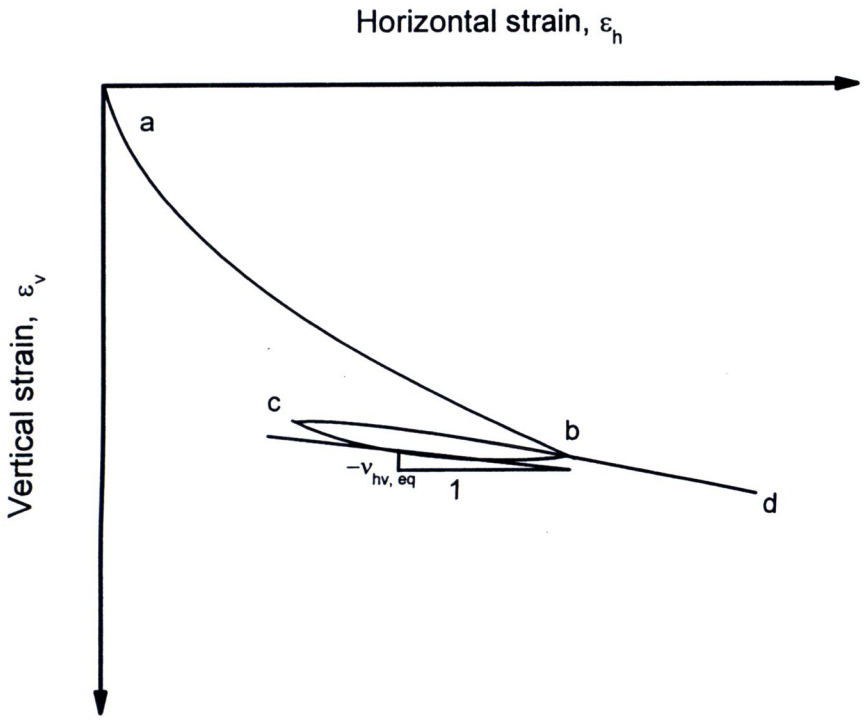

Figure 4.21(b) Definition of equivalent Poisson's ratio for horizontally compacted specimen

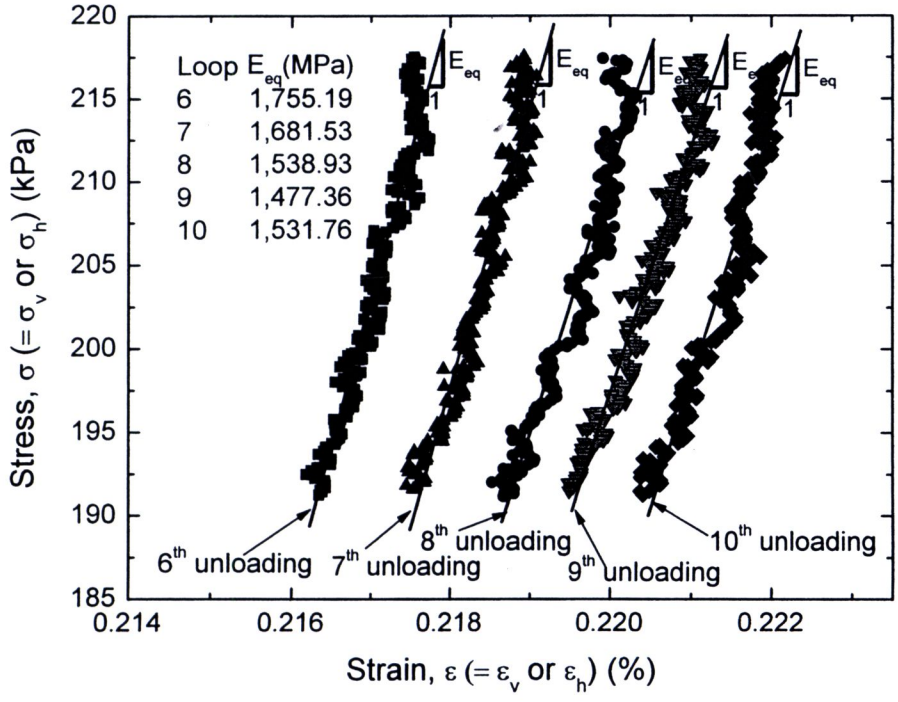

Figure 4.22(a) For example, to evaluations of equivalent elastic modulus at unloading from the sixth to the tenth loops at σ equal to 217 kPa

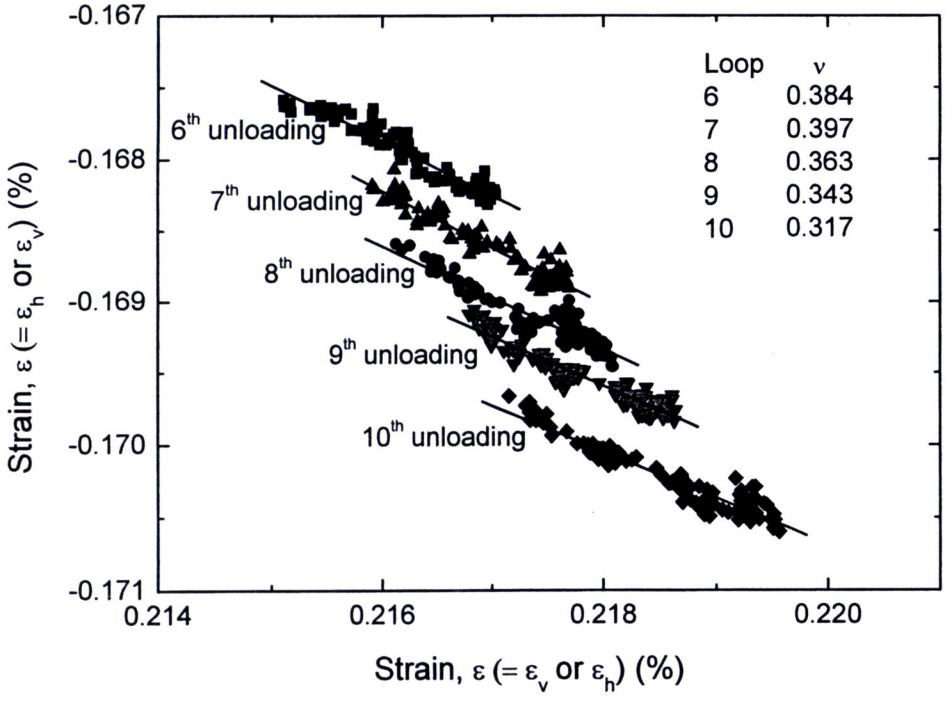

Figure 4.22(b) For example, to evaluations of equivalent Poisson's ration at unloading from the sixth to the tenth loops

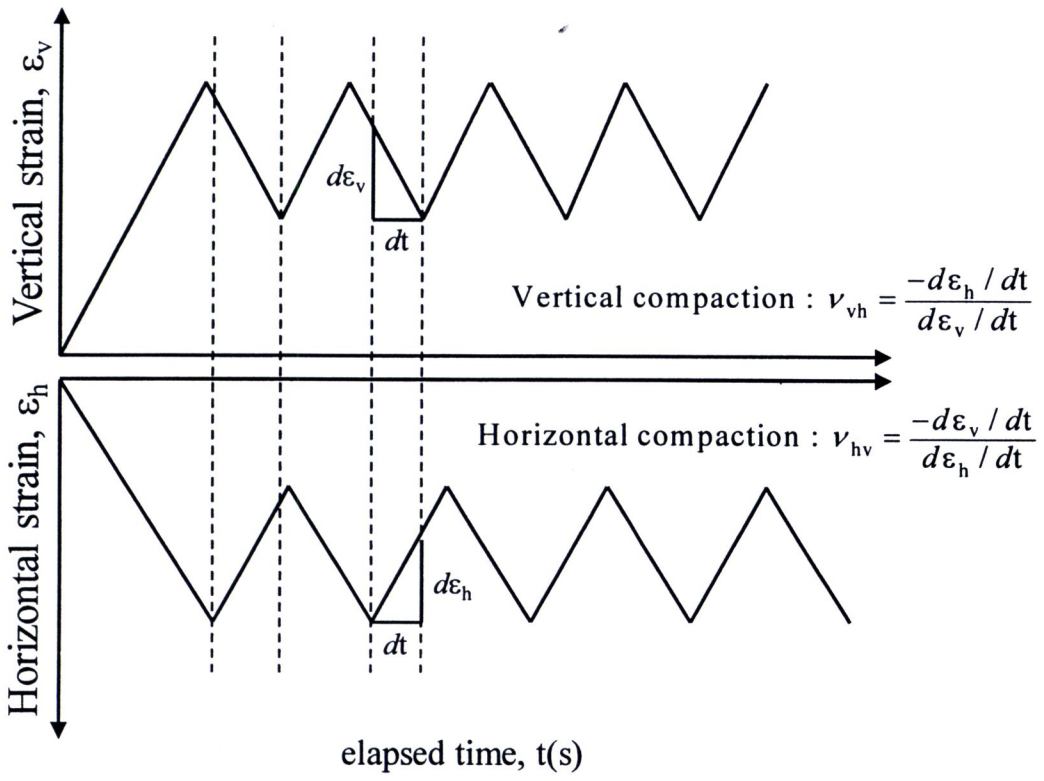

Figure 4.23 For example, to evaluations of equivalent Poisson's ration which determined from the ratio of the $d\varepsilon_h / dt$ to the $d\varepsilon_v / dt$ or the $d\varepsilon_v / dt$ to the $d\varepsilon_h / dt$

Table 4.3 Summary of voids in mineral aggregate and voids ratio of PMA in the vertical and horizontal compactions at different densities

Density (g/cm^3)	VMA (%)	Void ratio (e_0)	$f(e_0)$
1.90	31.369	0.457	2.014
2.15	22.339	0.288	2.752
2.37	14.392	0.168	3.431

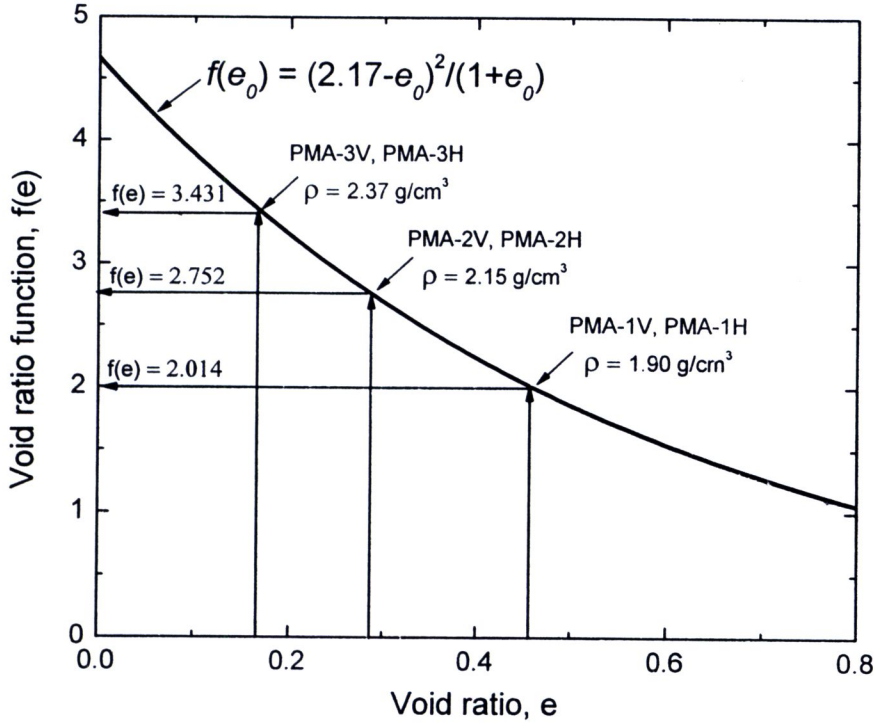

Figure 4.24 Relationships between the product of void ratio function and the void ratio for PMA-1V, PMA-1H, PMA-2V, PMA-2H, PMA-3V and PMA-3H

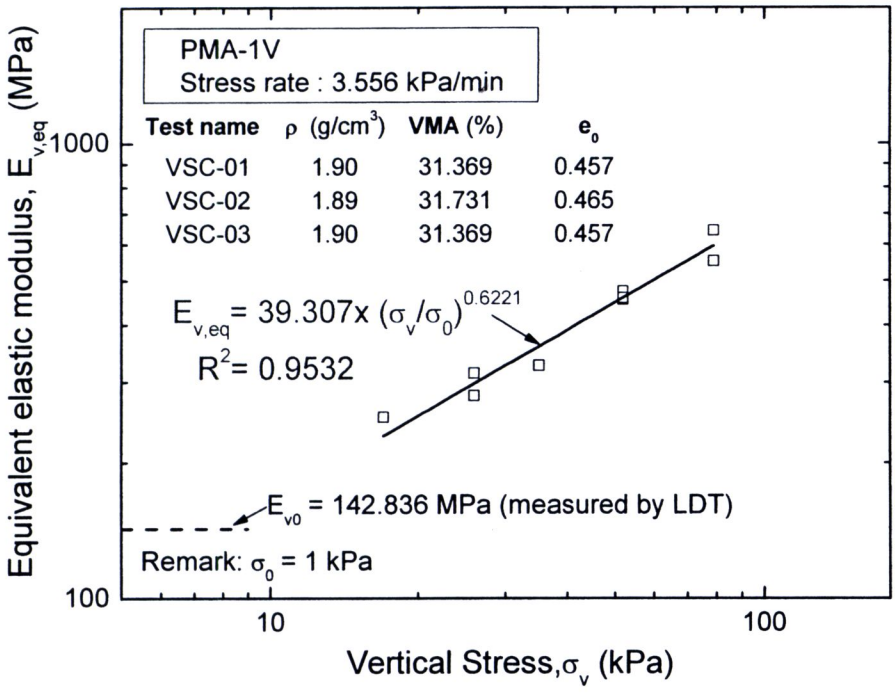

Figure 4.25(a) Relationships between equivalent elastic modulus and vertical stress for PMA-1V from tests VSC-01, VSC-02 and VSC-03

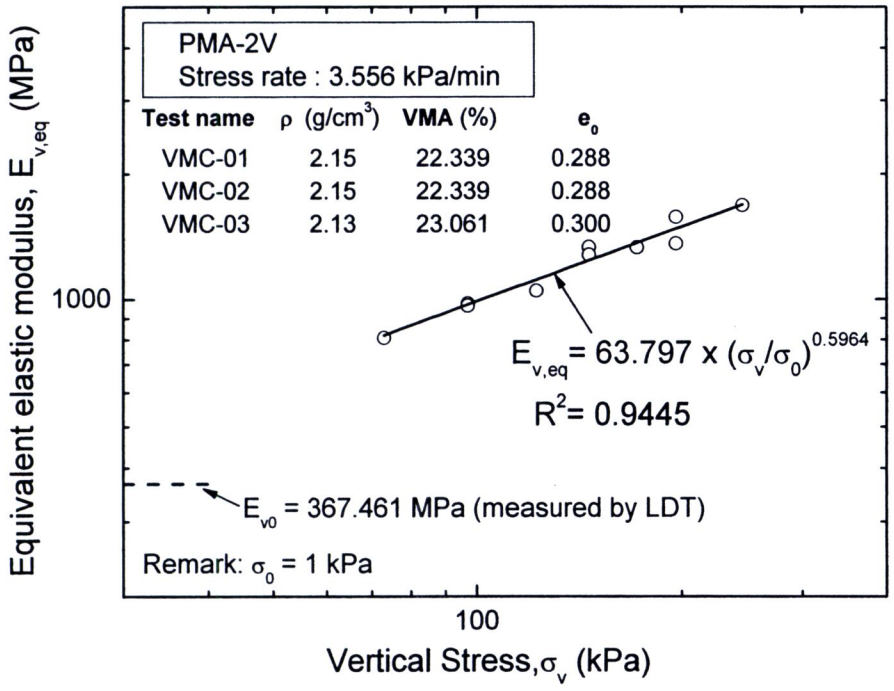

Figure 4.25(b) Relationships between equivalent elastic modulus and vertical stress for PMA-2V from tests VMC-01, VMC-02 and VMC-03

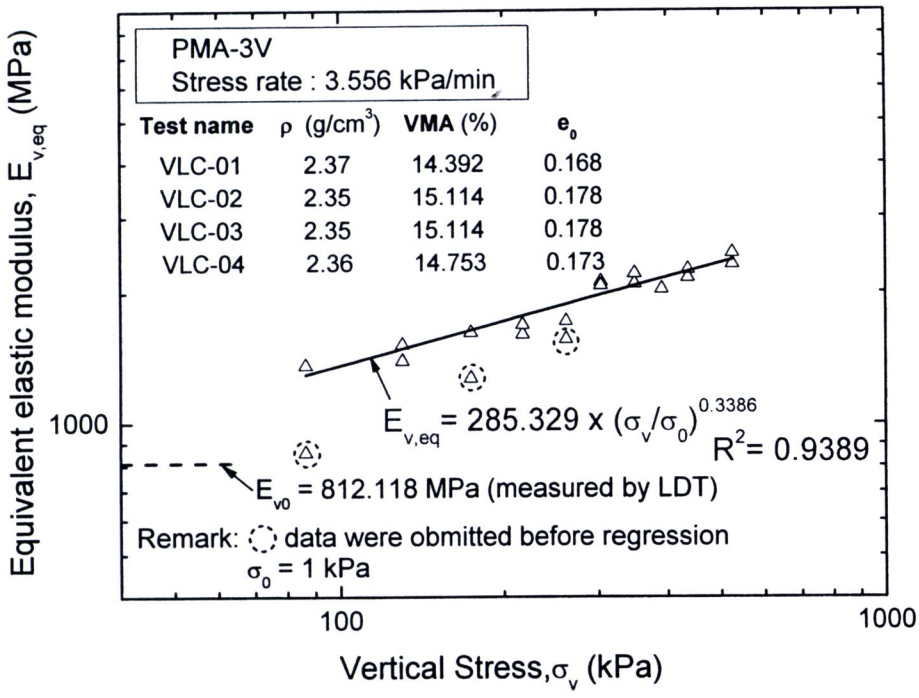

Figure 4.25(c) Relationships between equivalent elastic modulus and vertical stress for PMA-3V from tests VLC-01, VLC-02, VLC-03 and VLC-04

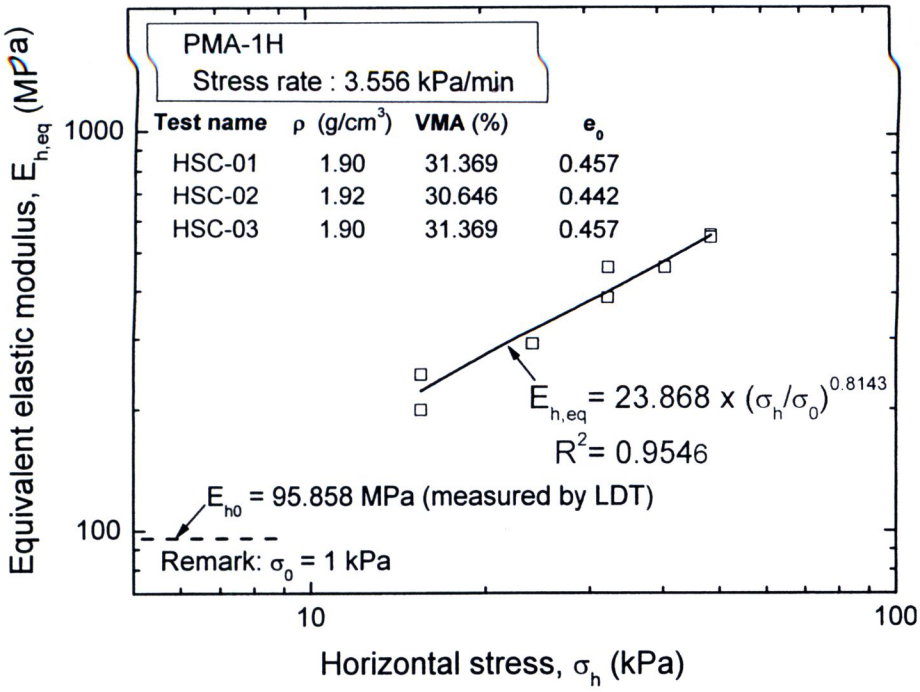

Figure 4.26(a) Relationships between equivalent elastic modulus and horizontal stress for PMA-1H from tests HSC-01, HSC-02 and HSC-03

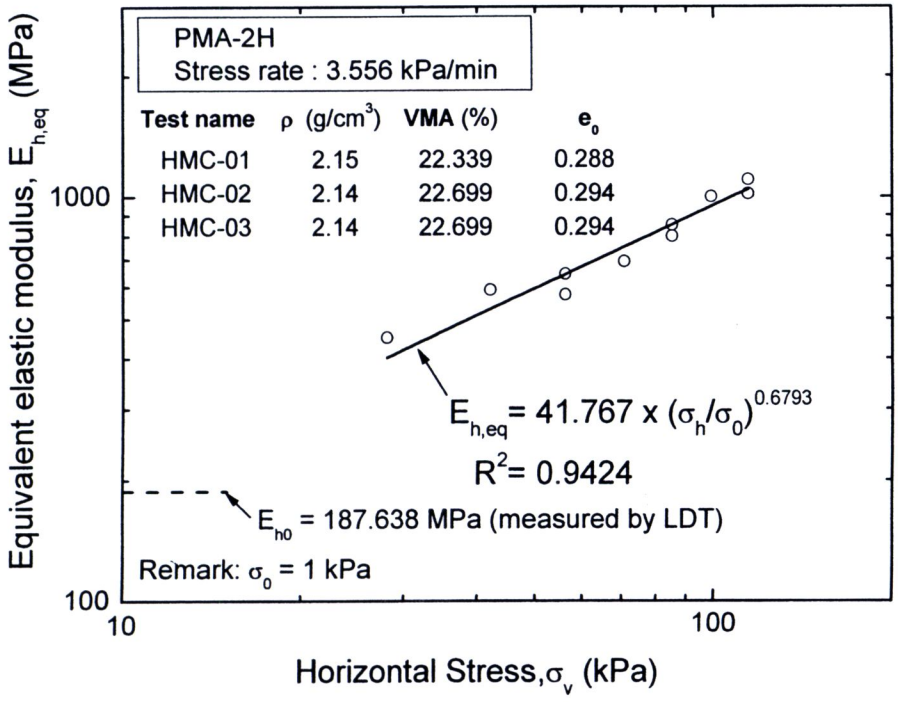

Figure 4.26(b) Relationships between equivalent elastic modulus and horizontal stress for PMA-2H from tests HMC-01, HMC-02 and HMC-03

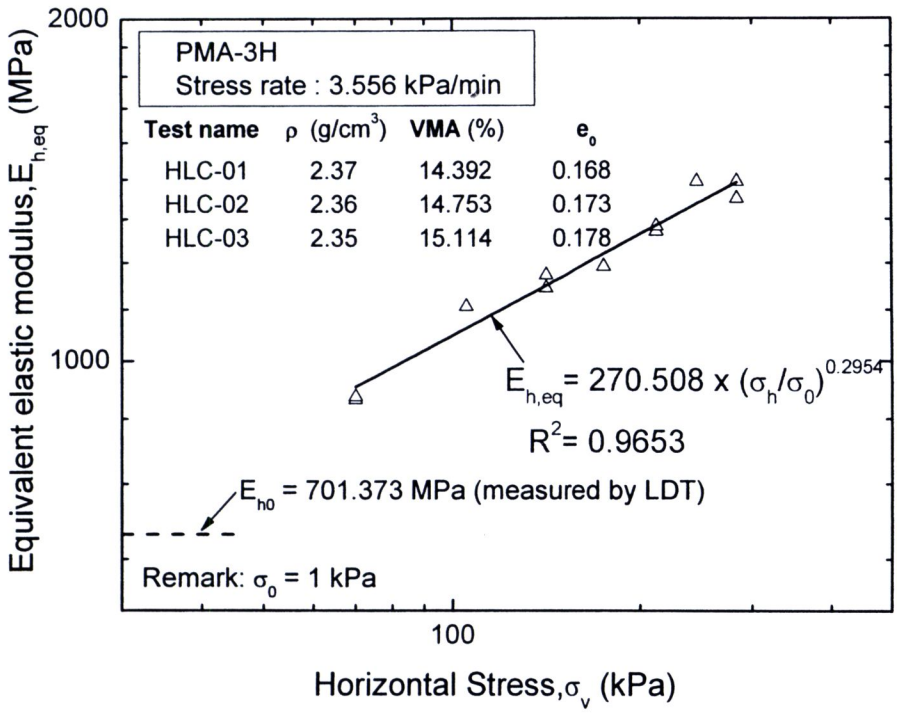

Figure 4.26(c) Relationships between equivalent elastic modulus and horizontal stress for PMA-3H from tests HLC-01, HLC-02 and HLC-03

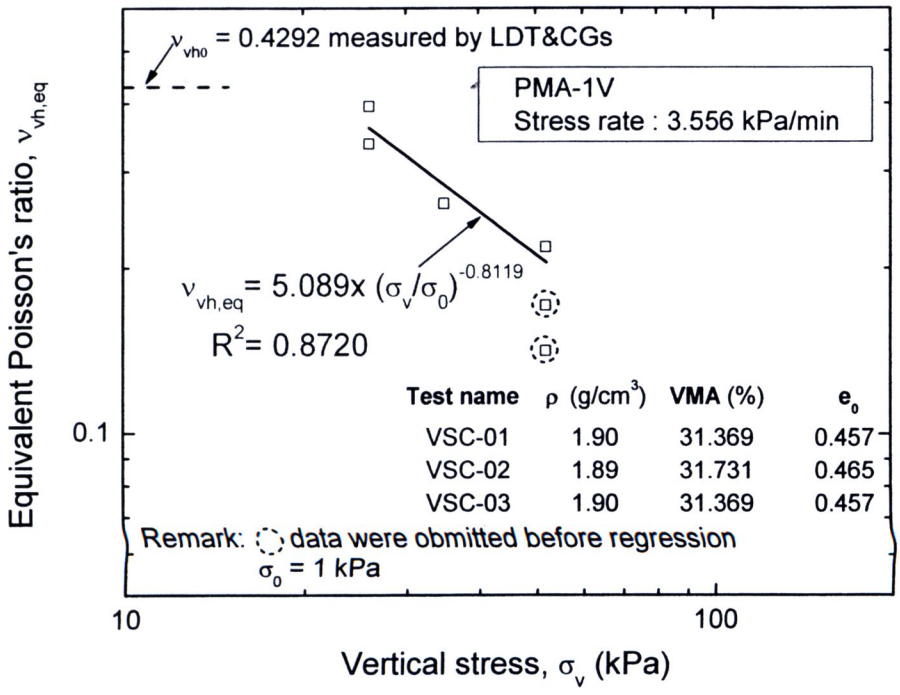

Figure 4.27(a) Relationships between equivalent Poisson's ratio and vertical stress for PMA-1V from tests VSC-01, VSC-02 and VSC-03

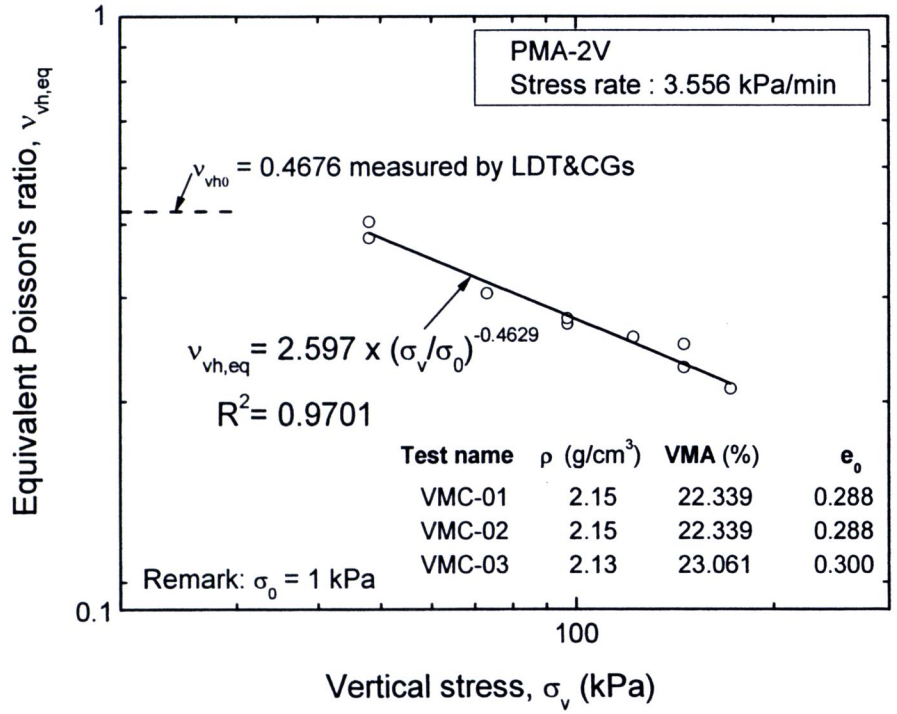

Figure 4.27(b) Relationships between equivalent Poisson's ratio and vertical stress for PMA-2V from tests VMC-01, VMC-02 and VMC-03

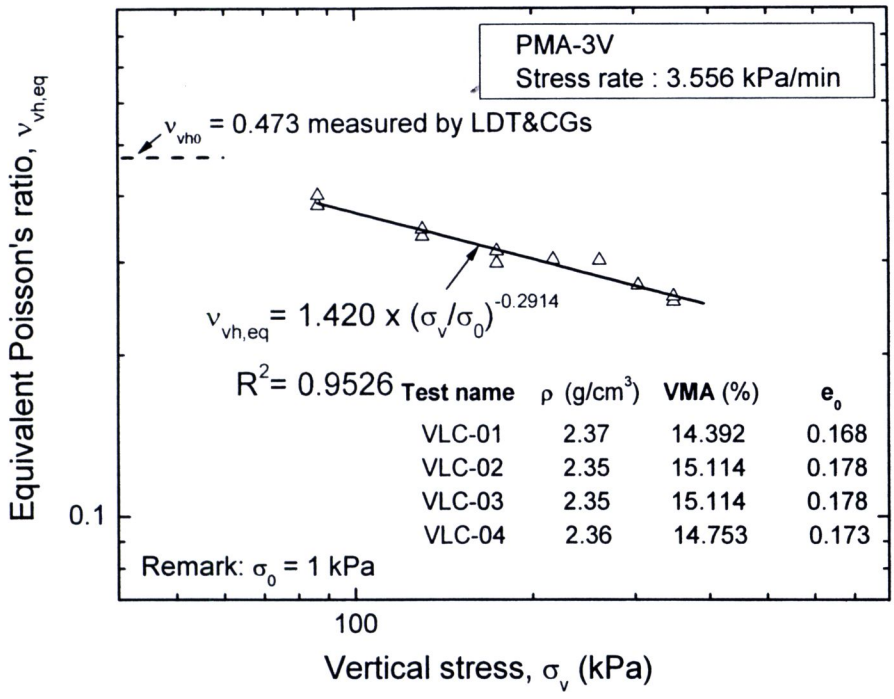

Figure 4.27(c) Relationships between equivalent Poisson's ratio and vertical stress for PMA-3V from tests VLC-01, VLC-02, VLC-03 and VLC-04

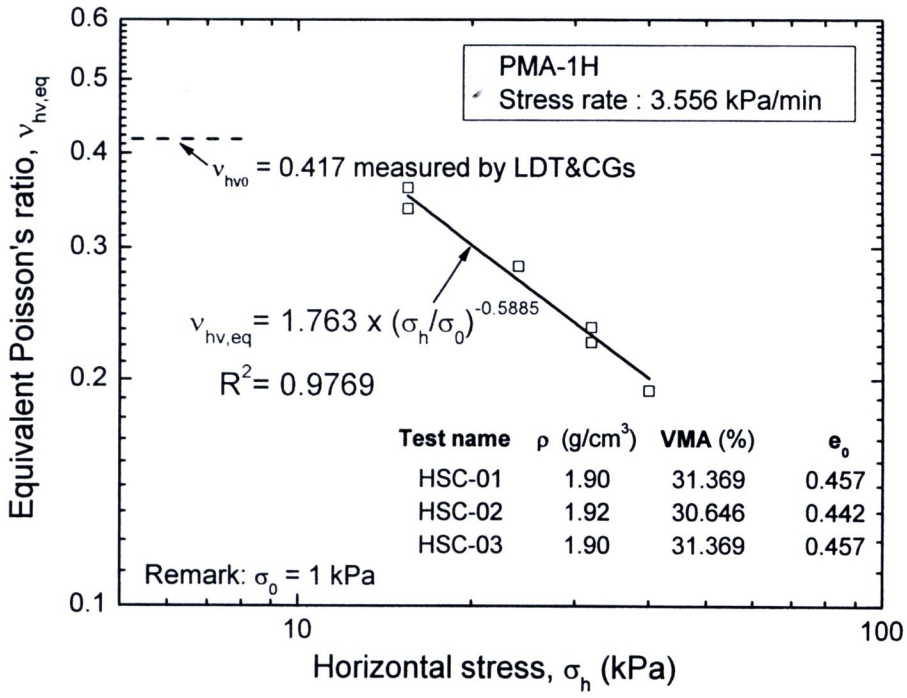

Figure 4.28(a) Relationships between equivalent Poisson's ratio and horizontal stress for PMA-1H from tests HSC-01, HSC-02 and HSC-03

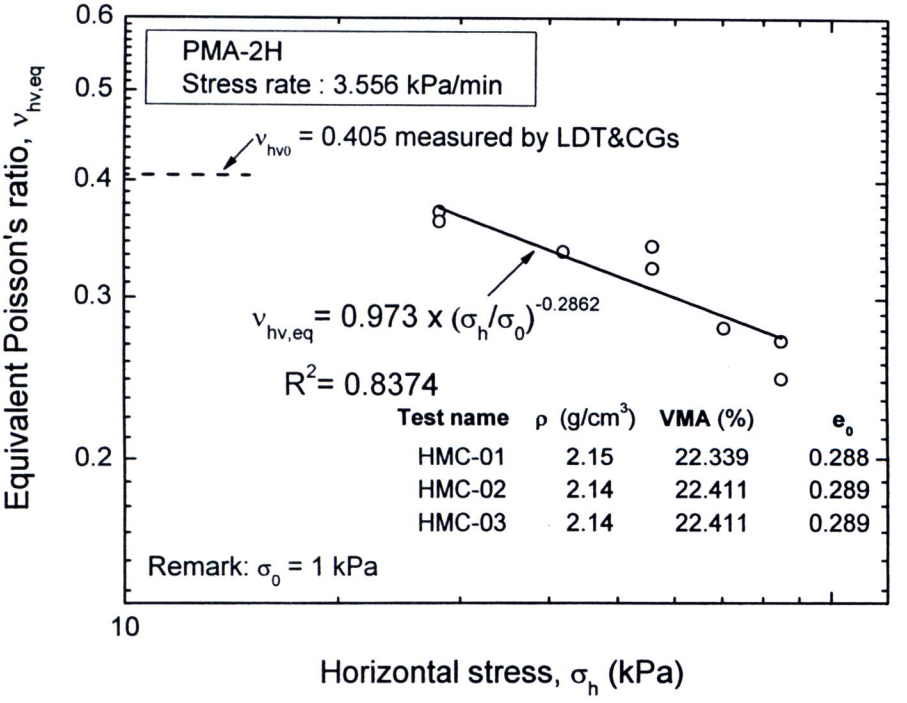

Figure 4.28(b) Relationships between equivalent Poisson's ratio and horizontal stress for PMA-2H from tests HMC-01, HMC-02 and HMC-03

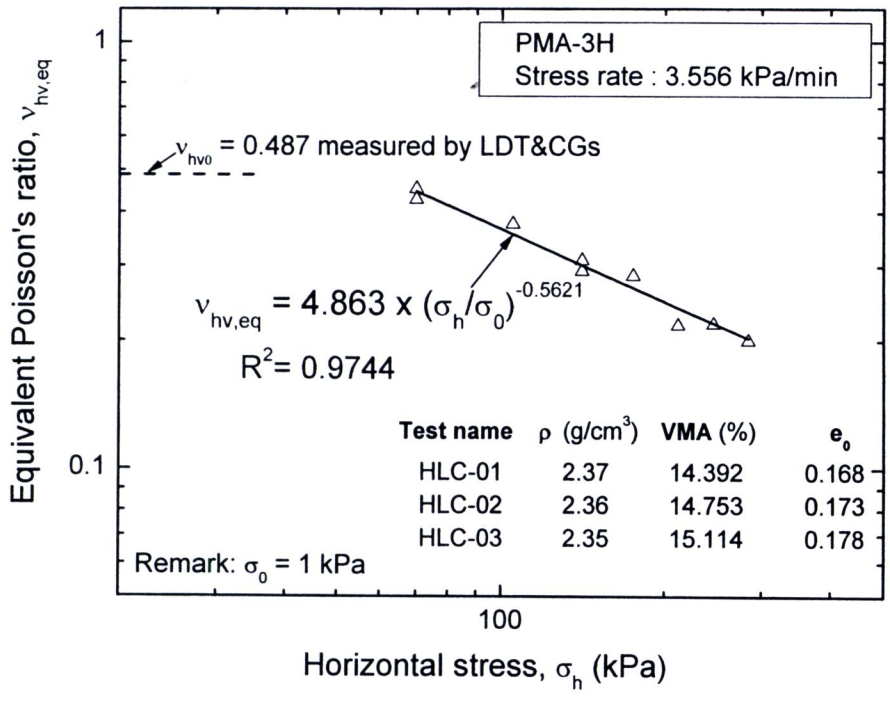

Figure 4.28(c) Relationships between equivalent Poisson's ratio and horizontal stress for PMA-3H from tests HLC-01, HLC-02 and HLC-03

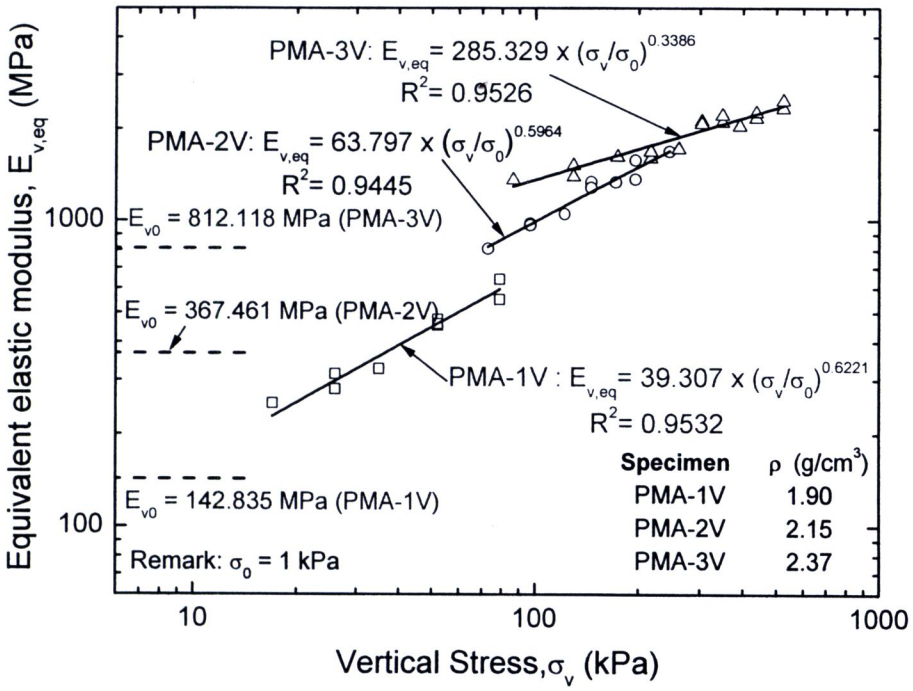

Figure 4.29(a) Comparisons of equivalent elastic modulus among PMA-1V, PMA-2V and PMA-3V as a function of vertical stress

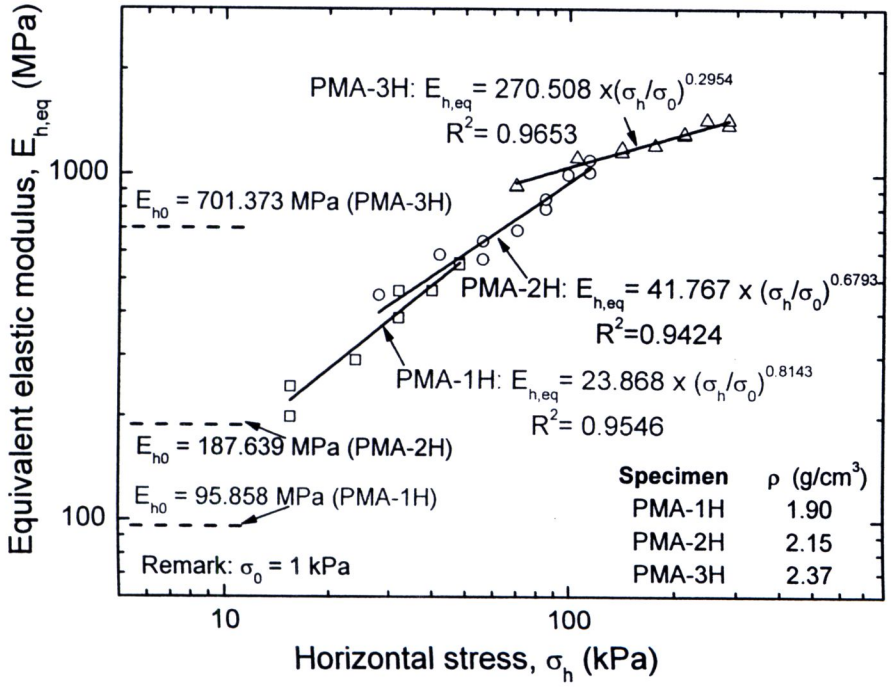

Figure 4.29(b) Comparisons of equivalent elastic modulus among PMA-1H, PMA-2H and PMA-3H as a function of horizontal stress

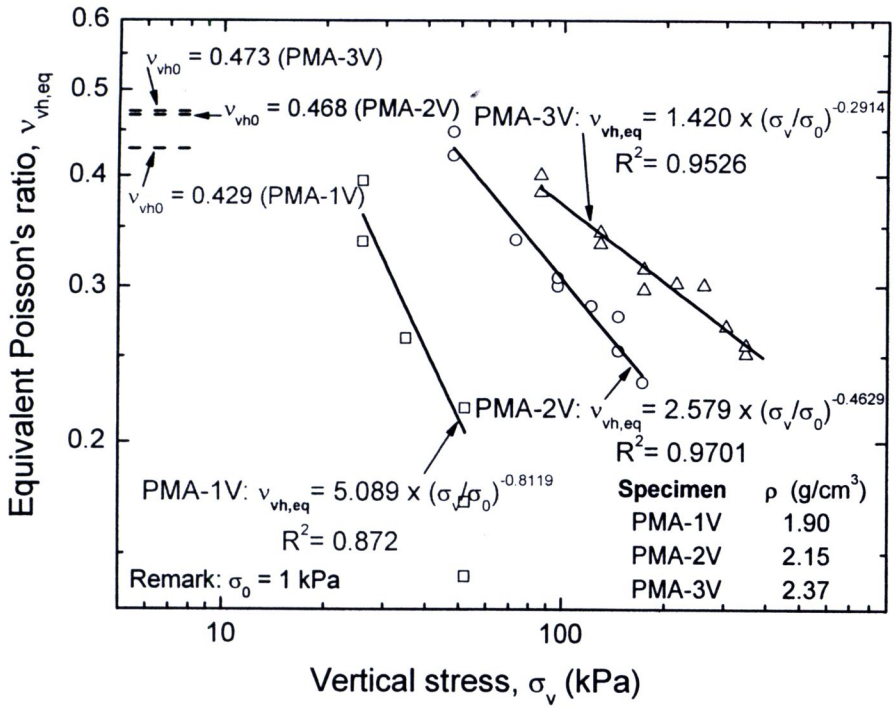

Figure 4.30(a) Comparison of equivalent Poisson's ratio among PMA-1V, PMA-2V and PMA-3V as a function of vertical stress

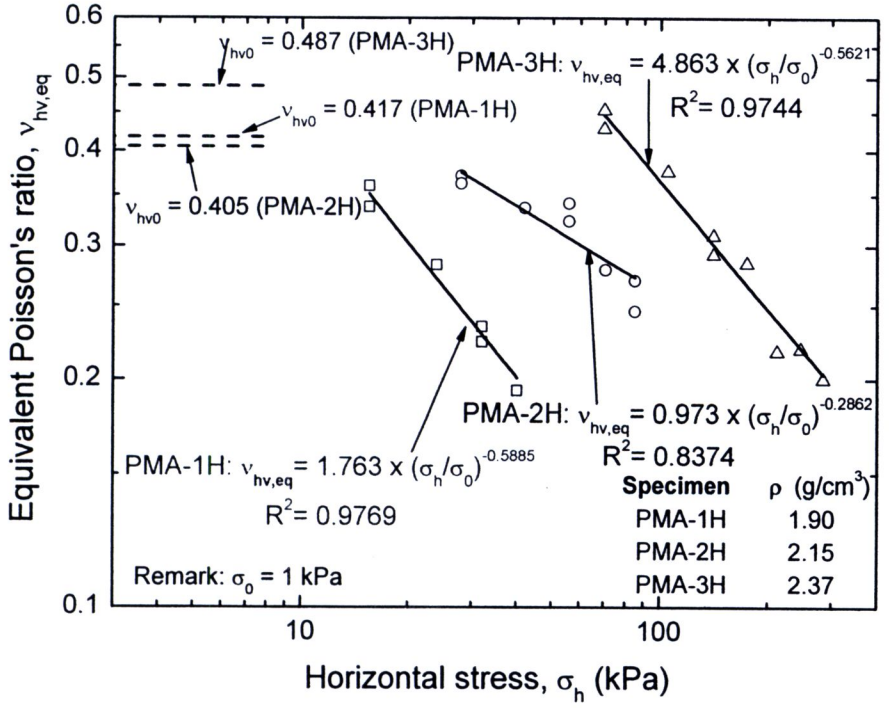

Figure 4.30(b) Comparison of equivalent Poisson's ratio among PMA-1H, PMA-2H and PMA-3H as a function of horizontal stress

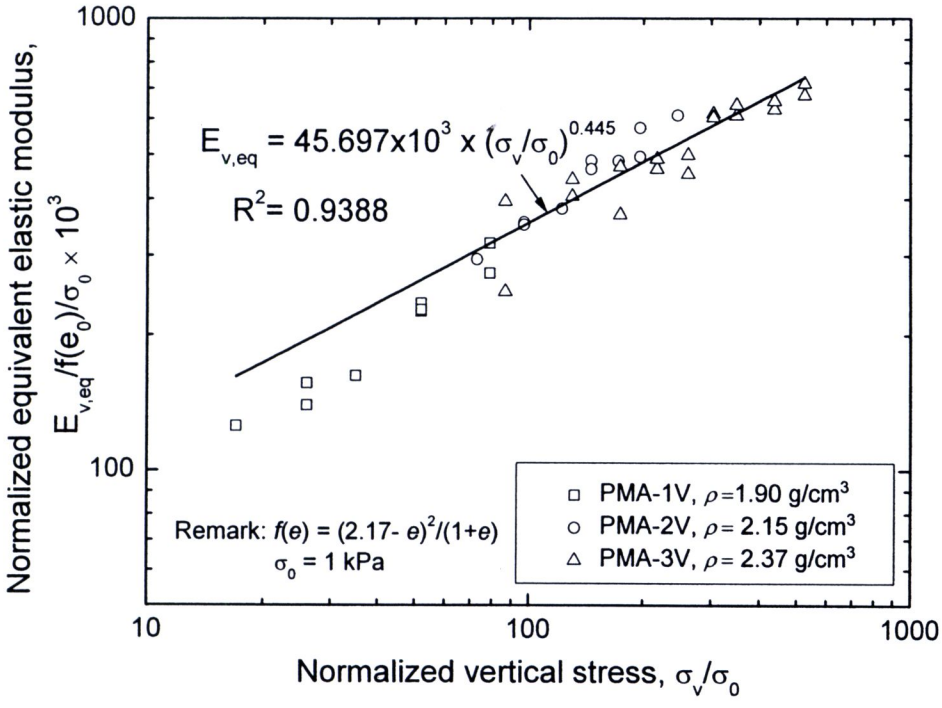

Figure 4.31(a) Equivalent elastic modulus for all densities of PMA-1V, PMA-2V and PMA-3V as a function of normalized vertical stress

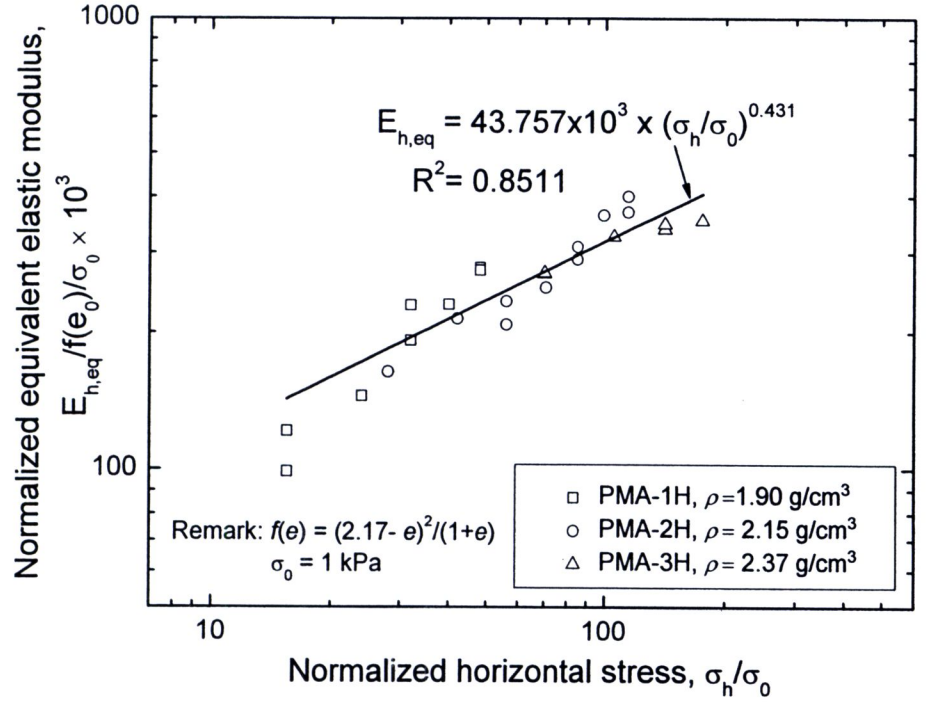

Figure 4.31(b) Equivalent elastic modulus for all densities of PMA-1H, PMA-2H and PMA-3H as a function of normalized horizontal stress

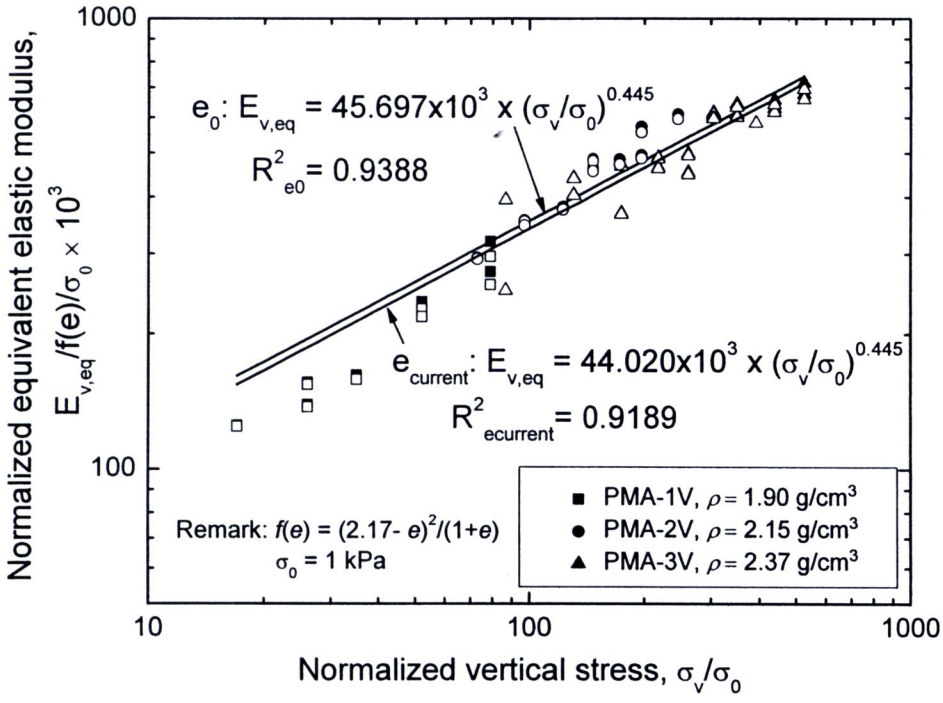

Figure 4.32(a) Equivalent elastic modulus normalized by different e_0 and $e_{current}$ for all densities of PMA-1V, PMA-2V and PMA-3V as a function of normalized vertical stress

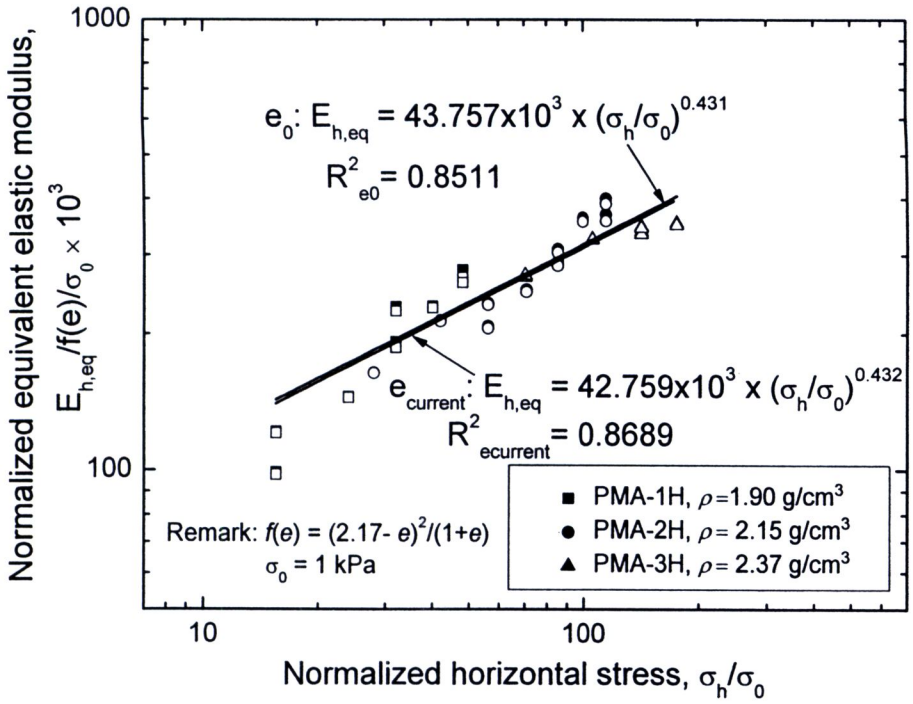

Figure 4.32(b) Equivalent elastic modulus normalized by different e_0 and $e_{current}$ for all densities of PMA-1H, PMA-2H and PMA-3H as a function of normalized horizontal stress

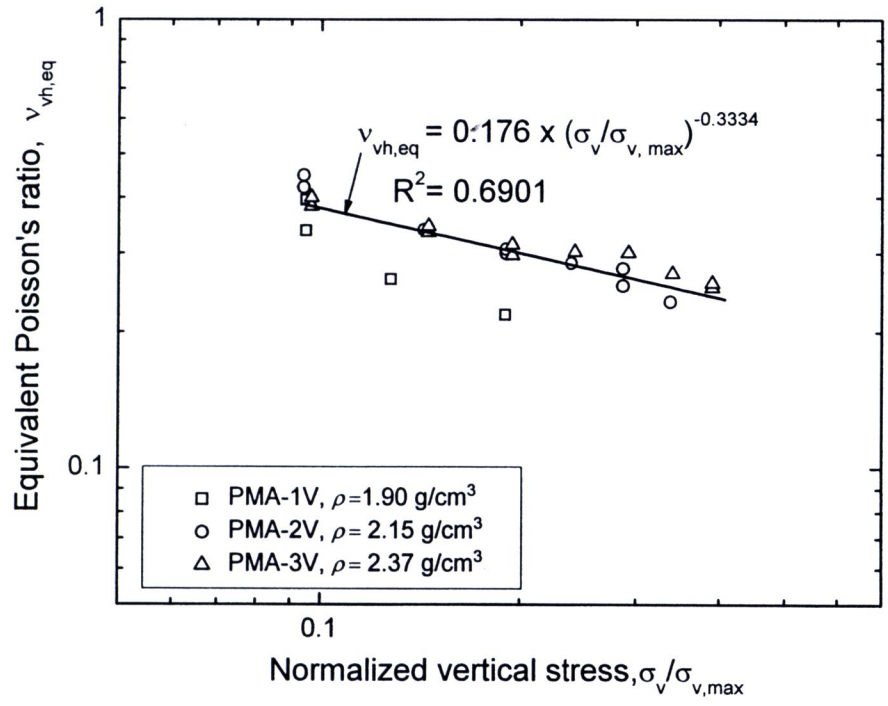

Figure 4.33(a) Equivalent Poisson's ratio for all densities of PMA-1V, PMA-2V and PMA-3V as a function of normalized vertical stress

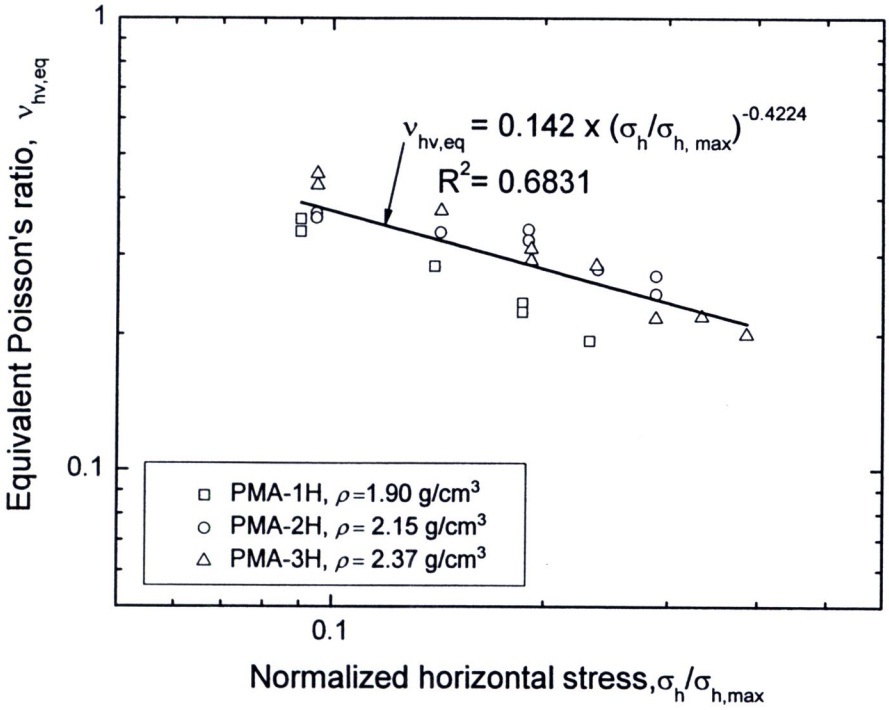

Figure 4.33(b) Equivalent Poisson's ratio for all densities of PMA-1H, PMA-2H and PMA-3H as a function of normalized horizontal stress

4.4 Comparison between the vertical stiffness and the horizontal stiffness

Figures 4.34(a) through 4.34(c) compare the vertical equivalent elastic modulus $E_{v,eq}$ -values with the horizontal equivalent elastic modulus $E_{h,eq}$ -values while Figs 4.35(a) through 4.35(c) compare the vertical to horizontal equivalent Poisson's ratio $\nu_{vh,eq}$ -values with the horizontal to vertical equivalent Poisson's ratio $\nu_{hv,eq}$ -values of PMA specimens at different densities equal to 1.90 g/cm^3 (PMA-1V, PMA-1H), 2.15 g/cm^3 (PMA-2V, PMA-2H) and 2.37g/cm^3 (PMA-3V, PMA-3H) and had the voids in mineral aggregates (VMA) of 31.369 %, 22.339 %, and 14.392 %, respectively. Fig 4.36(a) compared the normalized equivalent elastic modulus of all densities between the vertical and horizontal PMA specimen, linear fitted with different *m*-power values. On the other hand, Fig 4.36(b) compares the above-mentioned results when linear fitted with the average *m*-power. Fig 4.37(a) compares the normalized equivalent Poisson's ratio of all densities between $\nu_{vh,eq}$ and $\nu_{hv,eq}$ of PMA specimen, linear fitted with different *m*-power values. On the other hand, Fig 4.37(b) compares the above-mentioned results when linear fitted with the average *m*-power. The following trends of behavior may be seen from these figures:

1) Considering at the same density and stress, the vertical equivalent modulus, $E_{v,eq}$ evaluated from minute-amplitude unload and reload cycles applied after sustained loading is noticeably greater than the value of horizontal equivalent modulus $E_{h,eq}$.
2) Under consideration from 1) The vertical to horizontal equivalent Poisson's ratio, $\nu_{vh,eq}$ is noticeably greater than the value of horizontal to vertical equivalent Poisson's ratio, $\nu_{hv,eq}$.
3) Observation 1) implies that $E_{v,eq} > E_{h,eq}$ because the direction of compaction of the vertically compacted PMA specimen is parallel to the direction of loading. In addition, the joint between the layers and the arrangement of aggregate particles in the layer are normal to the direction of loading. Also, the force from the compaction can be treated as preloading in the same direction of the force from loading.
4) Poisson's ratio is the ratio between the lateral strain to the axial strain. For the same stress and density, $\nu_{vh,eq}$ from the vertically compacted specimens is greater than $\nu_{hv,eq}$ from the horizontally compacted one. This is also due to the observation 3).
5) From the comparisons of normalized equivalent modulus for all densities between the vertical and horizontal PMA specimen, the $E_{v,eq}$ - values of vertical specimen is greater than the $E_{h,eq}$ - values of horizontal specimen ($E_{v,eq}$ is greater than $E_{h,eq}$) when considering at the same level stress. It may be seen, therefore, that, the behaviors of PMA is anisotropic.
6) In comparison with the slope of equation (*m*-values) which is the "stress level dependency parameter" between the vertical and horizontal specimens, the *m*-values of $E_{v,eq}$ was close to that of $E_{h,eq}$ (m_v is similar to m_h). Therefore, the slope was averaged to find the net difference of the equation which represents the degree of anisotropic. The *m*-value after average is 0.438 (Fig. 4.36(b)).

7) Observation 6) implies that, the net difference between $E_{v,eq}$ and $E_{h,eq}$ under the same stress is 10.61%. In addition, there are the parameters for describing the anisotropic behavior that is "Inherent anisotropic ratio" (E_v / E_h) which is 1.12. And, the "stress-induced anisotropy" is represented by stress level dependency parameter (m) which is equal to 0.438.

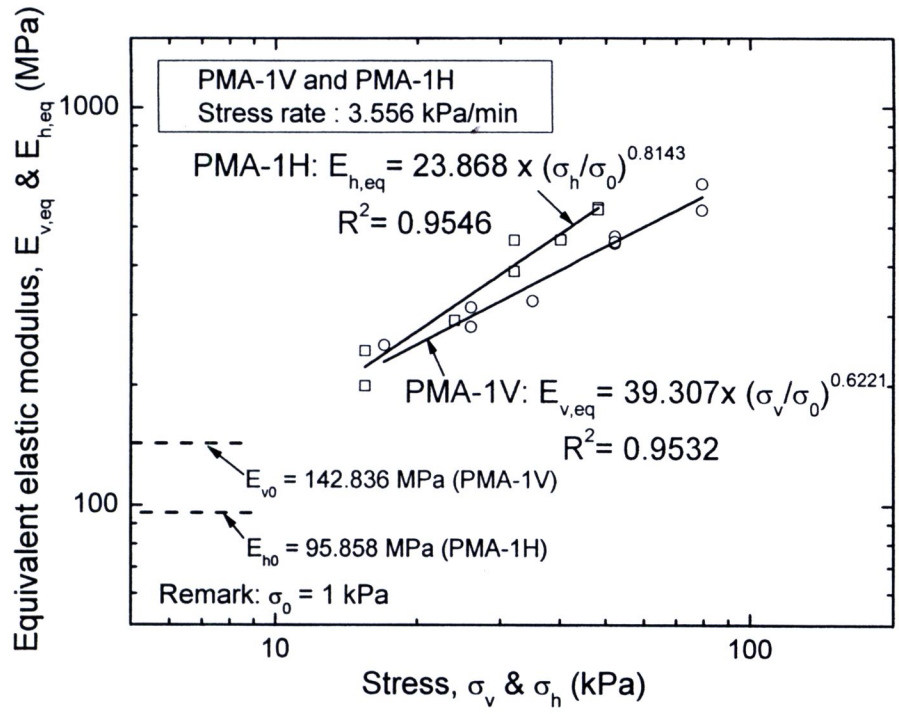

Figure 4.34(a) Comparisons between vertical and horizontal equivalent elastic modulus for PMA-1V and PMA-1H at density of 1.90 g/cm^3

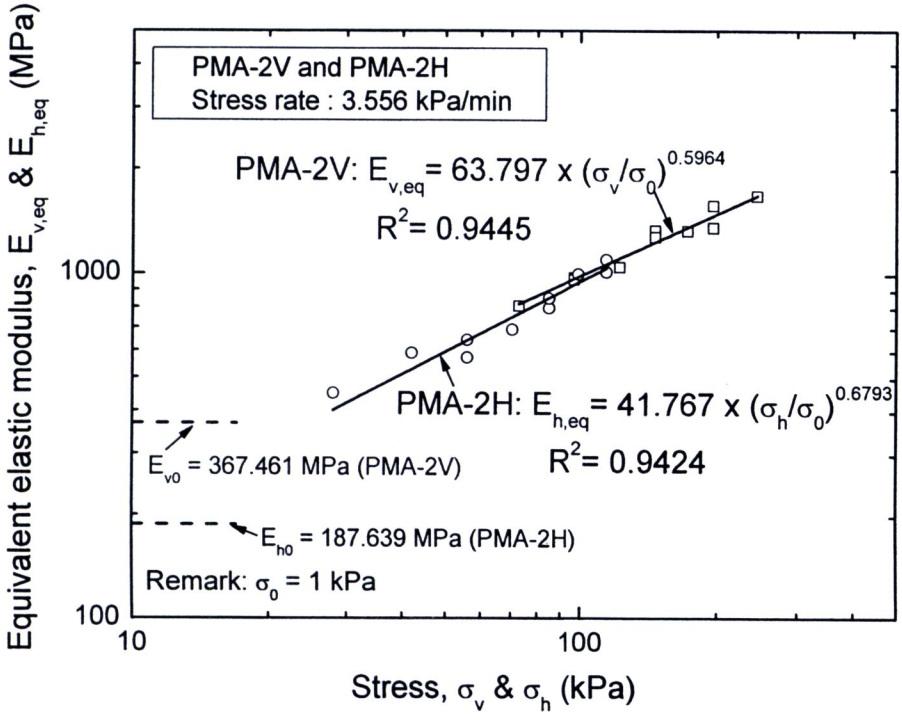

Figure 4.34(b) Comparisons between vertical and horizontal equivalent elastic modulus for PMA-2V and PMA-2H at density of 2.15 g/cm^3

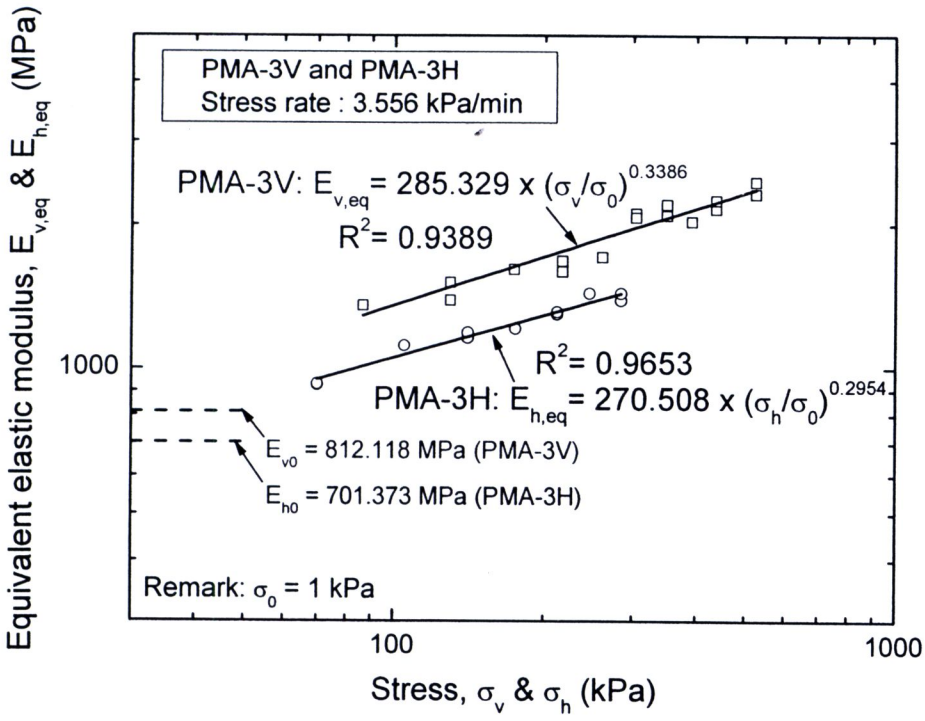

Figure 4.34(c) Comparisons between vertical and horizontal equivalent elastic modulus for PMA-3V and PMA-3H at density of 2.37 g/cm^3

THE NATIONAL RESEARCH COUNCIL OF THAILAND
RESEARCH LIBRARY

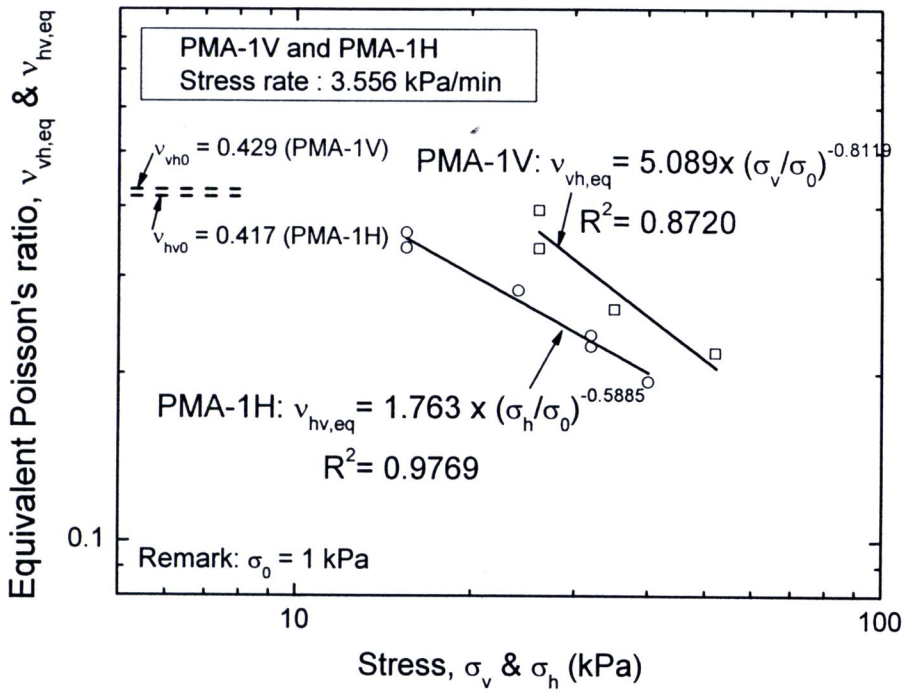

Figure 4.35(a) Comparisons between vertical and horizontal equivalent Poisson's ratio for PMA-1V and PMA-1H at density of 1.90 g/cm^3

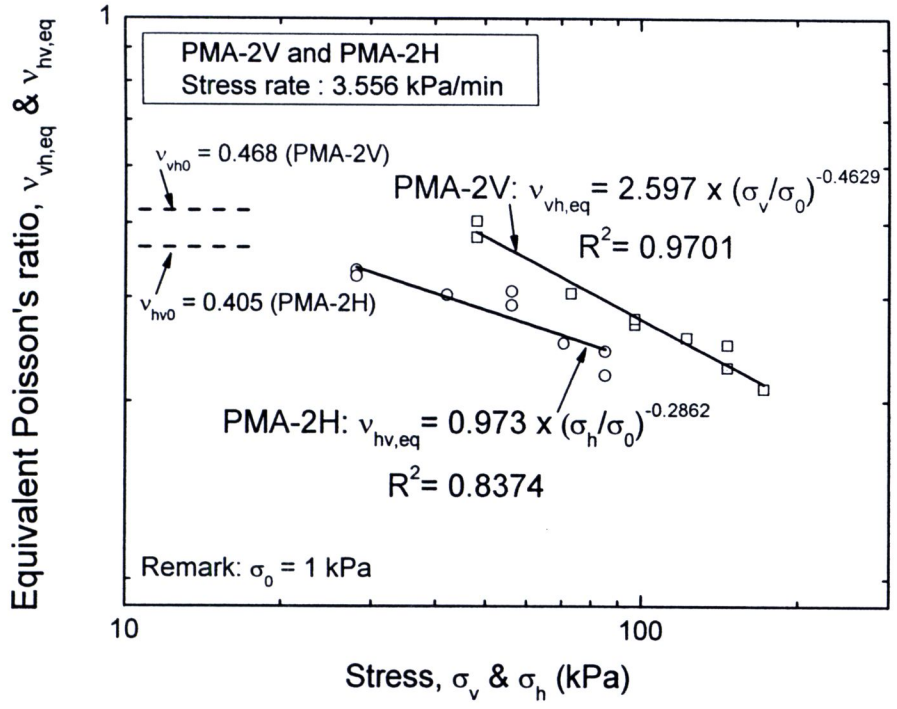

Figure 4.35(b) Comparisons between vertical and horizontal equivalent Poisson's ratio for PMA-2V and PMA-2H at density of 2.15 g/cm^3

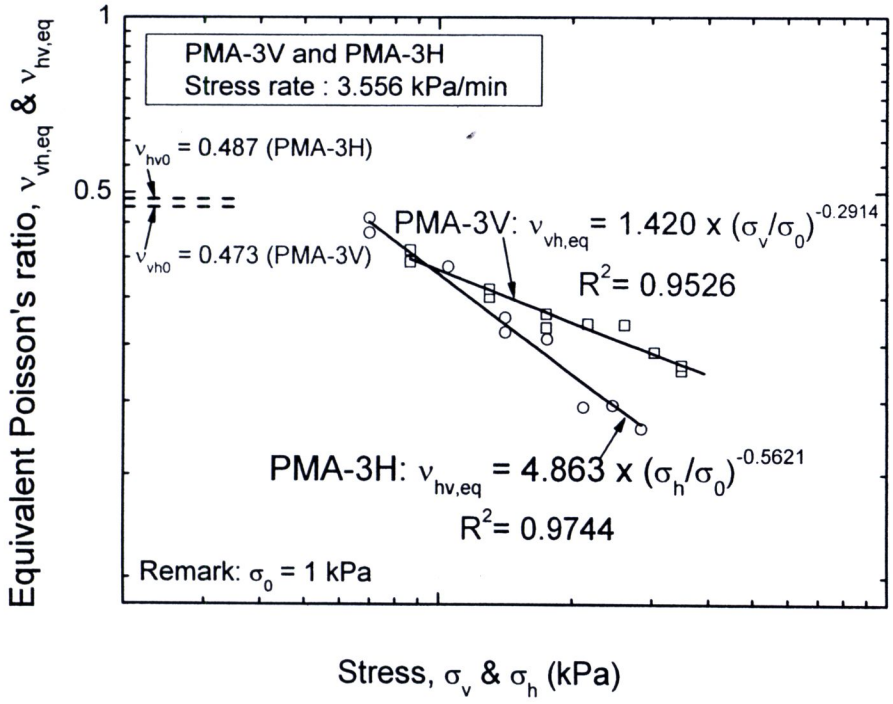

Figure 4.35(c) Comparisons between vertical and horizontal equivalent Poisson's ratio for PMA-3V and PMA-3H at density of 2.37 g/cm^3

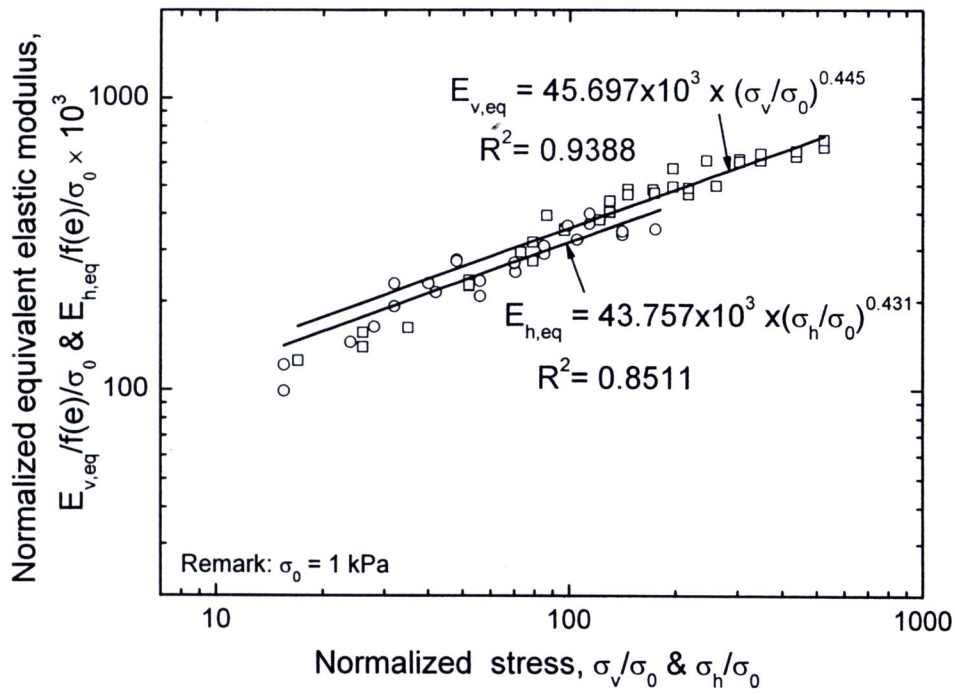

Figure 4.36(a) Comparisons between vertical and horizontal normalized equivalent elastic modulus for all densities, linear fitted with different *m*-power values

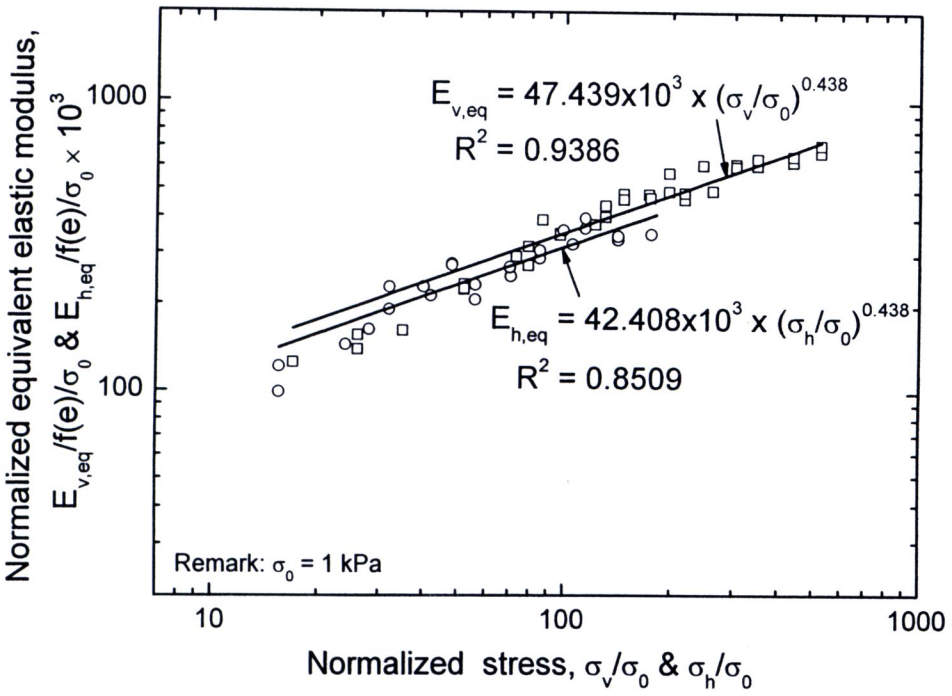

Figure 4.36(b) Comparisons between vertical and horizontal normalized equivalent elastic modulus for all densities, linear fitted with the average m-power

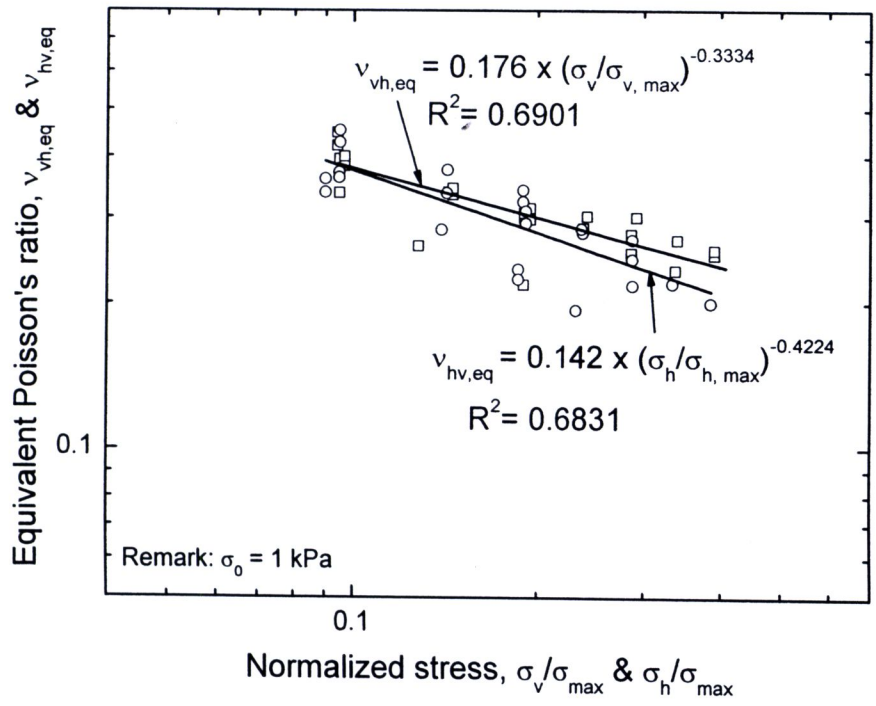

Figure 4.37(a) Comparisons between vertical and horizontal equivalent Poisson's ratio for all densities, linear fitted with different *m*-power values

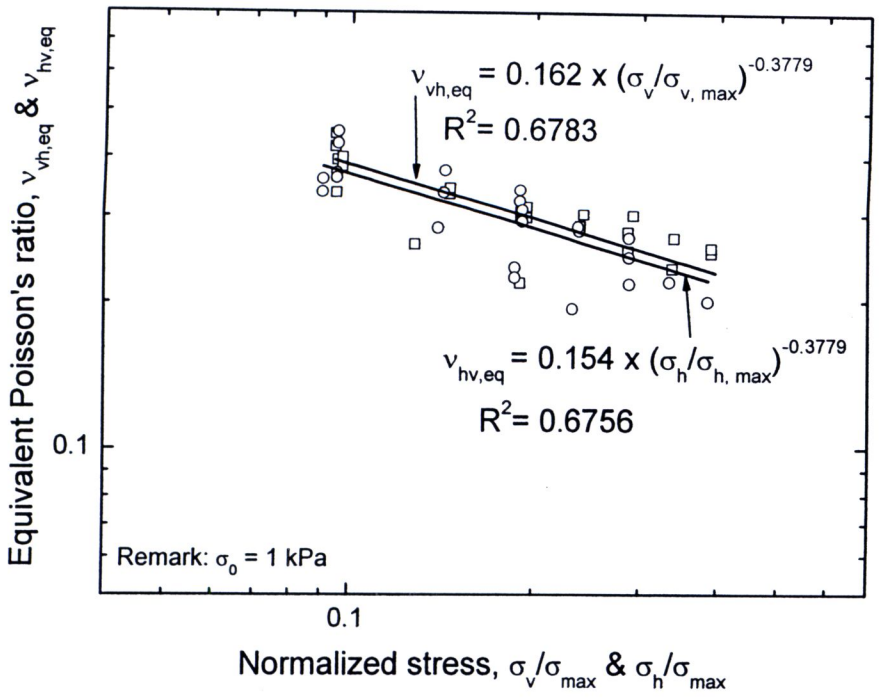

Figure 4.37(b) Comparisons between vertical and horizontal equivalent Poisson's ratio for all densities, linear fitted with the average *m*-power

4.5 Comparisons of stiffness between Polymer Modified Asphaltic Concrete (PMA) and Hot-mixed Asphaltic Concrete (HMA)

To make this research more complete and according to the objective of the study, the properties of PMA have been compared with the ones of HMA. Musika (2010) investigated small-strain properties on HMA. The HMA specimens were prepared by compaction to different directions of compaction (vertical compaction and horizontal compaction) with a controlled density equal to 1.90 g/cm^3, 2.15 g/cm^3 and 2.37 g/cm^3 similar to the ones in this study. In this section, the small-strain stiffness between PMA and HMA specimens in the vertical compaction and horizontal compactions were compared.

Figs. 4.38(a) through 4.38(c) and Figs. 4.40(a) through 4.40(c) show the comparisons of $E_{v,eq}$ - values and the $\nu_{vh,eq}$ - values for the vertically compacted specimens at the densities of 1.90 g/cm^3, 2.15 g/cm^3 and 2.37 g/cm^3, respectively. Figs. 4.39(a) through 4.39(c) and Figs. 4.41(a) through 4.41(c) show the comparisons of $E_{h,eq}$ - values and the $\nu_{hv,eq}$ - values for the horizontally compacted specimens at the densities of 1.90 g/cm^3, 2.15 g/cm^3 and 2.37 g/cm^3, respectively. Fig 4.42(a) and 4.42(b) show the comparisons of the relation between the equivalent elastic modulus normalized by the void ratio function and the stress, respectively for the vertically and horizontally compacted directions. Fig 4.43(a) and 4.43(b) show the comparisons of the relation between the equivalent Poisson's ratio and the normalized stress. Fig 4.44(a) and Fig 4.44(b) show the comparisons of the relation between the equivalent elastic modulus normalized by the void ratio function and the stress with other geomaterials. Fig 4.45(a) through 4.45(c) compared the normalized equivalent elastic modulus of HMA, Hime gravel and Toyoura sand, respectively when linear fitted with the average *m*-power values. The following trends of behavior may be seen from these figures:

1) Considering at the same density and direction of compaction, the $E_{v,eq}$ - values and $E_{h,eq}$ - values of the PMA specimen were higher than, respectively, the $E_{v,eq}$ - values and $E_{h,eq}$ - values of the HMA specimen. This behavior is more obvious with the specimens of greater density. When consider, at the same density, it was found that the $E_{v,eq}$ - values were higher than $E_{h,eq}$ - values ($E_{v,eq} > E_{h,eq}$).
2) All of specimen, the both $\nu_{vh,eq}$ and $\nu_{hv,eq}$ -values of PMA specimen is noticeably higher than the those of HMA specimen when compared at the same density.
3) Considering the equivalent elastic modulus normalized by the void ratio function $E_{v,eq} / f(e)$ and $E_{h,eq} / f(e)$ between the PMA and HMA specimens, the slope of PMA was close to that of HMA. It may be seen that, the behaviors of both HMA and PMA are similar in that the stress level dependency on the anisotropic elastic modulus is similar.
4) In the specimens compacted vertically, the $E_{v,eq}$ - values normalized by the void ratio function of PMA specimen was higher than the $E_{v,eq}$ - values normalized by the void ratio function of HMA specimen for about 1.6 times. This order of difference is also the case for the horizontally compacted specimens (i.e., $E_{h,eq}$ -values). This shows that PMA specimens have the stiffness properties quantitatively greater than HMA specimens

5) Considering the $\nu_{vh,eq}$ and $\nu_{hv,eq}$ - values of PMA and HMA specimens, both PMA specimens compacted vertically and horizontally have respectively $\nu_{vh,eq}$ and $\nu_{hv,eq}$ -values higher than the values of HMA specimens for about 1.8 times.
6) The PMA and HMA have the similar behavior in that stress level dependency on the anisotropic elastic modulus and Poisson's ratio is similar. However, when comparing at the same stress level the $E_{v,eq}$ and $E_{h,eq}$ - values of PMA were noticeably greater than those of HMA. All of the above shows that PM-AC plays an important role on the development of these properties.
7) When comparing for m_v and m_h - values between HMA, Hime gravel and Toyoura sand which prepared by pluviation through air (Hoque et al., 1998), it was found that the range of $m_v = 0.485 - 0.510$ and $m_h = 0.420 - 0.462$. It could be seen that, both m_v and m_h – values of this study are close to respectively m_v and m_h – values of other geomaterials. Therefore, PMA has the similar behavior when compared to other geomaterials in this respect because PMA made from geomaterials so, the behavior that express is the same as other geomaterials; however, the elastic modulus of PMA is greater than that of other geomaterials. This is due likely to the presence of binder which provides cohesion in addition to the friction at the interparticle contact.
8) From the comparisons of normalized equivalent modulus for the geomatertais between the vertical and horizontal specimens to find the "Inherent anisotropic ratio". The ratios are 1.12, 1.19, 1.67 and 1.11 for PMA, HMA, Hime gravel and Toyoura sand respectively. Considering the Inherent anisotropic ratio of Hime gravel, both Hime gravel has the maximum ratio. It may be seen, Hime gravel has the most anisotropic behaviors of geomaterials in this study. On the other hand, Toyoura sand has the minimum ratio. So, Toyoura sand has the least anisotropic behaviors of geomaterials in this study.
9) Considering the Inherent anisotropic ratio between PMA and HMA which prepared from the same materials, the Inherent anisotropic ratio of PMA is less than the ratio of HMA. Therefore PMA has anisotropic behaviors less than HMA. This is also due to the observation 7). It could be seen that, PM-AC can reduce the anisotropic behaviors of asphaltic concrete.

However, the E_{eq} value obtained from this study may be less than the E value for used to design the road because the result from this study without effect of the different rate of testing (rate-effect). Using the fast rate in the test that make the E values greater than use slow rate in the test which in this study was use slow rate (3.556 kPa/min) for the elastic behaviors (Kongsukprasert et al., 2007). Therefore, the E_{eq} value obtained from this study less than the E value for used to design the road for example, the stiffness value obtained from FWD tests is greater than the stiffness value obtained from PLT tests because the rate of testing FWD method more than PLT method.

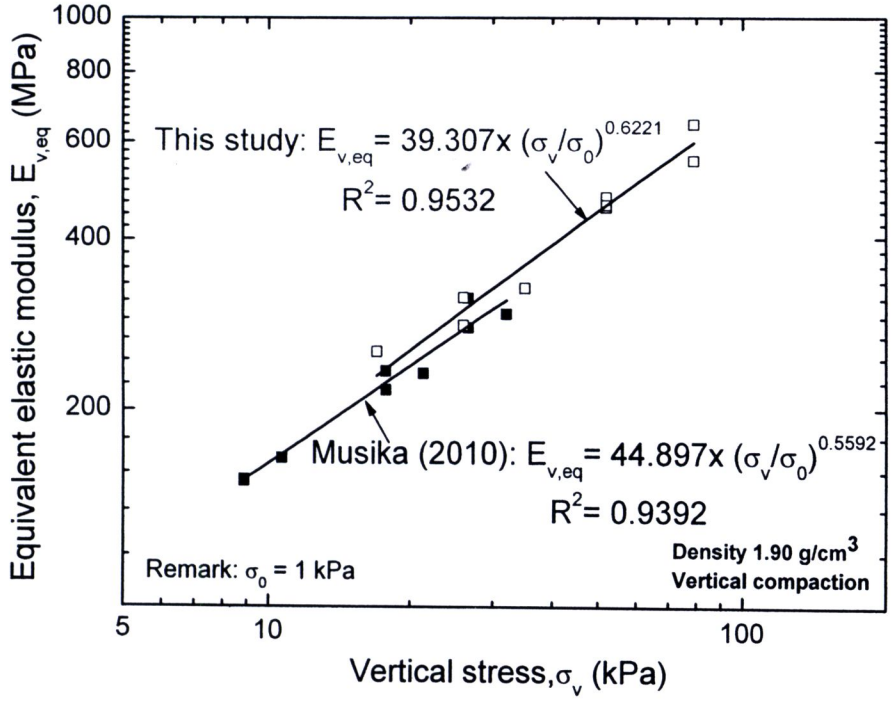

Figure 4.38(a) Comparisons of equivalent elastic modulus between PMA and HMA specimens as a function of vertical stress at density of 1.90 g/cm^3

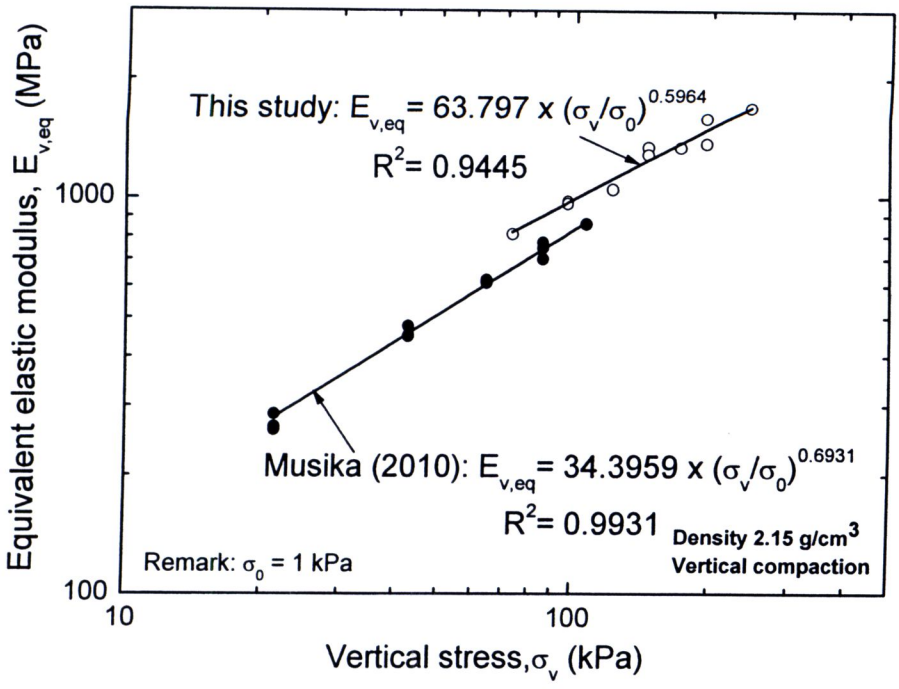

Figure 4.38(b) Comparisons of equivalent elastic modulus between PMA and HMA specimens as a function of vertical stress at density of 2.15 g/cm^3

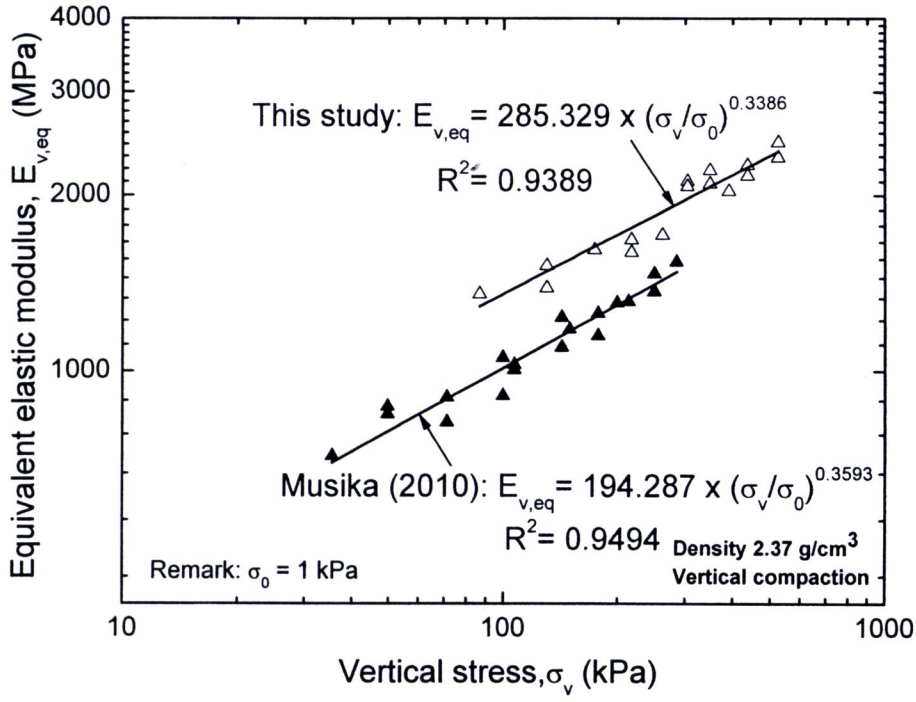

Figure 4.38(c) Comparisons of equivalent elastic modulus between PMA and HMA specimens as a function of vertical stress at density of 2.37 g/cm^3

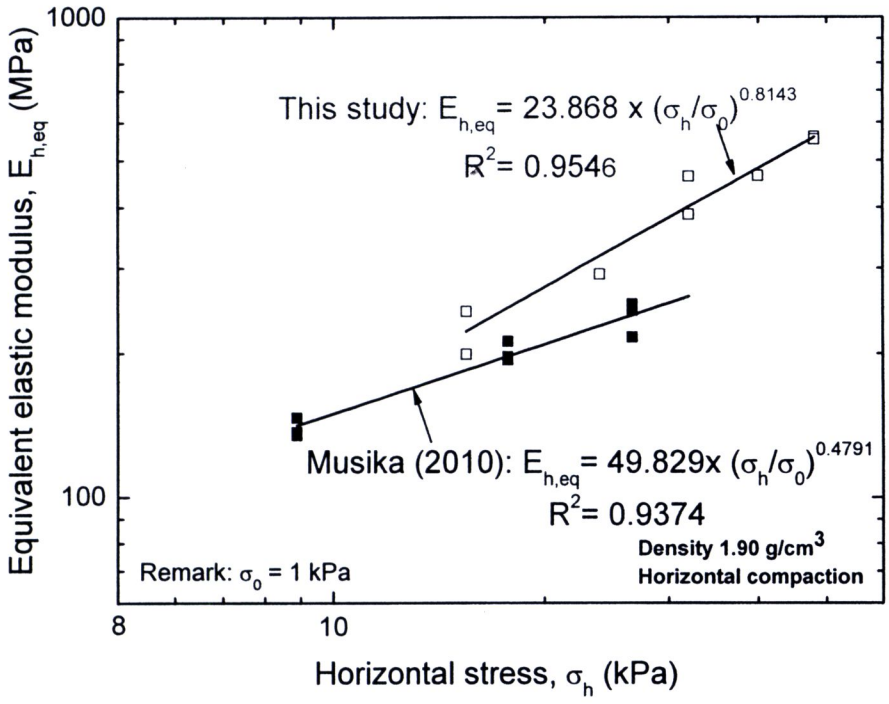

Figure 4.39(a) Comparisons of equivalent elastic modulus between PMA and HMA specimens as a function of horizontal stress at density of 1.90 g/cm^3

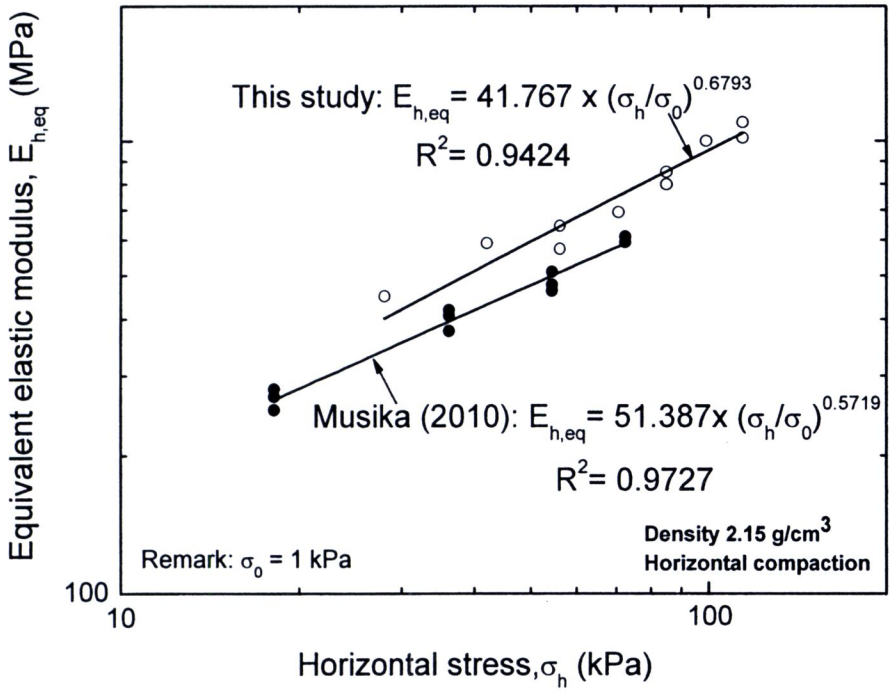

Figure 4.39(b) Comparisons of equivalent elastic modulus between PMA and HMA specimens as a function of horizontal stress at density of 2.15 g/cm^3

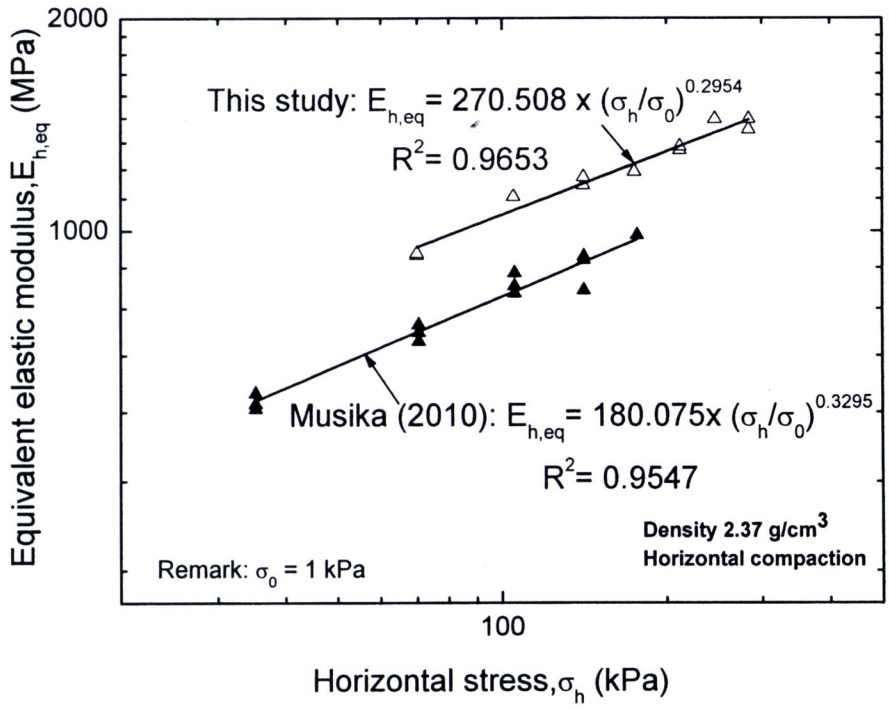

Figure 4.39(c) Comparisons of equivalent elastic modulus between PMA and HMA specimens as a function of horizontal stress at density of 2.37 g/cm^3

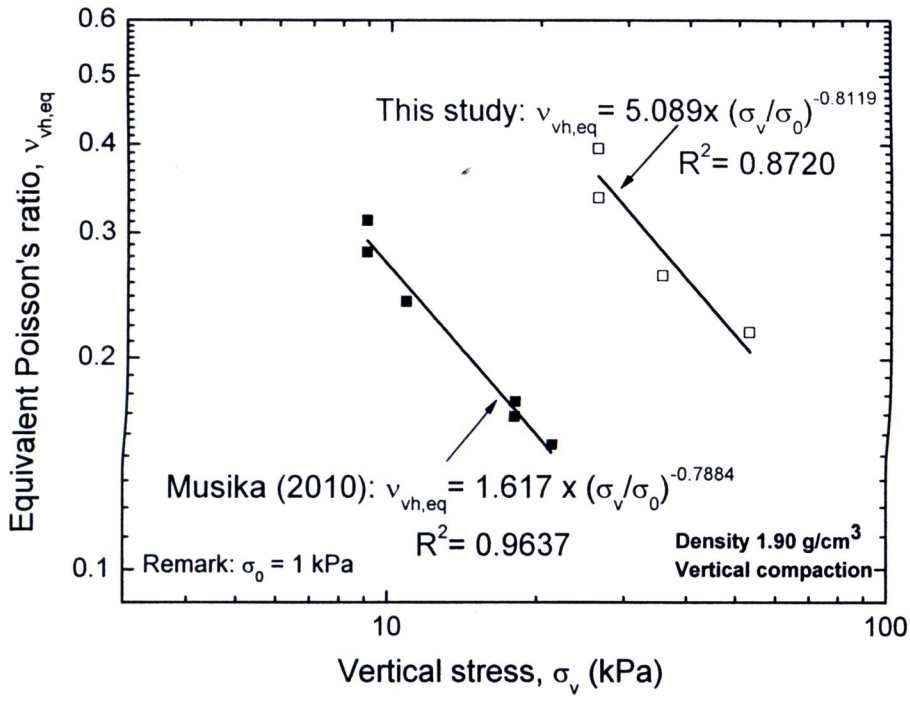

Figure 4.40(a) Comparisons of equivalent Poisson's ratio between PMA and HMA specimens as a function of vertical stress at density of 1.90 g/cm^3

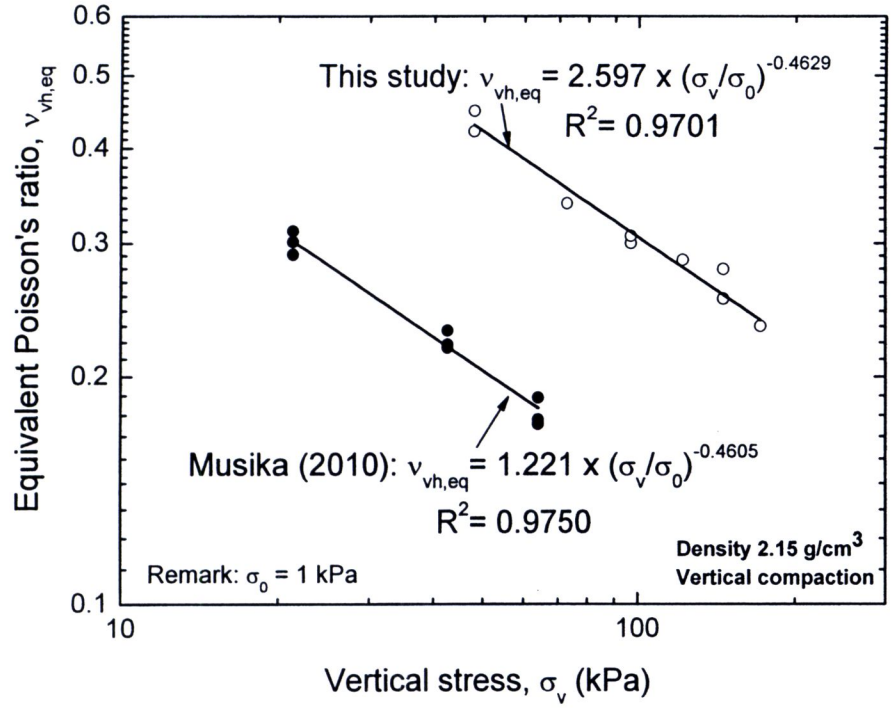

Figure 4.40(b) Comparisons of equivalent Poisson's ratio between PMA and HMA specimens as a function of vertical stress at density of 2.15 g/cm^3

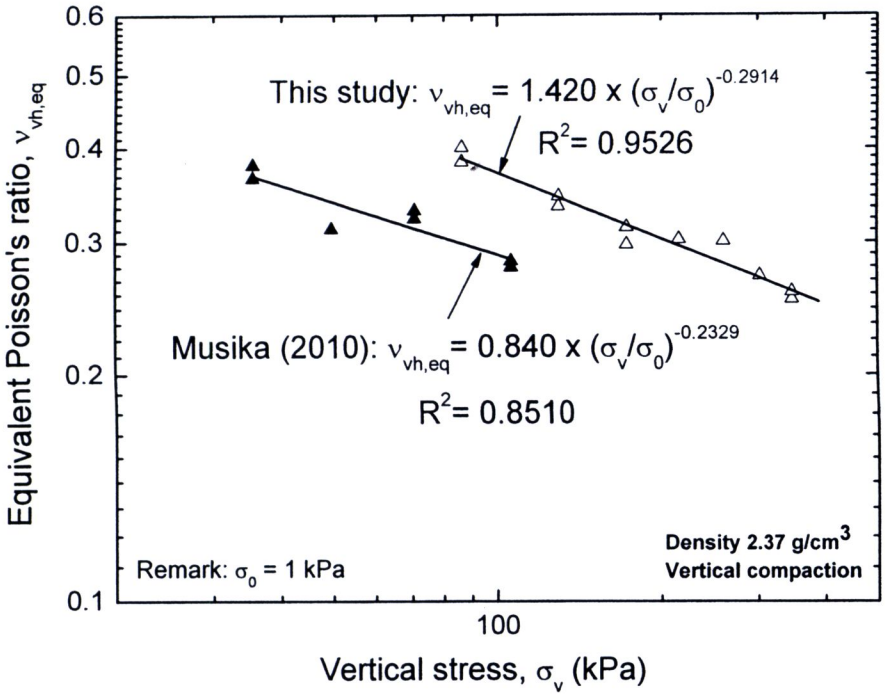

Figure 4.40(c) Comparisons of equivalent Poisson's ratio between PMA and HMA specimens as a function of vertical stress at density of 2.37 g/cm^3

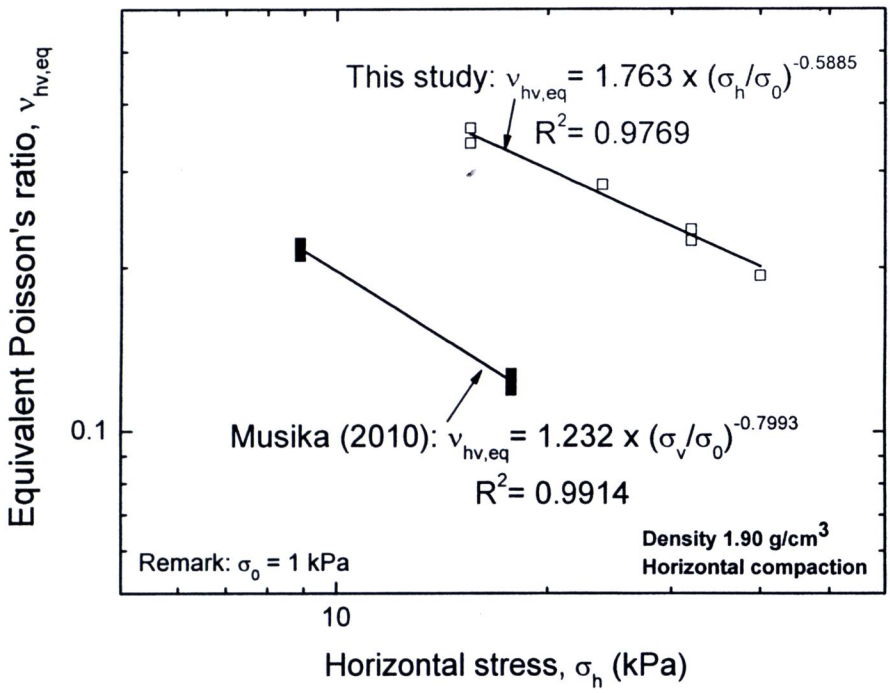

Figure 4.41(a) Comparisons of equivalent Poisson's ratio between PMA and HMA specimens as a function of horizontal stress at density of 1.90 g/cm^3

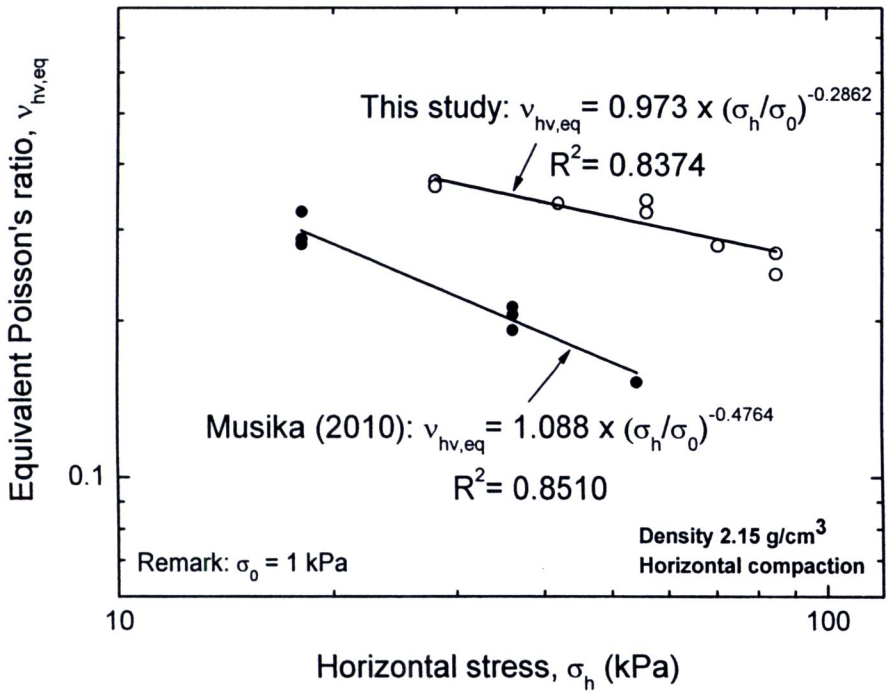

Figure 4.41(b) Comparisons of equivalent Poisson's ratio between PMA and HMA specimens as a function of horizontal stress at density of 2.15 g/cm^3

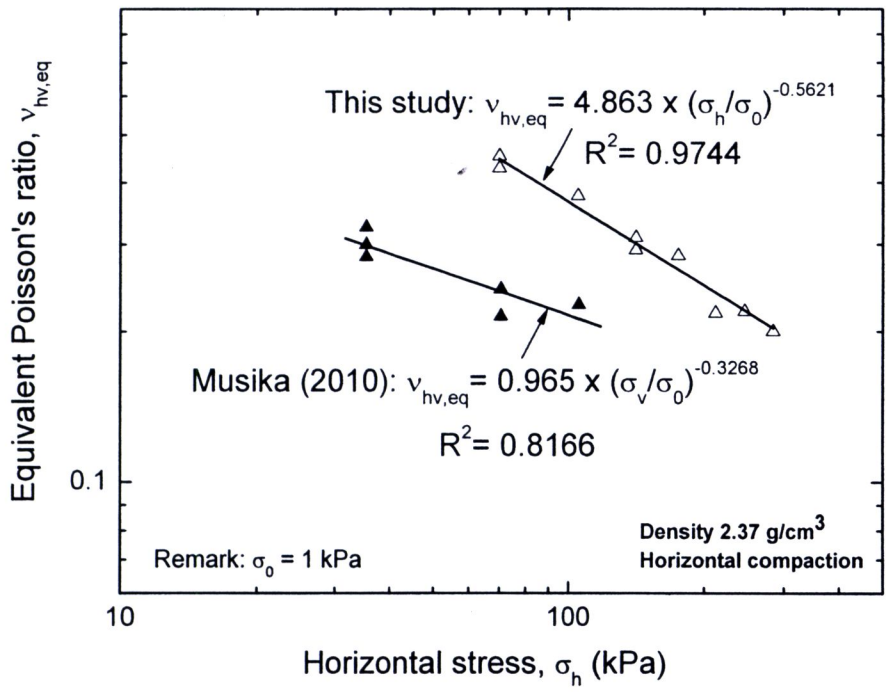

Figure 4.41(c) Comparisons of equivalent Poisson's ratio between PMA and HMA specimens as a function of horizontal stress at density of 2.37 g/cm^3

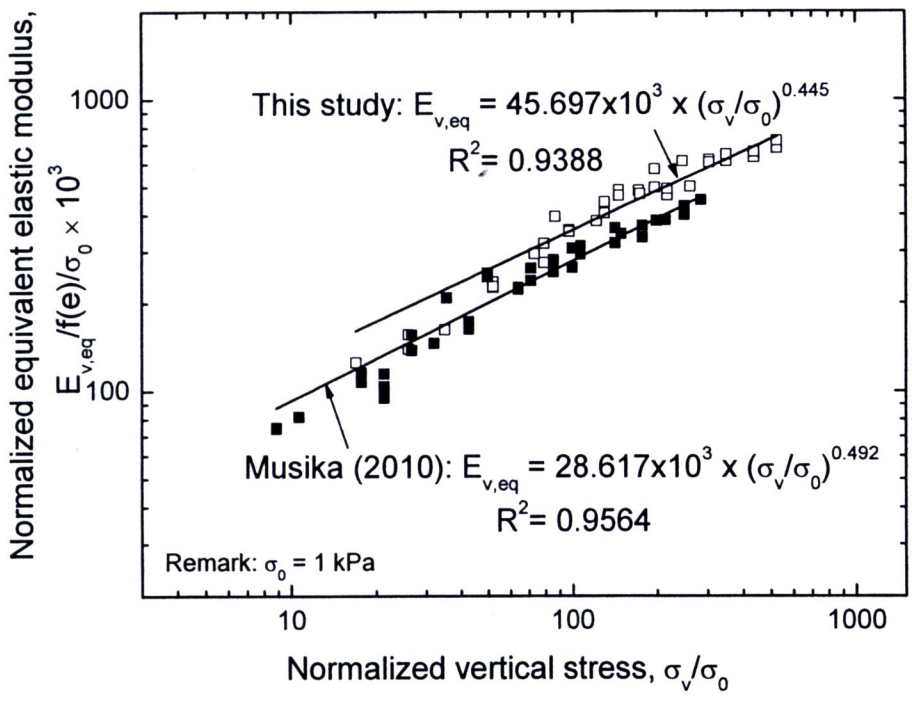

Figure 4.42(a) Comparisons of equivalent elastic modulus for all densities of PMA and HMA as a function of normalized vertical stress

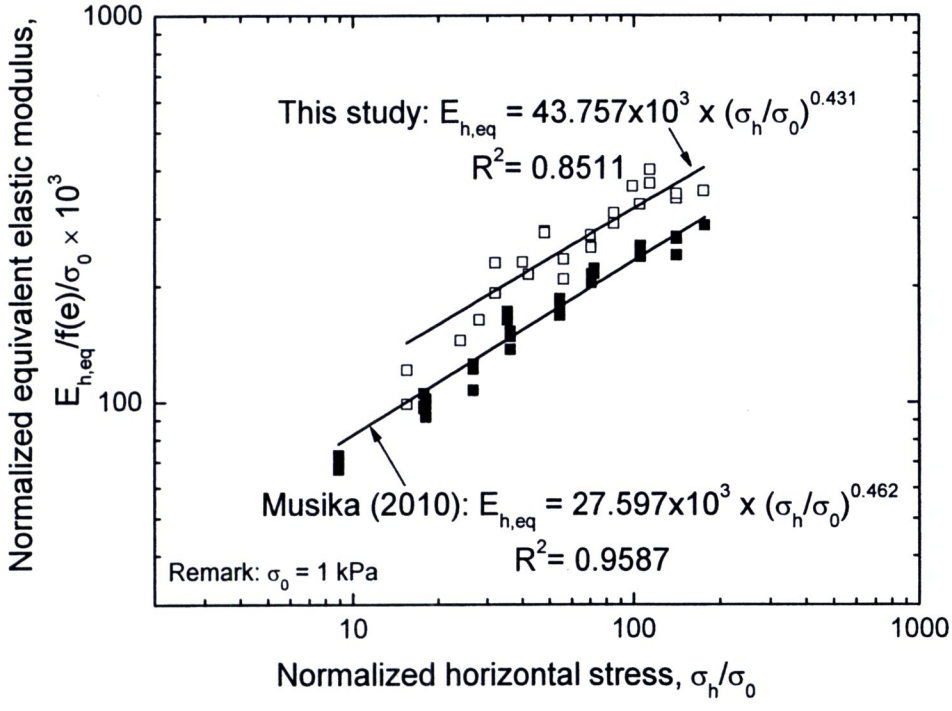

Figure 4.42(b) Comparisons of equivalent elastic modulus for all densities of PMA and HMA as a function of normalized horizontal stress

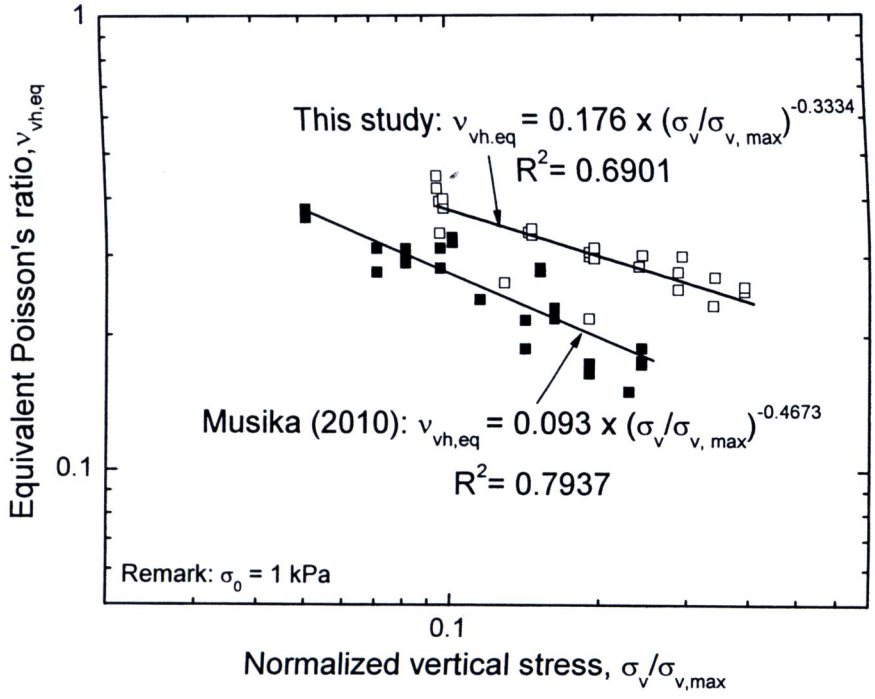

Figure 4.43(a) Comparisons of equivalent Poisson's ratio for all densities of PMA and HMA as a function of normalized vertical stress

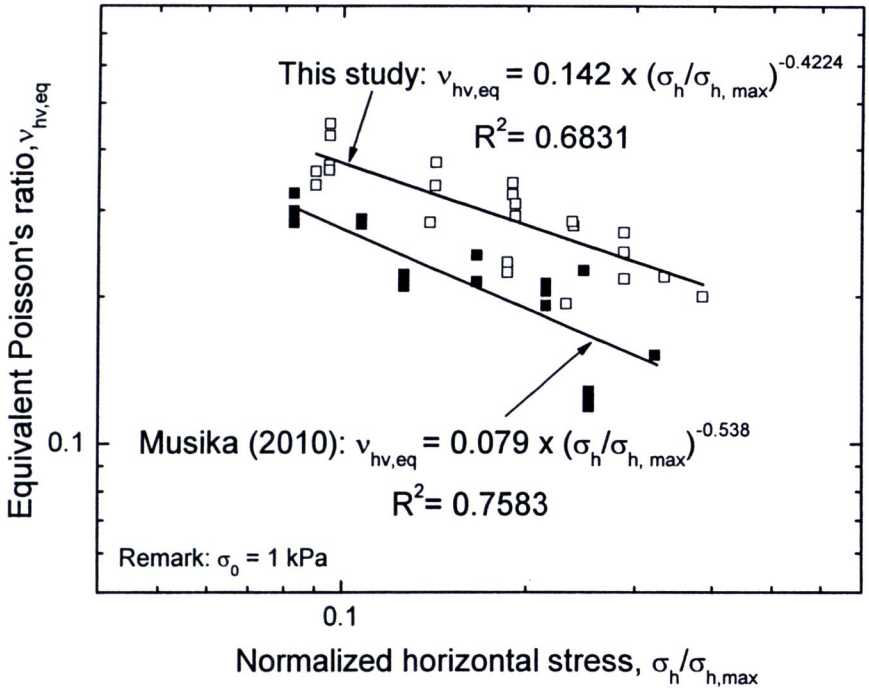

Figure 4.43(b) Comparisons of equivalent Poisson's ratio for all densities of PMA and HMA as a function of normalized horizontal stress

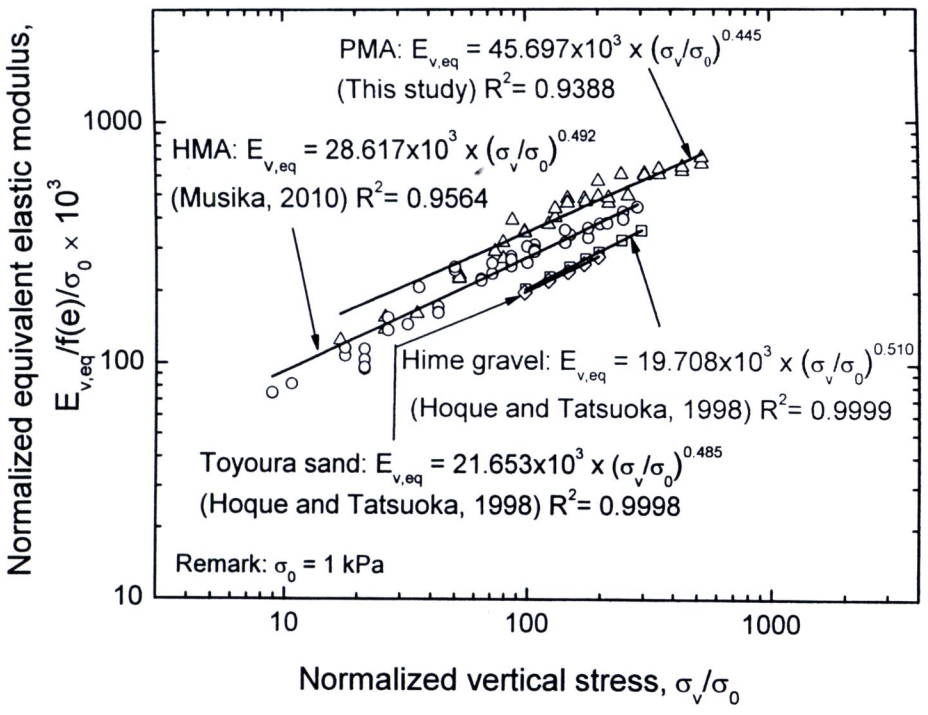

Figure 4.44(a) Comparisons of equivalent elastic modulus of PMA, HMA, Hime gravel and Toyoura sand as a function of normalized vertical stress

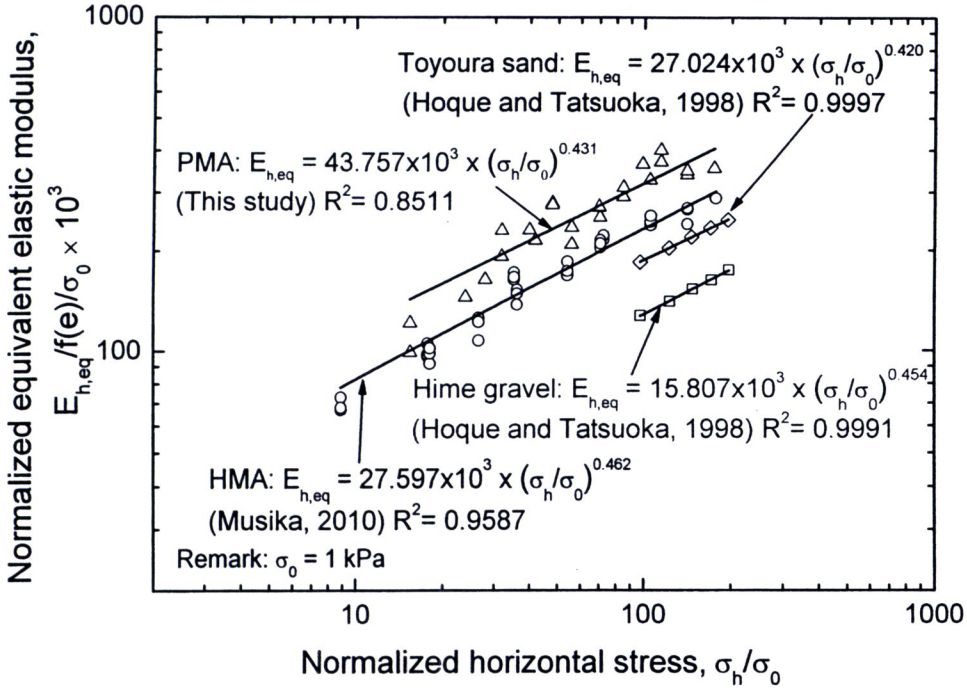

Figure 4.44(b) Comparisons of equivalent elastic modulus of PMA, HMA, Hime gravel and Toyoura sand as a function of normalized horizontal stress

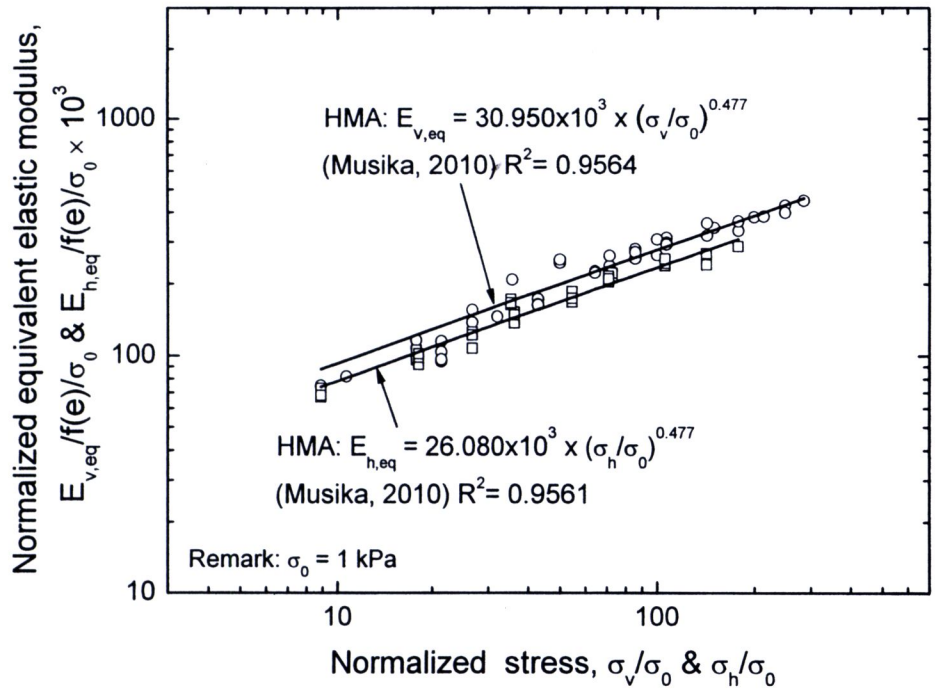

Figure 4.45(a) Comparisons between vertical and horizontal normalized equivalent elastic modulus of HMA, linear fitted with the average m-power

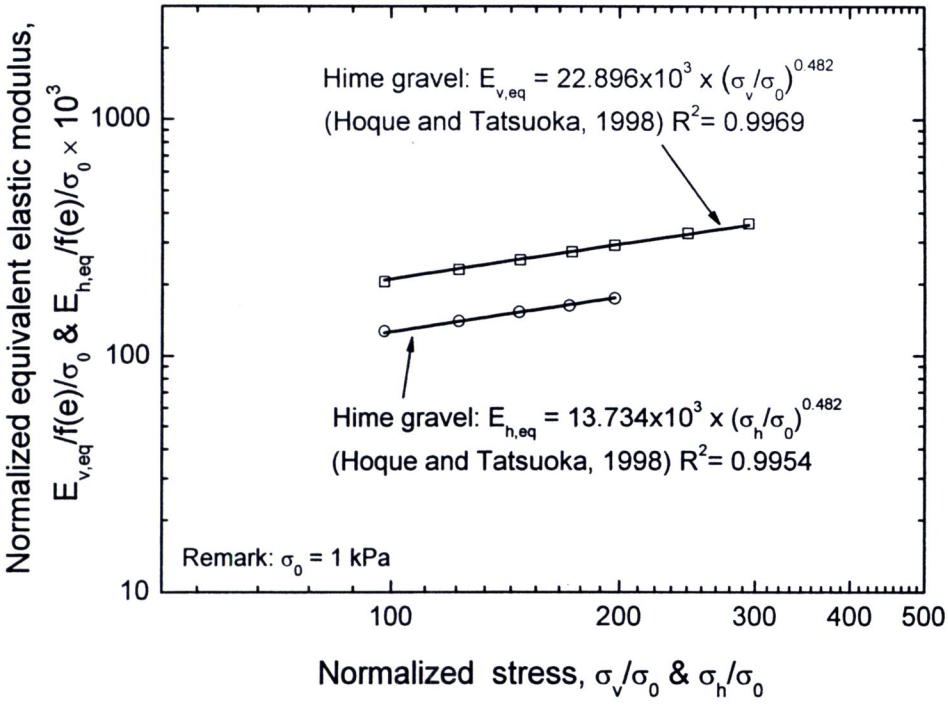

Figure 4.45(b) Comparisons between vertical and horizontal normalized equivalent elastic modulus of Hime gravel, linear fitted with the average m-power

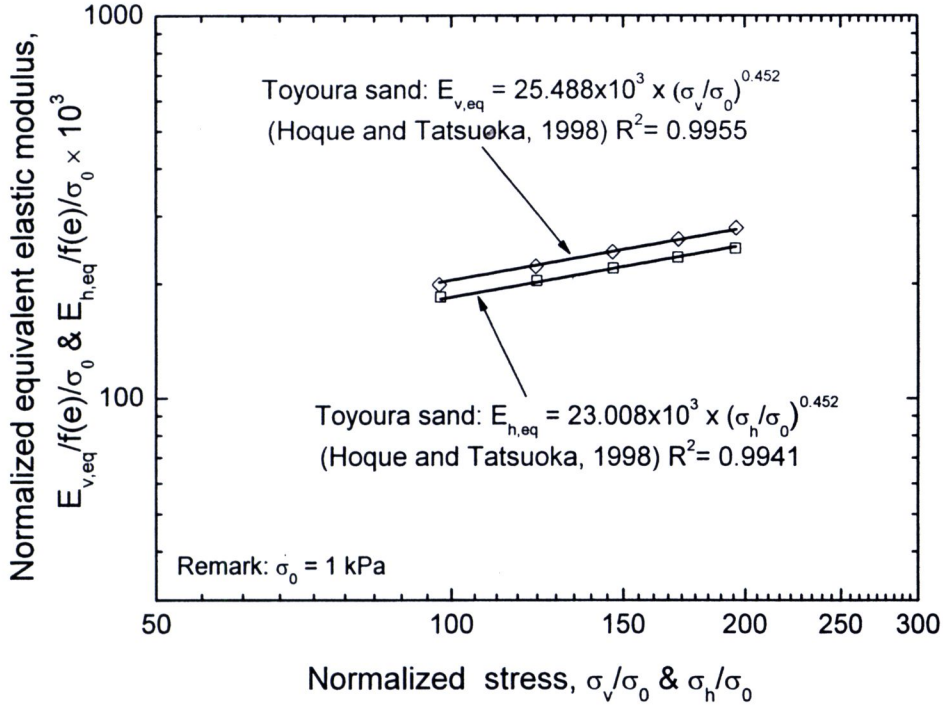

Figure 4.45(c) Comparisons between vertical and horizontal normalized equivalent elastic modulus of Toyoura sand, linear fitted with the average m-power